Linking Source, Fate/Transport and Chemical Composition of CDOM in the North Atlantic Subtropical Gyre

Dissertation in fulfilment of the requirements for the degree of Doctorate of Natural Sciences of the Faculty of Mathematics and Natural Sciences at Kiel University

submitted by
Natasha McDonald
Printed in San Francisco, USA 2020

Academic Advisor/First Examiner:	Prof. Eric P. Achterberg
Second Examiner:	Prof. Alexandra Z. Worden
Date of Oral Examination	27 May 2020

I, Natasha McDonald, declare that apart from the guidance of my supervisors, the content and design of this paper is solely my own work. No part of this thesis has been submitted as part of a doctoral degree to another examining body. Chapter 3 has undergone peer review and has been published in Frontiers in Marine Sciences (https://doi.org/10.3389/fmars.2019.00743) under a CC-BY license, such that it may be re-published without charge. I confirm that this thesis has been prepared subject to the Rules of Good Scientific Practice of the German Research Foundation and that I have not had an academic degree withdrawn from me.

_____

Natasha McDonald
19 February, 2020

Table of Contents

ABSTRACT

The oceanic reservoir of inorganic carbon is substantially larger than that of dissolved organic carbon (DOC) (ca. 38,000 vs. 660 Pg C). However, DOC plays an important role in carbon cycling in the ocean, and as such, efforts to constrain this pool of carbon are invaluable to our understanding of the global carbon cycle. A fraction of dissolved organic matter is chromophoric (CDOM) and accounts for approximately 50% of blue light absorption in the ocean. It also absorbs light in the visible portion of the spectrum and therefore regulates light available for photosynthesis. Furthermore, CDOM in the surface ocean can be observed in satellite measurements of ocean color, and in turn influences algorithmic predictions of chlorophyll and primary production. Despite its importance in ocean biogeochemistry and remote sensing, the sources, fate and composition of CDOM remain unresolved. This is especially true in the pelagic ocean, in regions such as the North Atlantic subtropical gyre. In this study, we investigated the sources and cycling of CDOM in the North Atlantic, using a decade-long time series of biogeochemical samples, as well as *in vitro* incubations of seawater collected from the Bermuda Atlantic Time Series in the Sargasso Sea (31° 40' N, 64° 10' W). We found that autochthonous processes contribute greatly to the oceanic CDOM pool. Both the heterotrophic production and microbial breakdown of CDOM appear to be taxon-specific, with two genera of marine archaeota demonstrating the ability to alter portions of lignin (a component of terrigenous CDOM) on a timescale of days. This reveals a linked cycle of terrigenous and autochthonous CDOM, in which breakdown of one component, can lead to the production of new CDOM. Additionally, we investigated the role of marine autotrophs and found a significant correlation ($R = 0.58$, $p < 0.01$) between CDOM and *Prochlorococcus* cell abundance at the depth of the CDOM maximum. Both were correlated with virioplankton abundance at the same depths ($R = 0.65$, $p < 0.01$). As such, we posit a scenario whereby CDOM is produced by the viral lysis of *Prochlorococcus*. As *Prochlorococcus* is the most abundant photosynthetic organism on Earth and its abundance is predicted to increase by 29% by 2100, this could have a significant effect on the global CDOM pool. Finally, we created a model to investigate the sources of CDOM in the bathypelagic ocean. Although it is thought that the majority of deep CDOM in the North Atlantic is transported via the North Atlantic Deep Water, *Prochlorococcus* abundance in the euphotic zone accounted for ~30% of the variance in our model, suggesting that particulate matter containing *Prochlorococcus* lysate or cells may be transported to the deep ocean, where it leaches CDOM. The results of our study highlight the influence of autochthonous processes in open ocean CDOM cycling, and suggest that the roles of *Prochlorococcus* and archaea may be especially important.

ZUSAMMENFASSUNG

Das ozeanische Reservoir an anorganisen Kohlenstoff ist wesentlich größer als das Reservoir an gelösten organischen Kohlenstoff (DOC) (ca. 38.000 vs. 660 Pg C). Das DOC spielt jedoch eine wichtige Rolle im Kohlenstoffkreislauf des Ozeans. Deshalb sind die Bemühungen, diesen Kohlenstoffpool zu quantifizieren von unschätzbarem Wert für unser Verständnis des globalen Kohlenstoffkreislaufs. Ein Bruchteil der gelösten organischen Substanz ist chromophorisch (CDOM) und macht etwa 50% der Absorption von blauem Licht im Ozean aus. Es absorbiert auch Licht im sichtbaren Spektrum und reguliert somit das für die Photosynthese verfügbare Licht. Darüber hinaus kann CDOM in der Ozeanoberfläche mithilfe von Satellitenmessungen der Ozeanfarbe beobachtet werden und trägt somit zur Vorhersage von Chlorophyll und Primärproduktion bei. Trotz ihrer Bedeutung für die Biogeochemie der Ozeane und die Fernerkundung sind die Quellen und die Zusammensetzung der CDOM nach wie vor ungeklärt. Dies gilt insbesondere für den pelagischen Ozean, in Regionen wie dem subtropischen Nordatlantik. In dieser Studie haben wir die Quellen und Zyklen von CDOM im Nordatlantik untersucht, wobei wir eine jahrzehntelange Zeitreihe von biogeochemischen Proben sowie vitro-Inkubationen von Meerwasser aus der Zeitreihe der Bermuda-Atlantiks in der Sargassosee (31° 40’ N, 64° 10’ W) verwenden. Wir haben festgestellt, dass autochthone Prozesse einen großen Beitrag zum ozeanischen CDOM-Pool leisten. Sowohl die heterotrophe Produktion als auch der mikrobielle Abbau von CDOM scheinen taxonspezifisch zu sein, wobei zwei Gattungen von Meeresarchäota die Fähigkeit zeigen, Teile des Lignin (ein Bestandteil der terrigenen CDOM) auf einer Zeitskala von Tagen zu verändern. Dies zeigt einen verknüpften Zyklus von terrigener und autochthoner CDOM, bei dem die Zersetzung einer Komponente zur Produktion neuer CDOM führen kann. Zusätzlich untersuchten wir die Rolle der marinen Autotrophen und fanden eine signifikante Korrelation ($R = 0{,}58$; $p < 0{,}01$) zwischen der CDOM- und *Prochlorokokken*-Zellhäufigkeit in der Tiefe des CDOM-Maximums. Beide korrelierten mit der Virioplanktonhäufigkeit in der gleichen Tiefe ($R = 0{,}65$; $p < 0{,}01$). Daher schlagen wir ein Szenario vor, bei dem CDOM durch die virale Lyse von *Prochlorokokken* erzeugt wird. Da *Prochlorokokken* der am häufigsten vorkommende fotosynthetische Organismus auf der Erde ist und sein Vorkommen bis 2100 voraussichtlich um 29% zunehmen wird, könnte dies erhebliche Auswirkungen auf den globalen CDOM-Pool haben. Schließlich haben wir ein Modell erstellt, um die Quellen von CDOM im tiefen Ozean zu untersuchen. Obwohl man annimmt, dass der Großteil der CDOM im Nordatlantik über das nordatlantische Tiefenwasser transportiert wird, machte die *Prochlorokokken*-Häufigkeit in der euphotischen Zone ~30% der Varianz in unserem Modell aus, was darauf hindeutet, dass Partikel, die *Prochlorokokken*-Lysat oder Zellen enthalten, in die Tiefsee transportiert werden können, wo sie CDOM auslaugen. Die Ergebnisse unserer Studie heben den Einfluss autochthoner Prozesse beim CDOM-Zyklus im offenen Ozean hervor und legen nahe, dass die Rolle von *Prochlorokokken* und Archaeen besonders wichtig sein könnte.

CHAPTER 1: General Introduction

Overview

The light-absorbing or chromophoric fraction of dissolved organic matter (CDOM) plays a key role in many chemical and biological processes in the oceans; however, its sources, chemical composition and cycling in the open ocean remain largely unresolved (Del Vecchio and Blough, 2004, Goldstone et al., 2004, Bricaud et al., 1981, Nelson and Siegel, 2002, Blough and Del Vecchio, 2002a, Nelson and Siegel, 2013, Kujawinski, 2016). CDOM has both terrigenous and autochthonous sources, which appear to be interrelated, but the influences of these sources on CDOM composition and cycling in the open ocean are unclear (Nelson et al., 2007, Nelson et al., 1998). In this study, we investigated the interrelated roles of terrigenous and autochthonous CDOM in the North Atlantic subtropical gyre, in order to achieve a better understanding of CDOM cycling in the open ocean. The Bermuda Atlantic Time-series Study site in the Sargasso Sea (31° 40' N, 64° 10' W) was utilized as an open ocean sampling location due to its removal from direct continental influence and the oligotrophic nature of the western North Atlantic subtropical gyre.

Role and importance of CDOM in ocean biogeochemistry and remote sensing

Over the past few decades, CDOM has received much interest as its role in biogeochemical cycles, including primary productivity, has become increasingly clear (Nelson et al., 2007, Nelson et al., 1998, Blough et al., 1993, Green and Blough, 1994, Kujawinski et al., 2004, Vodacek et al., 1997). CDOM is comprised of a vast mixture of organic compounds and is a complex component of the ocean carbon pool. It exhibits an absorbance spectrum that is characterized by an exponential increase in absorption with decreasing wavelength (Figure 1), and consequently regulates the amount of ultraviolet (UV) and visible light that is attenuated in the water column (Blough et al., 1993, Del Vecchio and Blough, 2002, Green and Blough, 1994, Vodacek et al., 1997). These controls on light availability can serve to protect organisms from harmful UV irradiation.

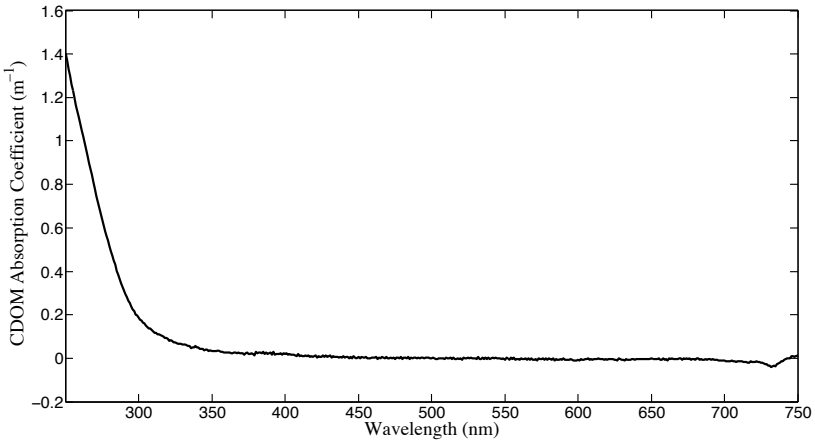

Figure 1. A typical open ocean CDOM absorbance spectrum (absorption coefficient (m^{-1}) from 250 – 750 nm) collected at the BATS site.

However, CDOM can also reduce photosynthetically active radiation (PAR) and therefore has a considerable impact on biological processes such as photosynthesis.

CDOM plays indirect roles in many chemical processes in the ocean. When photolyzed, CDOM products react with dissolved oxygen, generating reactive oxygen species (ROS; Thomas-Smith and Blough (2001)). The resulting secondary chemical reactions with ROS can impact redox cycling of trace metals and the oxidation of dimethyl sulfide (DMS) to dimethyl sulfoxide (DMSO; Green and Blough (1994), Blough and Del Vecchio (2002b)). Furthermore, its unique spectral properties allow us to determine its global surface ocean distribution using satellite sensors, and to differentiate CDOM from other chromophores in the ocean, such as chlorophyll (Behrenfeld et al., 2005, Siegel et al., 2005). In fact, colored dissolved and detrital materials control more than 50% of blue light absorption in the ocean (Siegel et al., 2002) and thus, CDOM absorbance properties have a significant impact on chlorophyll retrieval from satellite ocean color data. Maritorena et al. (2002) have included colored organic matter as an integral component of the Garver, Siegel, Maritorena (GSM) ocean color algorithm. Inclusion of this component results in up to 50% higher estimates of chlorophyll values in the subtropical gyres than predicted by other models (Siegel et al., 2005), which can in turn affect modeled rates of global net primary production (NPP). Therefore, a complete understanding of CDOM cycling based upon *in situ* data has critical implications for our understanding of many photochemical and biogeochemical processes in the ocean, as well as for ocean color-based measurements of chlorophyll, and in turn, estimates of primary productivity (Siegel et al., 2005).

Importance of the study region

Questions as to the sources, fate, transport and chemical composition of the global CDOM pool have been the subject of substantial interest, and have led to a significant number of investigations (Dittmar, 2015, Koch et al., 2005, Nelson and Siegel, 2013, Del Vecchio and Blough, 2004). However, in some parts of the oceans, the processes that govern CDOM cycling and composition remain unclear. The oligotrophic waters of the North Atlantic subtropical gyre (NASG; Figure 2) exhibit some of the lowest concentrations of CDOM because of low productivity, strong stratification and strong photochemical removal. Studies suggest that the processes governing dissolved organic carbon (DOC) concentrations in

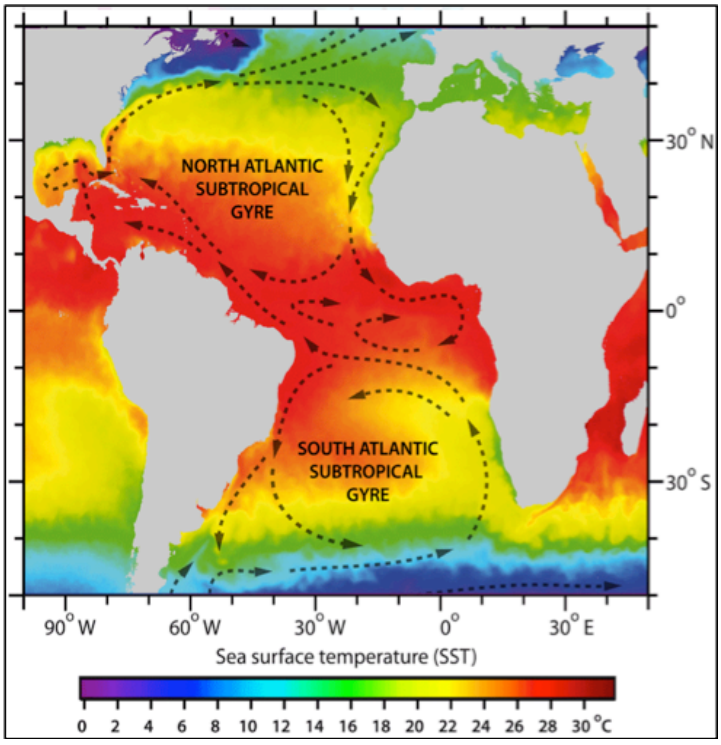

Figure 2. Surface ocean temperature distribution in the Atlantic. Boundaries indicated for the North and South Atlantic subtropical gyres.

surface waters in the NASG are crucially different from those regulating CDOM (Nelson and Siegel, 2002, Nelson and Siegel, 2013). In 2003, as part of the US CLIVAR/CO_2 Repeat Hydrography Survey, the distribution of CDOM throughout the North Atlantic was investigated. The lowest surface CDOM concentrations were observed in the subtropical gyres, while highest concentrations occurred in coastal waters and the subpolar gyre (Nelson et al., 2007, Nelson et al., 2010). The study also showed an increase in DOC mass-specific absorption of CDOM in deep waters with increased CFC-determined ventilation age, suggesting that CDOM is a relatively refractory part of the overall DOC pool (Nelson et al., 2010). Like CDOM, DOC exhibits not only spatial but also temporal variability. However, mid-latitude ocean zones, such as the oligotrophic western Sargasso Sea do not exhibit the same seasonality as nutrient-rich waters. Unlike high latitude, nutrient rich regions, where large increases in DOC concentrations are observed during phytoplankton blooms (Hansell, 2002), DOC concentrations in the western NASG are reduced during periods of highest primary productivity because light availability allows for overturn of the water column, and low DOC waters are mixed upward throughout the water column. During the summer, DOC concentrations increase, though the seasonal changes observed in these waters are on a much smaller scale than those observed in high latitude waters (Hansell, 2002, Goldberg et al., 2009, Hansell and Carlson, 1998, Lipschultz et al., 2002). This region is therefore of particular interest for the study of CDOM for several reasons, including the decoupling of DOC from CDOM that occurs in these waters and the number of discrete water masses including the North Atlantic Deep Water (NADW) that are advected to the NASG at depth and which contain CDOM of varying chemical composition. Dissolved organic matter (DOM) in the NASG is largely produced autochthonously; however, transport of terrigenous DOM from rivers and atmospheric deposition occurs, and it is not currently known how these inputs contribute to CDOM cycling – either directly or indirectly (Hernes and Benner, 2003). Therefore, the subtropical gyres can be considered a key "study zone" for OC cycles, and further investigation of the processes by which CDOM is produced, transported, chemically transformed and degraded could shed light on why DOC, CDOM and primary production (PP) are decoupled in the NASG and eventually provide a better understanding of DOM cycling throughout the global oceans. Finally, a large benefit of this study region is the availability of the long running Bermuda Atlantic Time Series Study (BATS) database of biogeochemical and physical measurements. This database, coupled with more than a decade of *in situ* CDOM measurements collected at the BATS site, allows for the investigation of long-term patterns and changes in open ocean DOM cycling.

Decoupling of CDOM and DOC in the open ocean

The increasing interest in the global carbon cycle over the past decades has undoubtedly been driven by increasing atmospheric CO_2 levels and the role of these increases in climate change. While inorganic carbon is by far the dominant form of carbon in the ocean (38,100 Pg C; (Fletcher et al., 2006), the concentration of oceanic DOC (~662 Pg C; (Hansell et al., 2009, Carlson and Hansell, 2015) is comparable to atmospheric CO_2 levels (~685 Pg; (Fasham et al., 2001, Carlson and Hansell, 2015). Net uptake of CO_2 by the ocean is ~2 Pg/year (Carlson and Hansell, 2015, Carlson et al., 2002, Hansell, 2002, Fletcher et al., 2006, Denning et al., 1999, Carlson, 2002), and this suggests that

oxidation of as little as 1% of ocean DOC within 1 year, with transfer to the atmosphere, would create a CO_2 flux larger than that produced annually by the combustion of fossil fuels (Carlson and Hansell, 2015, Ridgwell and Arndt, 2015, Carlson, 2002). While it is presently unlikely that oxidation on this scale could occur over short time periods, these calculations illustrate the degree to which small changes in the oceanic DOC pool can affect the ocean-atmosphere balance of CO_2 and in turn, global climate change. DOM and DOC also have significant impacts on ecological and biological cycles in the ocean. A portion of ocean DOC is produced in the planktonic food web and subsequently utilized by heterotrophic bacteria, after which it can be transported to higher trophic levels, exported to the deep ocean or remineralized (Carlson, 2002, Carlson and Hansell, 2015). Therefore, understanding the production, sinks and biogeochemical processes that govern DOC cycling in the ocean is essential.

The ability to obtain accurate measurements of global DOC concentrations has proven difficult. Current methods of DOC quantification entail the combustion of sample material (Carlson et al., 2010) and are highly prone to contamination. Additionally, the process of combusting the samples precludes the measurement of volatile organic compounds, which some studies have shown to be significant in the ocean (Carini et al., 2014, Arrieta et al., 2016). Finally, the nature of the analysis also precludes *in situ* measurements of DOC using sensors or even 'lab-on-a-chip' technologies, thus limiting the scope and resolution of global measurements. The chromophoric nature of CDOM would ostensibly lend to its potential use as a tracer of the global dissolved organic pool (DOC) pool, with the light-absorbing fraction of dissolved organic matter (DOM) in constant proportion to DOC concentration (Nelson et al., 2007, Siegel et al., 2005, Stedmon and Nelson, 2015). The ability to predict DOC concentrations from CDOM absorbance measurements would be a quick, easy and cost-effective method that would be invaluable in endeavors to constrain the global carbon cycle. However, the proportion of colored to 'uncolored' DOM is not constant; there is some degree of relationship evident in coastal waters with minimal degradation processes and simple mixing of a single high-DOM freshwater with a low-DOM, high-salinity seawater endmember. However, in most regions, photooxidation, microbial degradation and mixing result in a decoupling of DOC and CDOM (Stedmon and Nelson, 2015). This is particularly evident in open ocean regions, such as the subtropical gyres.

Links between terrigenous and autochthonous components of CDOM and implications for modeling ocean DOC

Complicating the matter of relating CDOM to DOC is the fact that cycling of DOC in the open ocean is not yet entirely understood. The oceanic DOC pool is one of the largest reservoirs of organic carbon on earth (Hedges et al., 2002, Carlson and Hansell, 2015, Goni et al., 1996). It has been shown that a portion of DOC escapes loss within the microbial loop, resulting in a decoupling of biological production and removal processes. An accumulation of up to ~70 μmol/kg of DOC in surface waters of the oligotrophic subtropical gyres, convincingly demonstrates that not all DOM is labile (Carlson and Hansell, 2015, Dittmar, 2015, Moran et al., 2016). The majority of recalcitrant DOM in the open ocean is thought to be produced by microbes (Carlson, 2002, Carlson and Hansell, 2015, Koch et al., 2005); however, terrigenous inputs, although small, may also

play a role. On the basis of measurements of lignin phenol concentrations, it has been shown that less than 2% of ocean DOC is terrigenous (Hernes and Benner, 2006), yet if estimates of annual riverine export to the ocean and of atmospheric deposition of dissolved or water soluble organic carbon to the surface ocean are considered, these concentrations should be higher (Williams and Druffel, 1987, Hedges et al., 1997, Koch et al., 2005). This raises a number of questions about the fate and transport of terrigenous DOM in the open ocean. It has been postulated that a combination of photodegradation and microbial transformation of a fraction of terrigenous DOM accounts for its low concentrations in the upper ocean (Koch et al., 2005, Mopper et al., 2015). It has also been shown that photooxidation of these terrigenous compounds can yield labile degradation products that can in turn be utilized by marine heterotrophs, thereby inducing bacterial growth (Hernes and Benner, 2003, Hedges et al., 1997, Fichot et al., 2016). In fact, some estimates show that nutrient requirements for bacterial populations in many ocean environments could be largely met by photodegradation products of organic matter (Moran and Zepp, 1997). The photodegradation products of the nitrogen-based components of DOM can meet up to 30% of nitrogen required by bacteria, which is important for microbial communities in oligotrophic waters (Moran and Zepp, 1997). By this removal mechanism, a large portion of photodegradation products from terrigenous DOM in surface waters could be 'recycled' by marine microbes. However, photolysis of some DOM constituents actually produces refractory byproducts, and others are resistant to photodegradation, especially those compounds with low molecular weight (LMW) (Beaupre and Druffel, 2012). Furthermore, geographic location and depth influence whether or not carbon will be bioavailable (Carlson and Hansell, 2015, Hansell et al., 2009, Goldberg et al., 2011, Hawkes et al., 2015). For instance, 1.9 Pg C resists microbial degradation in the epipelagic, but only 0.2 Pg C persist below 500 meters (Carlson and Hansell, 2015). A study at BATS has shown that DOC in surface waters that is resistant to microbial degradation, is quickly utilized by microbes and removed within timescales of weeks when exported to the mesopelagic region (Carlson and Hansell, 2015, Goldberg et al., 2009). This could indicate that key micronutrients or vitamins, necessary to make degradation of surface DOC energetically worthwhile, are present at depth, or it could suggest taxon-specific differences in microbial community ability to degrade more refractory DOC, or even genetic differences within in the same species. Like the DOM pool in its entirety, CDOM also has terrigenous and autochthonous sources in the open ocean, and there is evidence that these two inputs are interlinked. The role of marine microbes in the CDOM cycle does not appear to be solely limited to utilizing CDOM degradation products as a nutrient source. Marine microbes have been shown to produce CDOM in controlled incubations of oligotrophic waters. Nelson et al. (2004) observed and quantified production of CDOM by heterotrophic bacteria after amendment with various nutrient mixtures. However, researchers are still unclear as to the exact mechanisms and processes driving the molecular composition of marine DOM, and CDOM. The molecular composition of bulk marine DOM has been characterized in a number of studies (Kujawinski et al., 2004, Mopper et al., 2015, Dittmar et al., 2005, Koch et al., 2005, Stedmon and Bro, 2008, Coble, 1996, Del Castillo et al., 1999, Hansell et al., 2009), but never in regards to investigating the interrelated roles of terrigenous and autochthonous compounds in the cycling of oceanic DOM. It is currently unknown how marine microbes affect the molecular composition of terrigenous DOM, or how

degradation and/or utilization of terrigenous DOM affect the composition of microbially-produced DOM. A comprehensive understanding of these processes is therefore crucial to detangling the relationship between CDOM and DOM in the open ocean.

While many light-absorbing compounds in the oceans, including chlorophyll, have well-defined molecular properties, the exact chemical composition of CDOM remains largely unknown (Hansell et al., 2009, Del Vecchio and Blough, 2004, Kujawinski et al., 2004, Nelson and Siegel, 2002). Studies suggest that the characteristic excitation and emission spectra of CDOM are not simply a supposition of individual spectra from a mixture of compounds (Blough and Del Vecchio, 2002a, Del Vecchio and Blough, 2002, Del Vecchio and Blough, 2004). This implies photochemical interactions amongst molecules, and makes an understanding of this crucial component of the global carbon pool more difficult to achieve (Boyle et al., 2009, Del Vecchio and Blough, 2004). Photochemical and spectroscopic studies have revealed that one compound, lignin, is a known component of some optically active organic matter, and is present ubiquitously in natural waters (Hernes and Benner, 2002, Hernes and Benner, 2006). Lignin is a racemic natural organic polymer, found solely in tissues of woody vascular plants, and can therefore be used as a tracer of terrigenous organic matter. Despite its terrigenous origin, lignin is found in the pelagic ocean as a component of open ocean CDOM (Hernes and Benner, 2006). While terrigenous DOC is rapidly remineralized in the ocean via photochemical and microbial processes, lignin phenols have an average residence time of ~35 years in the Atlantic Ocean, indicating that at least some components of lignin are relatively refractory (Hernes and Benner, 2006). Reactivities within the Atlantic vary widely though, with photooxidation of lignin phenols in some surface waters within days, to lignin in deep water persisting for decades. A study by Hernes and Benner (2003) found that at salinities > 25 psu, photooxidation was the leading removal mechanism for lignin phenols. Photooxidation was seen to dramatically decrease the high molecular weight (HMW) fraction of lignin phenols. While the overall composition of lignin phenols was only altered by photooxidation, experiments on the microbial degradation of lignin phenols demonstrated some removal of these compounds. Hernes and Benner (2003) noted a loss of 21% of lignin phenols in the dark control for one of their photooxidation experiments, presumably from microbial degradation. Additionally, they analyzed lignin degradation in a long-term dark incubation of Mississippi plume water after a period of 1.7 years and found ~50% loss of lignin phenol concentrations and 37% loss of DOC (Hernes and Benner, 2003). Another similar study, using estuarine waters showed DOC losses of ~10% after 51 days of dark incubation (Moran et al., 2000). Despite several preliminary studies (Moran et al., 2000, Hernes and Benner, 2003), investigations of lignin degradation by microbial processes have not been carried out using natural pelagic oceanic waters, particularly those from nutrient-limited subtropical gyres. Nor have preliminary studies delineated taxon-specific responses to lignin, assessed the changes in molecular composition of the DOM throughout the incubations, or linked microbial degradation of lignin with the optical properties of CDOM. Additionally, studies have shown that the open ocean CDOM pool is not solely comprised of terrigenous matter, and production of CDOM has been evidenced in correlation with increased microbial growth in incubations of natural seawater assemblages (Nelson et al., 2004). Questions then arise as to the specific role lignin serves in open ocean cycles of organic matter and our study

suggests that it may actually be utilized by marine microbes on rapid time scales (days) and could therefore play a crucial part in microbial nutrient requirements, leading in turn to microbial production of 'marine' CDOM.
The connection between removal of terrigenous DOM in the open ocean and changes in the chemical composition and optical properties of marine CDOM could be the keystone in a comprehensive understanding of DOM cycling in the open ocean. It is clear that CDOM plays a crucial role in many ocean processes, and that it has potential to serve as a useful tracer of organic carbon. To effectively model DOC cycling using CDOM absorbance measurements, the chemical constituents that contribute to the optically active component of DOM must be elicited and linked to pertinent physical, biological and chemical processes in the marine environment. This cannot be achieved without an understanding of how microbial processes serve as a link between terrigenous and autochthonous DOM.

Autotrophic production of CDOM: a disparity between in situ and in vitro studies
Studies of autochthonous production of CDOM in the ocean have largely focused on marine heterotrophs. This is in part due to the lack of correlation observed between CDOM and chlorophyll *a* at the CDOM and deep chlorophyll maxima in the pelagic ocean (Nelson et al., 1998, Siegel et al., 2002, Nelson and Siegel, 2002, Nelson and Siegel, 2013). Blue light solar attenuation coefficients in the Sargasso Sea vary seasonally, but do not coincide with chlorophyll *a* concentrations (Nelson et al., 1998, Nelson and Siegel, 2013). Furthermore, although absorbance of particulate matter in the euphotic zone correlates strongly with chlorophyll *a*, the same is not true for CDOM. This has led researchers to believe that this blue light attenuation is related to CDOM and not particulate matter. Additionally, CDOM production in the euphotic zone is at a maximum in the summer and early autumn, when phytoplankton biomass is at an annual low (Steinberg et al., 2001, Nelson et al., 1998). The fact that the summer CDOM profile does not correlate with chlorophyll *a* and that it is qualitatively similar to the shape of bacterial abundance and thymidine uptake profiles has led researchers to posit that *in situ* CDOM in the open ocean is the result of heterotrophic activity. However, the conclusion that open ocean CDOM has a predominantly non-phytoplankton source is at odds with *in vitro* studies in which axenic cultures of marine phytoplankton and cyanobacteria species have been shown to produce CDOM. Studies have shown that prokaryotic cyanobacteria such as *Trichodesmium* spp. can produce CDOM in culture (Steinberg et al., 2004). Additionally, axenic cultures of *Chaetoceros*, *Skeletonema*, *Prorocentrum*, and *Micromonas* have each exhibited production of CDOM (Romera-Castillo et al., 2010), demonstrating that eukaryotic phytoplankton including diatoms, dinoflagellates and green algae can serve as CDOM sources. The lack of an *in situ* correlation between CDOM and chlorophyll *a* can therefore possibly be attributed to the fact that phytoplankton-derived CDOM is highly labile and is rapidly degraded in the water column. Chemical characterizations of the fluorophores produced in culture by phytoplankton revealed that this DOM was comprised of N-groups such as amino acids and carbohydrates (Romera-Castillo et al., 2010), suggesting that phytoplankton DOM is labile and unlikely to persist and accumulate in the water column. However, the comparison of CDOM with bulk chlorophyll *a* measurements may not reveal correlations with individual groups of phytoplankton. For instance, picocyanobacteria such as *Prochlorococcus* and

Synechococcus have been shown to produce CDOM in axenic cultures (Zhao et al., 2017), but to our knowledge, the contribution of picocyanobacteria to oceanic CDOM cycling has never been investigated. Considering that *Prochlorococcus* is the most abundant photosynthetic organism on earth (Amann et al., 1990, Becker et al., 2014, Biller et al., 2015) and it exhibits a seasonal maximum during the summer and early autumn at BATS, its role in the production of CDOM warrants exploration.

CDOM cycling in the deep ocean

While it is evident that autochthonous biological processes play an important role in CDOM cycling in the upper ocean, it is thought that the majority of CDOM in the deep waters of the North Atlantic is terrigenous. CDOM throughout the global ocean basins is found to increase throughout the main thermocline and in the North Atlantic subtropical gyre, it remains elevated in the bathypelagic zone. While CDOM is significantly correlated to apparent oxygen utilization (AOU) in the Pacific and Indian oceans (Carlson et al., 2010, Nelson and Siegel, 2013), no correlation exists in the North Atlantic below the main thermocline. Deep CDOM in the North Atlantic has been speculated to result from the advection of the Antarctic Intermediate Water (AAIW) and the North Atlantic Deep Water (NADW). Studies have suggested that the CDOM concentrations and distribution at depth in the North Atlantic subtropical gyre are a reflection of the concentrations and composition found in AAIW and NADW source waters. However, no correlation between pCFC-12 age and CDOM is found below 1000 m (Nelson and Siegel, 2013). Furthermore, CDOM profiles in the deep waters of the North Atlantic are homogenous and exhibit no significant variance between depths below the main thermocline. This is hypothesized to be the result of rapid advection and isopycnal mixing (Nelson et al., 2007). However, autochthonous sources of deep CDOM have not been fully investigated. It is assumed that the lack of correlation with AOU precludes a biogenic source in the deep Atlantic; however, the AOU profile at BATS does not reflect known microbial activity at depth. For instance, the SAR202 clade has been shown to be present below 1000 m, and is a known copiotroph that can remineralize semi-refractory organic compounds (Saw et al., 2019) – however, its signature of processing of organic material is not evident in AOU measurements (Landry, 2017). In fact, water mass input from the NADW is reflected in the deep AOU profile throughout the North Atlantic. At latitudes greater than 50°N, DOC and AOU values reflect the NADW formation (Carlson et al., 2010); however, the influence of the NADW is observed in AOU profiles as far south as the North Atlantic subtropical gyre. If deep CDOM in the North Atlantic was entirely terrigenous, there should be a correlation between AOU and CDOM, reflecting the input of the NADW in both. The absence of a correlation between AOU and CDOM in the deep ocean suggests that additional processes must govern deep CDOM distributions and that autochthonous sources must be examined.

Outline

Chapter 2 – Methods – Sample Collection and Analysis

In this chapter, an outline of data collection and analytical techniques are summarized to familiarize the reader with the methodological approach. These methods are discussed in detail within Chapters 3-5.

Chapter 3 – The Role of Heterotrophic Bacteria and Archaea in the Transformation of Lignin in the Open Ocean

Terrigenous and autochthonous production of CDOM have both been evidenced, yet the connection between the two is not entirely understood. This study sought to better delineate the links between terrigenous and biogenic CDOM by determining the microbial community composition and changes in the shape and intensity of CDOM spectra throughout incubations of seawater from the BATS site. Incubations were carried out in the dark and consisted of filtered surface water inoculated with unfiltered water from the local bacteria maximum. Samples were then amended with various mixtures of nutrients or left as unamended controls. A subset of samples was amended with lignin, to determine if marine heterotrophs could utilize semi-refractory, terrigenous carbon sources. In addition to heterotrophic bacteria, the abundance of two groups of Archaea was also measured throughout the experiments to determine if they play a role in utilization and production of CDOM. The results demonstrated a significant taxon-specific response to lignin-amended treatments over controls, corresponding to changes in CDOM spectra. Of particular interest was the growth response by Thaumarchaeota, which has been previously investigated for its mixotrophic nature and highlights a previously uninvestigated role for Archaea in CDOM cycling.

Chapter 4 -- Prochlorococcus is Linked to the Production of Chromophoric Dissolved Organic Matter in the North Atlantic Subtropical Gyre

The majority of oceanic CDOM studies focus on heterotrophic production, yet marine autotrophs have been shown to produce CDOM *in vitro*. Here, we examine the possible link between *in situ* production of CDOM and marine autotrophs, including picocyanobacteria. A decade-long dataset of CDOM and picocyanobacteria measurements collected at the BATS site was utilized in our study to investigate potential correlations between *Prochlorococcus* and *Synechococcus* and production of CDOM in the open ocean. Additionally, 7 parameters indicative of biological processes, including chlorophyll *a* and chlorophyll *b* concentrations, *Prochlorococcus*, *Synechococcus* and total bacterioplankton cell abundances, as well as net primary production (NPP) and bacterial production (BP) rates were performed at discrete depths throughout the time series record at BATS. The contribution of other marine autotrophs to the CDOM pool was also investigated using a suite of phytopigment time series data. Our findings indicate that *Prochlorococcus* is significantly correlated to the eutrophic CDOM maximum at BATS, while *Synechococcus* cell abundance and 12 marker pigments indicative of other phytoplankton groups were not statistically related to CDOM.

Chapter 5 – The Cycling of Deep Ocean Chromophoric Dissolved Organic Matter in the North Atlantic Subtropical Gyre

CDOM in the upper ocean is largely held to be autochthonous; yet, it has been suggested that CDOM in the deep ocean is terrigenous and the result of the water mass advection. However, CDOM data from the bathypelagic zone at BATS exhibits homogeneity between depths and monthly temporal variations that cannot be explained by advection alone. To determine if autochthonous organic matter contributes to deep ocean CDOM, we developed a model, using inputs of picoplankton abundance, POC flux from sediment

traps, deep ocean organic carbon data and potential density anomaly. Additionally, we used neutral density surfaces to delineate advected water masses at BATS and to investigate the correlation of water mass input with deep CDOM. Our findings indicate a deep ocean CDOM pattern related to *Prochlorococcus* abundance in the upper ocean, supporting recent studies that have predicted the export of picoplankton OM to depth.

Chapter 6 – Final Discussion and Future Work
Here, we summarize the findings of Chapters 3-5 and discuss possible future investigations to expand upon the work.

Summary
The previous *in vitro* and *in situ* studies highlight the complexity of CDOM cycling in the open ocean and demonstrate the need for a better understanding of how biological, chemical and physical processes in the ocean are interconnected. An enhanced understanding of CDOM cycling would have implications for the fields of remote sensing and ocean biogeochemistry, as well as global carbon cycling. The ability to model DOC and DOM from CDOM and FDOM measurements would greatly enhance the resolution of global carbon data and would allow for better constraint of the global carbon cycle, allowing for more accurate predictions of climate change. As such, the specific aims of this study were 1) to determine the role of terrigenous material in the autochthonous production of CDOM, 2) to ascertain if marine autotrophs contribute to *in situ* CDOM production and 3) to determine the factors controlling the accumulation and distribution of CDOM in surface waters and the bathypelagic zone in the North Atlantic subtropical gyre.

References

AMANN, R. I., BINDER, B. J., OLSON, R. J., CHISHOLM, S. W., DEVEREUX, R. & STAHL, D. A. 1990. COMBINATION OF 16S RIBOSOMAL-RNA-TARGETED OLIGONUCLEOTIDE PROBES WITH FLOW-CYTOMETRY FOR ANALYZING MIXED MICROBIAL-POPULATIONS. *Applied and Environmental Microbiology,* 56**,** 1919-1925.

ARRIETA, J. M., DUARTE, C. M., SALA, M. M. & DACHS, J. 2016. Out of Thin Air: Microbial Utilization of Atmospheric Gaseous Organics in the Surface Ocean. *Frontiers in Microbiology,* 6.

BEAUPRE, S. R. & DRUFFEL, E. R. M. 2012. Photochemical reactivity of ancient marine dissolved organic carbon. *Geophysical Research Letters,* 39.

BECKER, J. W., BERUBE, P. M., FOLLETT, C. L., WATERBURY, J. B., CHISHOLM, S. W., DELONG, E. F. & REPETA, D. J. 2014. Closely related phytoplankton species produce similar suites of dissolved organic matter. *Frontiers in Microbiology,* 5.

BEHRENFELD, M. J., BOSS, E., SIEGEL, D. A. & SHEA, D. M. 2005. Carbon-based ocean productivity and phytoplankton physiology from space. *Global Biogeochemical Cycles,* 19.

BILLER, S. J., BERUBE, P. M., LINDELL, D. & CHISHOLM, S. W. 2015. Prochlorococcus: the structure and function of collective diversity. *Nature Reviews Microbiology,* 13**,** 13-27.

BLOUGH, N. V. & DEL VECCHIO, R. 2002a. *In:* HANSELL, D. & CARLSON, C. (eds.) *Biogeochemistry of Marine Dissolved Organic Matter.* San Diego: Academic Press.

BLOUGH, N. V. & DEL VECCHIO, R. 2002b. Chromophoric DOM in the Coastal Environment. *In:* HANSELL, D. A. C., C. (ed.) *Biogeochemistry of Marine Dissolved Organic Matter.* Academic Press.

BLOUGH, N. V., ZAFIRIOU, O. C. & BONILLA, J. 1993. OPTICAL-ABSORPTION SPECTRA OF WATERS FROM THE ORINOCO RIVER OUTFLOW - TERRESTRIAL INPUT OF COLORED ORGANIC-MATTER TO THE CARIBBEAN. *Journal of Geophysical Research-Oceans,* 98**,** 2271-2278.

BOYLE, E. S., GUERRIERO, N., THIALLET, A., DEL VECCHIO, R. & BLOUGH, N. V. 2009. Optical Properties of Humic Substances and CDOM: Relation to Structure. *Environmental Science & Technology,* 43**,** 2262-2268.

BRICAUD, A., MOREL, A. & PRIEUR, L. 1981. ABSORPTION BY DISSOLVED ORGANIC-MATTER OF THE SEA (YELLOW SUBSTANCE) IN THE UV AND VISIBLE DOMAINS. *Limnology and Oceanography,* 26**,** 43-53.

CARINI, P., WHITE, A. E., CAMPBELL, E. O. & GIOVANNONI, S. J. 2014. Methane production by phosphate-starved SAR11 chemoheterotrophic marine bacteria. *Nature Communications,* 5.

CARLSON, C. 2002. Production and Removal Processes. *In:* HANSELL, D. & CARLSON, C. (eds.) *Biogeochemistry of Marine Dissolved Organic Matter.* San Diego: Academic Press.

CARLSON, C. & HANSELL, D. 2015. DOC Sources, Sinks, Reactivity, and Budgets. *In:* HANSELL, D. & CARLSON, C. (eds.) *Biogeochemistry of Marine Dissolved Organic Matter, 2nd Edition.* USA: Academic Press.

CARLSON, C. A., GIOVANNONI, S. J., HANSELL, D. A., GOLDBERG, S. J., PARSONS, R., OTERO, M. P., VERGIN, K. & WHEELER, B. R. 2002. Effect of nutrient amendments on bacterioplankton production, community structure, and DOC utilization in the northwestern Sargasso Sea. *Aquatic Microbial Ecology,* 30**,** 19-36.

CARLSON, C. A., HANSELL, D. A., NELSON, N. B., SIEGEL, D. A., SMETHIE, W. M., KHATIWALA, S., M., M. M. & HALEWOOD, E. R. 2010. Dissolved organic carbon export and subsequent remineralization in the mesopelagic and bathypelagic realms of the North Atlantic basin. . *Deep Sea Research II,* 57**,** 1433-1445.

COBLE, P. G. 1996. Characterization of marine and terrestrial DOM in seawater using excitation emission matrix spectroscopy. *Marine Chemistry,* 51**,** 325-346.

DEL CASTILLO, C. E., COBLE, P. G., MORELL, J. M., LOPEZ, J. M. & CORREDOR, J. E. 1999. Analysis of the optical properties of the Orinoco River plume by absorption and fluorescence spectroscopy. *Marine Chemistry,* 66**,** 35-51.

DEL VECCHIO, R. & BLOUGH, N. V. 2002. Photobleaching of chromophoric dissolved organic matter in natural waters: kinetics and modeling. *Marine Chemistry,* 78**,** 231-253.

DEL VECCHIO, R. & BLOUGH, N. V. 2004. On the origin of the optical properties of humic substances. *Environmental Science & Technology,* 38**,** 3885-3891.

DENNING, A. S., TAKAHASHI, T. & FRIEDLINGSTEIN, P. 1999. Can a strong atmospheric CO2 rectifier effect be reconciled with a "reasonable" carbon budget? *Tellus Series B-Chemical and Physical Meteorology,* 51**,** 249-253.

DITTMAR, T. 2015. Reasons Behind the Long-Term Stability of Dissolved Organic Matter. *In:* HANSELL, D. & CARLSON, C. (eds.) *Biogeochemistry of Marine Dissolved Organic Matter, 2nd Edition.* San Diego: Academic Press.

DITTMAR, T., KATTNER, G. & KOCH, B. 2005. New molecular approaches for tracing dissolved organic matter through marine systems. *Abstracts of Papers of the American Chemical Society,* 230**,** U1787-U1788.

FASHAM, M. J. R., BALINO, B. M., BOWLES, M. C., ANDERSON, R., ARCHER, D., BATHMANN, U., BOYD, P., BUESSELER, K., BURKILL, P., BYCHKOV, A., CARLSON, C., CHEN, C. T. A., DONEY, S., DUCKLOW, H., EMERSON, S., FEELY, R., FELDMAN, G., GARCON, V., HANSELL, D., HANSON, R., HARRISON, P., HONJO, S., JEANDEL, C., KARL, D., LE BORGNE, R., LIU, K. K., LOCHTE, K., LOUANCHI, F., LOWRY, R., MICHAELS, A., MONFRAY, P., MURRAY, J., OSCHLIES, A., PLATT, T., PRIDDLE, J., QUINONES, R., RUIZ-PINO, D., SAINO, T., SAKSHAUG, E., SHIMMIELD, G., SMITH, S., SMITH, W., TAKAHASHI, T., TREGUER, P., WALLACE, D., WANNINKHOF, R., WATSON, A., WILLEBRAND, J. & WONG, C. S. 2001. A new vision of ocean biogeochemistry after a decade of the Joint Global Ocean Flux Study (JGOFS). *Ambio***,** 4-31.

FICHOT, C. G., BENNER, R., KAISER, K., SHEN, Y., AMON, R. M. W., OGAWA, H. & LU, C.-J. 2016. Predicting Dissolved Lignin Phenol Concentrations in the Coastal Ocean from Chromophoric Dissolved Organic Matter (CDOM) Absorption Coefficients. *Frontiers in Marine Science,* 3.

FLETCHER, S. E. M., GRUBER, N., JACOBSON, A. R., DONEY, S. C., DUTKIEWICZ, S., GERBER, M., FOLLOWS, M., JOOS, F., LINDSAY, K., MENEMENLIS, D., MOUCHET, A., MULLER, S. A. & SARMIENTO, J. L. 2006. Inverse estimates of anthropogenic CO2 uptake, transport, and storage by the ocean. *Global Biogeochemical Cycles,* 20.

GOLDBERG, S. J., CARLSON, C. A., BRZEZINSKI, M., NELSON, N. B. & SIEGEL, D. A. 2011. Systematic removal of neutral sugars within dissolved organic matter across ocean basins. *Geophysical Research Letters,* 38.

GOLDBERG, S. J., CARLSON, C. A., HANSELL, D. A., NELSON, N. B. & SIEGEL, D. A. 2009. Temporal dynamics of dissolved combined neutral sugars and the quality of dissolved organic matter in the Northwestern Sargasso Sea. *Deep-Sea Research Part I-Oceanographic Research Papers,* 56**,** 672-685.

GOLDSTONE, J. V., DEL VECCHIO, R., BLOUGH, N. V. & VOELKER, B. M. 2004. A multicomponent model of chromophoric dissolved organic matter photobleaching. *Photochemistry and Photobiology,* 80**,** 52-60.

GONI, M. A., EGLINTON, T. I., BOON, J. J., PUREVEEN, J., HOUSEL, E. & HEDGES, J. L. 1996. Quantitative constraints on organic matter degradation. *Abstracts of Papers of the American Chemical Society,* 212**,** 55-GEOC.

GREEN, S. A. & BLOUGH, N. V. 1994. OPTICAL-ABSORPTION AND FLUORESCENCE PROPERTIES OF CHROMOPHORIC DISSOLVED ORGANIC-MATTER IN NATURAL-WATERS. *Limnology and Oceanography,* 39**,** 1903-1916.

HANSELL, D. 2002. DOC in the Global Ocean Carbon Cycle. *In:* HANSELL, D. A. C., C. (ed.) *Biogeochemistry of Marine Dissolved Organic Matter.* Academic Press.

HANSELL, D. A. & CARLSON, C. A. 1998. Deep-ocean gradients in the concentration of dissolved organic carbon. *Nature,* 395**,** 263-266.

HANSELL, D. A., CARLSON, C. A., REPETA, D. J. & SCHLITZER, R. 2009. DISSOLVED ORGANIC MATTER IN THE OCEAN A CONTROVERSY STIMULATES NEW INSIGHTS. *Oceanography,* 22**,** 202-211.

HAWKES, J. A., ROSSEL, P. E., STUBBINS, A., BUTTERFIELD, D., CONNELLY, D. P., ACHTERBERG, E. P., KOSCHINSKY, A., CHAVAGNAC, V., HANSEN, C. T., BACH, W. & DITTMAR, T. 2015. Efficient removal of recalcitrant deep-ocean dissolved organic matter during hydrothermal circulation. *Nature Geoscience,* 8**,** 856-+.

HEDGES, J. I., BALDOCK, J. A., GELINAS, Y., LEE, C., PETERSON, M. L. & WAKEHAM, S. G. 2002. The biochemical and elemental compositions of marine plankton: A NMR perspective. *Marine Chemistry,* 78**,** 47-63.

HEDGES, J. I., KEIL, R. G. & BENNER, R. 1997. What happens to terrestrial organic matter in the ocean? *Organic Geochemistry,* 27**,** 195-212.

HERNES, P. J. & BENNER, R. 2002. Transport and diagenesis of dissolved and particulate terrigenous organic matter in the North Pacific Ocean. *Deep-Sea Research Part I-Oceanographic Research Papers,* 49**,** 2119-2132.

HERNES, P. J. & BENNER, R. 2003. Photochemical and microbial degradation of dissolved lignin phenols: Implications for the fate of terrigenous dissolved organic matter in marine environments. *Journal of Geophysical Research-Oceans,* 108.

HERNES, P. J. & BENNER, R. 2006. Terrigenous organic matter sources and reactivity in the North Atlantic Ocean and a comparison to the Arctic and Pacific oceans. *Marine Chemistry,* 100**,** 66-79.

KOCH, B. P., WITT, M. R., ENGBRODT, R., DITTMAR, T. & KATTNER, G. 2005. Molecular formulae of marine and terrigenous dissolved organic matter detected by electrospray ionization Fourier transform ion cyclotron resonance mass spectrometry. *Geochimica Et Cosmochimica Acta,* 69**,** 3299-3308.

KUJAWINSKI, E. B., DEL VECCHIO, R., BLOUGH, N. V., KLEIN, G. C. & MARSHALL, A. G. 2004. Probing molecular-level transformations of dissolved organic matter: insights on photochemical degradation and protozoan modification of DOM from electrospray ionization Fourier transform ion cyclotron resonance mass spectrometry. *Marine Chemistry,* 92**,** 23-37.

KUJAWINSKI, E. B., LONGNECKER, K., BAROTT, K.L., WEBER, R.J.M., SOULE KIDO, M.C. 2016. Microbial community structure affects marine dissolved organic matter composition. *Frontiers in Marine Science,* 3.

LANDRY, Z. C., SWAN, B., HERNDL, G., STEPANAUSKAS, R., GIOVANNONI, S. 2017. SAR202 Genomes from the Dark Ocean Predict Pathways for the Oxidation of Recalcitrant Dissolved Organic Matter. *mBio,* 8**,** e00413-17.

LIPSCHULTZ, F., BATES, N. R., CARLSON, C. A. & HANSELL, D. A. 2002. New production in the Sargasso Sea: History and current status. *Global Biogeochemical Cycles,* 16.

MARITORENA, S., SIEGEL, D. A. & PETERSON, A. R. 2002. Optimization of a semianalytical ocean color model for global-scale applications. *Applied Optics,* 41**,** 2705-2714.

MOPPER, K., KIEBER, D. J. & STUBBINS, A. 2015. Marine Photochemistry of Organic Matter. *In:* HANSELL, D. & CARLSON, C. (eds.) *Biogeochemistry of Marine Dissolved Organic Matter, 2nd Edition.* San Diego: Academic Press.

MORAN, M. A., KUJAWINSKI, E. B., STUBBINS, A., FATLAND, R., ALUWIHARE, L. I., BUCHAN, A., CRUMP, B. C., DORRESTEIN, P. C., DYHRMAN, S. T., HESS, N. J., HOWE, B., LONGNECKER, K., MEDEIROS, P. M., NIGGEMANN, J., OBERNOSTERER, I., REPETA, D. J. & WALDBAUER, J. R. 2016. Deciphering ocean carbon in a changing world. *Proceedings of the National Academy of Sciences of the United States of America,* 113**,** 3143-3151.

MORAN, M. A., SHELDON, W. M. & ZEPP, R. G. 2000. Carbon loss and optical property changes during long-term photochemical and biological degradation of estuarine dissolved organic matter. *Limnology and Oceanography,* 45**,** 1254-1264.

MORAN, M. A. & ZEPP, R. G. 1997. Role of photoreactions in the formation of biologically labile compounds from dissolved organic matter. *Limnology and Oceanography,* 42**,** 1307-1316.

NELSON, N. B., CARLSON, C. A. & STEINBERG, D. K. 2004. Production of chromophoric dissolved organic matter by Sargasso Sea microbes. *Marine Chemistry,* 89**,** 273-287.

NELSON, N. B. & SIEGEL, D. A. 2002. Chromophoric DOM in the Open Ocean. *In:* HANSELL, D. & CARLSON, C. (eds.) *Biogeochemistry of Marine Dissolved Organic Matter.* Academic Press.

NELSON, N. B. & SIEGEL, D. A. 2013. The Global Distribution and Dynamics of Chromophoric Dissolved Organic Matter. *Annual Review of Marine Science***,** 447-76.

NELSON, N. B., SIEGEL, D. A., CARLSON, C. A., SWAN, C., SMETHIE, W. M. & KHATIWALA, S. 2007. Hydrography of chromophoric dissolved organic matter in the North Atlantic. *Deep-Sea Research Part I-Oceanographic Research Papers,* 54**,** 710-731.

NELSON, N. B., SIEGEL, D. A., CARLSON, C. A. & SWAN, C. M. 2010. Tracing global biogeochemical cycles and meridional overturning circulation using chromophoric dissolved organic matter. *Geophysical Research Letters,* 37.

NELSON, N. B., SIEGEL, D. A. & MICHAELS, A. F. 1998. Seasonal dynamics of colored dissolved material in the Sargasso Sea. *Deep-Sea Research Part I-Oceanographic Research Papers,* 45**,** 931-957.

RIDGWELL, A. & ARNDT, S. 2015. Why Dissolved Organics Matter: DOC in Ancient Oceans and Past Climate Change. *In:* HANSELL, D. & CARLSON, C. (eds.) *Biogeochemistry of Marine Dissolved Organic Matter, 2nd Edition.* San Diego: Academic Press.

ROMERA-CASTILLO, C., SARMENTO, H., ALVAREZ-SALGADO, X. A., GASOL, J. M. & MARRASE, C. 2010. Production of chromophoric dissolved organic matter by marine phytoplankton (vol 55, pg 446, 2010). *Limnology and Oceanography,* 55**,** 1466-1466.

SAW, J., NUNOURA, T., HIRAI, M., TAKAKI, Y., PARSONS, R., MICHELSEN, M., LONGNECKER, K., KUJAWINSKI, E., STEPANAUSKAS, R., LANDRY, Z., CARLSON, C. & GIOVANNONI, S. 2019. Pangenomics reveal diversification of enzyme families and niche specialization in globally abundant SAR202 bacteria.

SIEGEL, D. A., MARITORENA, S., NELSON, N. B., BEHRENFELD, M. J. & MCCLAIN, C. R. 2005. Colored dissolved organic matter and its influence on the satellite-based characterization of the ocean biosphere. *Geophysical Research Letters,* 32.

SIEGEL, D. A., MARITORENA, S., NELSON, N. B., HANSELL, D. A. & LORENZI-KAYSER, M. 2002. Global distribution and dynamics of colored dissolved and detrital organic materials. *Journal of Geophysical Research-Oceans,* 107.

STEDMON, C. A. & BRO, R. 2008. Characterizing dissolved organic matter fluorescence with parallel factor analysis: a tutorial. *Limnology and Oceanography-Methods,* 6**,** 572-579.

STEDMON, C. A. & NELSON, N. B. 2015. The Optical Properties of DOM in the Ocean. *In:* HANSELL, D. & CARLSON, C. (eds.) *Biogeochemistry of Marine Dissolved Organic Matter, 2nd Edition.* San Diego: Academic Press.

STEINBERG, D. K., CARLSON, C. A., BATES, N., JOHNSON R. J., F., M. A. & KNAP, A. H. 2001. Overview of the US JGOFS Bermuda Atlantic Time-series Study (BATS): a decade-scale look at ocean biology and biogeochemistry. *deep-Sea Research II,* 48**,** 1405-1447.

STEINBERG, D. K., NELSON, N. B., CARLSON, C. A. & PRUSAK, A. C. 2004. Production of chromophoric dissolved organic matter (CDOM) in the open ocean by zooplankton and the colonial cyanobacterium Trichodesmium spp. *Marine Ecology Progress Series,* 267**,** 45-56.

THOMAS-SMITH, T. E. & BLOUGH, N. V. 2001. Photoproduction of hydrated electron from constituents of natural waters. *Environmental Science & Technology,* 35**,** 2721-2726.

VODACEK, A., BLOUGH, N. V., DEGRANDPRE, M. D., PELTZER, E. T. & NELSON, R. K. 1997. Seasonal variation of CDOM and DOC in the Middle Atlantic Bight: Terrestrial inputs and photooxidation. *Limnology and Oceanography,* 42**,** 674-686.

WILLIAMS, P. M. & DRUFFEL, E. R. M. 1987. RADIOCARBON IN DISSOLVED ORGANIC-MATTER IN THE CENTRAL NORTH PACIFIC-OCEAN. *Nature,* 330**,** 246-248.

ZHAO, Z., GONSIOR, M., LUEK, J., TIMKO, S., IANIRI, H., HERTKORN, N., SCHMITT-KOPPLIN, P., FANG, X. T., ZENG, Q. L., JIAO, N. Z. & CHEN, F. 2017. Picocyanobacteria and deep-ocean fluorescent dissolved organic matter share similar optical properties. *Nature Communications,* 8.

CHAPTER 2: Methods – Sample Collection and Analysis

Sample collection

All samples were collected at the Bermuda Atlantic Time Series (BATS) site (31° 40' N, 64° 10' W) between July 2006 and June 2016 onboard the R/V Atlantic Explorer. Samples for microbial incubations were collected in July 2014. Samples were collected from Niskin bottles (General Oceanics) mounted on a steel rosette affixed with a conductivity, temperature and depth (CTD) sensor package (Seabird SBE 9/11 Plus).

CDOM: Samples were filtered directly from the Niskin bottles through a 0.2 μm capsule filter (Whatman Polycap 75 AS) using acid-washed Teflon-lined Tygon tubing (Saint Gobain) and collected in muffled amber glass vials (I-Chem) with Polytetrafluoroethylene-lined caps (I-Chem). Samples were stored in the dark at 4°C until analysis.

Bacterial abundance/FISH/CARDFISH and Microbial incubations: Samples for bacterial cell abundance and *Fluorescence in situ Hybridization (FISH) and Catalyzed Reporter Deposition-FISH (CARD-FISH)* consisted of 40 mL of unfiltered seawater water collected directly from the Niskin bottles into 50-mL polypropylene Falcon tubes (USA Scientific). The samples were fixed with 4 mL of 0.1-μm filtered (Supore, Pall, USA) formalin (37% formaldehyde; VWR), gently inverted to mix, and stored upright at -80 °C until analysis. Water for microbial incubations was collected from 1 m and 60 m. The 1 m water was filtered using a 0.2 μm filter (Whatman Polycap AS), and 14-L aliquots were transferred into 20-L polycarbonate carboys (Nalgene, USA) that were pre-cleaned with 10% hydrochloric acid. Water for the inoculum was collected from a depth of 60 m (where maximum bacterioplankton concentrations can typically be observed at BATS), and 7 L of inoculum was added, unfiltered, to each carboy, thereby diluting the filtered surface seawater to 70% of the total volume. The incubations were then either amended with a suite of nutrient substrates or left unamended as controls. A full description of the amendments is given in Chapter 3.

Collection and Solid Phase Extraction (SPE) of DOM: *Synechococcus* and *Prochlorococcus* cultures were grown using established procedures and filtered to collect DOM as described in detail in Zhao et al. (Zhao et al., 2017). All samples were acidified to pH 2 using formic acid (Sigma Aldrich) for an established solid-phase extraction (SPE) procedure (Dittmar, 2008) using Agilent Bond Elut PPL cartridges. Samples were drawn through clean Teflon tubing and connected to PPL cartridges at a flow rate of ~4 mL/min until sample solutions had passed through the cartridges. After extraction, cartridges were rinsed with 0.1% formic acid water (Sigma Aldrich), dried under N_2, and eluted with 10 mL pure methanol (LC-MS Chromasolv, Sigma Aldrich). Methanol extracts were stored at -20 °C prior to mass spectrometric analysis.

Ancillary Measurements: Ancillary data included measurements collected monthly as part of the BATS time series. Measurements for depth (m), temperature (ITS-90; °C), salinity (PSS-78), total organic carbon (TOC; μmol kg^{-1}), HPLC-quantified phytopigment concentration (ng kg^{-1}), oxygen, picoplankton abundance (cells mL^{-1}) and sediment trap organic carbon flux (C_{org}; mg m^{-2} d^{-1}) were collected according to methods outlined in the Joint Global Ocean Flux Study (JGOFS) protocols and have been made available at www.bats.bios.edu/bats_methods.html. The

potential density anomaly ($\sigma\theta$) was defined as $\sigma_{\theta,S,0} = \rho_{\theta,S,0}$ - 1000 kg/m^3, where θ is the potential temperature, S is the *in situ* salinity and ρ_0 is the potential density, referenced to the pressure at the ocean surface.

Instrumental Analysis

CDOM absorbance: Changes in CDOM concentrations were determined by UV-Visible spectroscopy. Prior to analysis, samples were removed from cold storage and allowed to equilibrate to room temperature (20 °C) to avoid the development of bubbles. Absorbance measurements were made using a Perkin Elmer Lambda-18 dual-beam spectrophotometer, equipped with a photo-multiplier tube. Samples were analyzed in quartz cuvettes with a 10 cm pathlength and were blank corrected against de-ionized water in a matched cuvette. Blank-corrected spectra were reported as absorption coefficients (m^{-1}) using the equation:

$$a = 2.303A / l \quad (1)$$

where a is the absorption coefficient (m^{-1}), A is the absorbance and l is the pathlength (m). Spectra were measured between 250 and 750 nm and were blank corrected. Spectra were quality controlled by performing a log-linear fit on spectra in the range of 320 – 450 nm and discarding any data with a correlation coefficient R of < 0.9 or if the least squares estimated log slope < -0.07. Additionally, the mean and standard deviation were calculated and flagged as bad if the values were outside 2 SD of the mean. Absorbance values at discrete wavelengths in the near-UV spectrum (325 nm and 350 nm) were then selected from individual spectra over time to measure changes in concentration and changes in CDOM components.

Enumeration of bacterioplankton abundance: Bacterioplankton abundance samples (40 mL) were fixed with formalin (10% final concentration), and stored at -80 °C until slide preparation. Samples were thawed and 5 – 10 mL aliquots were filtered onto Irgalan Black pre-stained 0.2 µm polycarbonate filters (Whatman), under gentle vacuum (~100 mm Hg). The samples were stained with 4'-6'-di- amidino-2-phenylidole dihydrochloride (DAPI 5 µg mL^{-1}; Sigma Aldrich); (Porter and Feig, 1980), and were then mounted onto slides with Resolve immersion oil (high viscosity; Resolve, Richard-Allan Scientific, Kalamazoo, MI) and stored at -20 °C. Slides were then enumerated using an AX70 epifluorescence microscope (Olympus, Tokyo, Japan) under ultraviolet excitation at 1000X magnification. At least 500 cells per slide (10 fields) were counted for bacterioplankton abundance.

Enumeration of specific bacterioplankton lineages by Fluorescence in situ Hybridization (FISH) and Catalyzed Reporter Deposition-FISH (CARD-FISH): FISH was utilized to quantify the abundance of the major bacterioplankton phylotypes present in the seawater. The FISH probes used for this study (Table S3) have previously been validated *in silico* for specificity using Probe Match on the Ribosomal Database Project (Cole et al., 2009) and TestProbe and Probebase on the SILVA website (Loy A, 2007). The bacterial and archaeal groups quantified included the SAR11 clade (152R, 441R, 542R, 732R probes), Alteromonas spp. (AC137R), Flavobacteria II (CFB563R), Rhodobacteraceae (536R), SAR202 (103R, 311R), Euryarchaeota (Eury806), and Thaumarchaeota (Thaum537).

Samples were fixed with formalin (10% final concentration) and known volumes (3-20 mL) were filtered onto 0.2 μm polycarbonate filters (Whatman), under gentle vacuum (~100 mm Hg) and stored at -20 °C with desiccant. Quarter filters were washed in 95% ethanol and then probed according to previous protocols (Morris et al., 2002, Morris et al., 2005, Parsons et al., 2011a, Parsons et al., 2015, McNally et al., 2017). Archaeal enumeration was performed using CARD-FISH (Herndl et al., 2005, Teira et al., 2004). Permeabilization of the cell membrane was conducted using 0.1 N HCl (ACS reagent, 37%; Sigma Aldrich) with no prior embedding in agarose. The probes and their specific hybridization settings are summarized in Table S3. The resulting filters from FISH and CARD-FISH were mounted with 20 μL of 1.67 μg mL^{-1} 0, 6-diamidino-2-phenylindole dihydrochloride (DAPI, SIGMA-Aldrich, St. Louis, MO, USA) in citifluor solution (Ted Pella Inc. Reading, USA), sealed with nail polish and stored frozen (-80 °C) in the dark (Parsons et al., 2011a). FISH and CARD-FISH slides were imaged with epifluorescence microscopy (Olympus AX70 microscope) under ultra-violet excitation and by excitation of Cy3 dye (532 nm; Invitrogen). Images were captured on a Toshiba (Irvine, CA, USA) CCD video camera with a Pro-series capture kit version 4.5 (Media Cybernetics, Bethesda, MD, USA) and processed with Image Pro software (version 7.0; Media Cybernetics) as previously described (Carlson et al., 2009, Parsons et al., 2011b, Parsons et al., 2015).

Picocyanobacteria Enumeration: Samples for picoplankton enumeration by flow cytometry (FCM) were collected, unfiltered, directly from Niskin bottles, into sterile 2.0 mL cryogenic vials (Thermo Scientific) and immediately fixed with paraformaldehyde (0.5% final volume; reagent grade; Sigma Aldrich). Samples were refrigerated for 1-2 hours and then stored in liquid nitrogen or at -80°C until analysis. A Becton Dickinson Influx cell sorter (BD Biosciences, NJ, USA) was used for the FCM analysis (ex = 488 nm; bandpass filters = 692 ± 20 nm and 580 ± 15 nm for chlorophyll *a* and phycoerythrin, respectively). 0.53 μm and 2.88 μm sized beads were used to perform daily calibrations (Spherotech Inc, USA). *Synechococcus* and *Prochlorococcus* were distinguished by size and whether phycoerythrin fluorescence was observed. Cell abundances were calculated using the volume analyzed method of Sieracki, Verity et al. (1993).

High Performance Liquid Chromatography (HPLC) Pigments Identification and Quantification: To obtain pigment samples, 4 liters of seawater were collected directly from niskin bottles (General Oceanics; Miami, USA) affixed to a rosette equipped with a conductivity, temperature and depth (CTD) sensor package (Seabird SBE 9/11 Plus) into pre-cleaned polycarbonate bottles (Nalgene) and were immediately filtered at a pressure of ≤ 5 inches Hg, through 0.7 μm, 47 mm glass fiber filters (Whatman, GF/F; Chicago, USA). The filters were then placed into aluminum foil and flash frozen in liquid nitrogen. Samples were subsequently stored at -80°C until analysis. Samples were analyzed by the Bermuda Atlantic Time-series Study (BATS) lab, according to methods outlined in Bidigare (1991) and Wright et al (1991) . For analysis, samples were extracted overnight at -20 °C in 5 mL of acetone (ACS grade; Fisher Scientific) and then an additional 5 mL of acetone was added to each sample. The HPLC system (Agilent 1100 Series with a Waters Spherisorb ODS2 silica-based reversed phased C_{18} column) was equilibrated with a primary solvent mixture (80:20, v:v, methanol: 0.5M ammonium acetate, aq., pH 7.2; Sigma HPLC grade > 99.99% purity) at a flow rate of 1 mL/min. A continuous gradient of 3 eluents was used (in decreasing order of polarity) consisting of the primary solvent mixture (Eluent A), 90:10 v:v acetonitrile:water (Eluent B; Sigma HPLC grade > 99.99% purity) and ethyl acetate (Eluent C; Sigma HPLC grade > 99.99% purity). A 1 mL aliquot of each sample was combined

with 400 μL of de-ionized water, agitated and placed in the dark for 5 min. A sample volume of 200 μL was injected into the sample loop. Retention times and visible spectrum, referenced to certified standards (DHI Labs, Denmark) were used to determine the identity and concentration of pigments in each sample.

Quantification of dissolved organic carbon: Dissolved organic carbon was sampled in duplicate and filtered through 0.7 μm pre-combusted glass fiber filters (Whatman, GF/F) into pre-combusted borosilicate glass vials (40 mL; I-Chem) fitted with acid-washed Teflon-lined caps and stored frozen at -20°C until analysis. All DOC samples were sent to the University of California for analysis. Samples were analyzed using high-temperature combustion on Shimadzu TOC-V analyzers, with slight modifications from the manufacturer model as described in Carlson et al. (2010). In order to minimize the machine blanks, expansive conditioning of the combustion tube with repeated injections of low carbon water (LCW) as well as deep seawater was performed. A daily standardization of the system response was performed using a four-point standardization calibration curve of glucose solution in LCW. In order to guarantee comparability between sample sets, all samples were systematically referenced against LCW, deep Sargasso Sea reference waters (2600 m), and surface Sargasso Sea water every 6-8 analyses.

High-resolution Mass Spectrometry: Ultra-high resolution mass spectrometry was used to characterize the molecular composition of *Prochlorococcus* and *Synechococcus* SPE-DOM using a Bruker Solarix 12 Tesla Fourier transform (FT) ion cyclotron resonance (ICR) mass spectrometer housed at Helmholtz Zentrum, Munich, Germany. Ionization was achieved using negative ion mode electrospray ionization (ESI) with an electrospray voltage of –3.6 kV. Samples were infused at a flow rate of 120 μL h^{-1} and 500 scans were averaged. The resolution (>500,000 at *m/z* 400) and the mass error (<0.2 ppm) were sufficiently precise to compute exact molecular formulae (Koch BP, 2007, Herzsprung P, 2014) based on the following atomic numbers: $^{12}C_{0-\infty}$, $^{1}H_{0-\infty}$, $^{16}O_{0-30}$, $^{14}N_{0-10}$ and $^{32}S_{0-2}$, as well as the ^{13}C and ^{34}S isotopologues (Herzsprung P, 2014, Koch BP, 2007). Van Krevelen or elemental diagrams were used to visualize the chemical space FT-ICR MS data by plotting assigned molecular formulas according to their hydrogen to carbon (H/C) and oxygen to carbon (O/C) ratios (Van Krevelen, 1950). A number of parameters were calculated to gain information based on assigned molecular formulas. For instance, double bond equivalents (DBE), or the number of unsaturations plus rings in a molecule, were determined for assigned molecular formulas according to the equation below (Koch BP, 2016, Koch BP, 2006).

$$DBE = 1 + C - O - S - \tfrac{1}{2}(N + H) \quad (1)$$

An additional parameter, the modified aromaticity index (AI_{mod}), or the DBE to carbon ratio, was introduced to be indicative or aromatic structures in DOM when AI_{mod} is greater than 0.5 according to the following equation (7, 8).

$$AI_{mod} = DBE/C = (1 + C - O - S - \tfrac{1}{2}(N + H))/(C - O - N - S) \quad (2)$$

For compounds containing only carbon, hydrogen, and oxygen (CHO) the average carbon oxidation state (COS) was approximated by

$$COS = (2O - H)/C \quad (3)$$

where a formula with COS less than or equal to 0 is reduced and that greater than 0 is oxidized.

Statistical Analyses and Data Visualization

All data analysis and visualization was performed using either Matlab (2014b) or R Studio (v. 1.1463). CDOM data were interpolated to remove missing values and then again to create an evenly-spaced time series of CDOM absorbance (325 nm) measurements. Row-wise followed by column-wise linear interpolation of data matrices was used to remove and replace missing (NA) values and then a linear time interpolation was performed for all variables to create evenly-spaced data. The use of cubic spline instead of linear interpolation resulted in a difference of < 1% in the outcome of modeled data. The interpolated time was defined as t = 732924 : 34.19 : 736138, where the first and last argument are serial date numbers, representing the sampling date range in reference to January 0, 0000, and 34.19 is the average sampling interval (days). To plot data with different value ranges on the same graph, the data for each parameter was standardized such that all variable vectors had a mean of zero and a standard deviation of one. The time series comprised data from 24 discrete depths ranging from 1 – 3000 m, collected between 2006 and 2015. Significant correlations and confidence intervals were tested by calculating Pearson's correlation coefficients (product moment), or with reduced major axis (geometric mean) model II regression, using Matlab code provided by Ed Peltzer at MBARI, available at https://www.mbari.org/index-of-downloadable-files/, with standard deviation calculated according to Ricker (1973). *R*-values with *p*-values < 0.05, corresponding to 95% confidence, were considered statistically significant, although most values were < 0.01 and noted as such.

Cross correlations were calculated using the fast Fourier transform-based cross correlation theorem, such that $f * g = \mathcal{F}^{-1}[\overline{F}(\nu)\,\overline{G}(\nu)]$, where $f * g$ is the cross correlation of $f(t)$ and $g(t)$ and $\mathcal{F}$ is the Fourier transform applied to each column of data. The number of degrees of displacement of the first dataset relative to the second, or 'lags', was set to 20 (months), with the center lag set equal to zero. Cross correlation plots included 95% confidence boundaries.

Changes in the frequency domain of time series spectra were analyzed by generating evolutionary power spectra using the Lomb-Scargle algorithm for un-evenly spaced time-series data as follows:

$$P_x(\omega) = \frac{1}{2\sigma}\left\{\frac{\left[\sum_j (y_j-\overline{y})\cos\omega(t_j-\tau)\right]^2}{\sum_j \cos^2\omega(t_j-\tau)} + \frac{\left[\sum_j (y_j-\overline{y})\sin\omega(t_j-\tau)\right]}{\sum_j \sin^2\omega(t_j-\tau)}\right\}$$

where N is the number of data points for y(t), ω is the angular frequency (2πf), τ is an offset that allows $P_x\omega$ (the periodogram) to be independent of uneven time spacing and

$$\overline{y} = \frac{1}{N}\sum_{i=1}^{N} y_i$$

and

$$s^2 = \frac{1}{N-1}\sum_{i=1}^{N}(y_i-\overline{y})^2$$

are the mean and variance of the dataset, respectively. To observe the power spectra for all measured depths simultaneously, a '3D' Lomb-Scargle periodogram was compiled for 1 – 250 m depth by creating a filled contour plot with frequency ($days^{-1}$) on the x-axis, depth (m) on the y-axis and the unitless power intensity on the z-axis. Frequencies at statistically significant power intensities were converted to periods ($t = \omega^{-1}$).

References

BIDIGARE, R. R. 1991. *In:* HURD, S. A. (ed.) *The analysis and characterization of marine particles.* Washington, D.C.: American Geophysical Union.

CARLSON, C. A., MORRIS, R., PARSONS, R., GIOVANNONI, S. J. & VERGIN, K. 2009. Seasonal dynamics of SAR11 populations in the euphotic and mesopelagic zones of the northwestern Sargasso Sea. *ISME Journal,* 3**,** 283-295.

COLE, J. R., WANG, Q., CARDENAS, E., FISH, J., CHAI, B., FARRIS, R. J., KULAM-SYED-MOHIDEEN, A. S., MCGARRELL, D. M., MARSH, T., GARRITY, G. M. & TIEDJE, J. M. 2009. The Ribosomal Database Project: improved alignments and new tools for rRNA analysis. *Nucleic Acids Research,* 37**,** D141-D145.

DITTMAR, T., KOCH, B., HERTKORN, N., KATTNER, G. 2008. A simple and efficient method for the solid-phase extraction of dissolved organic matter (SPE-DOM) from seawater. . *Limnology and Oceanography Methods,* 6**,** 230-235.

HERNDL, G. J., REINTHALER, T., TEIRA, E., VAN AKEN, H., VETH, C., PERNTHALER, A. & PERNTHALER, J. 2005. Contribution of Archaea to total prokaryotic production in the deep Atlantic Ocean. *Applied and Environmental Microbiology,* 71**,** 2303-2309.

HERZSPRUNG P, E. A. 2014. Understanding molecular formula assignment of Fourier transform ion cyclotron resonance mass spectrometry data of natural organic matter from a chemical point of view. *Analytical and Bioanalytical Chemistry,* 406**,** 7977-7987.

KOCH BP, D. T. 2006. From mass to structure: An aromaticity index for high-resolution mass data of natural organic matter. *Rapid Communications in Mass Spectrometry,* 20**,** 926-932.

KOCH BP, D. T. 2016. Erratum: From mass to structure: An aromaticity index for high-resolution mass data of natural organic matter *Rapid Communications in Mass Spectrometry,* 30**,** 250.

KOCH BP, D. T., WITT M, KATTNER G 2007. Fundamentals of Molecular Formula Assignment to Ultrahigh Resolution Mass Data of Natural Organic Matter. *Analytical Chemistry,* 79**,** 1758-1763.

LOY A, M. F., WAGNER M, HORN M 2007. probeBase - an online resource for rRNA-targeted oligonucleotide probes: new features 2007. *Nucleic Acids Res,* 35**,** 800-804.

MCNALLY, S. P., PARSONS, R. J., SANTORO, A. E. & APPRILL, A. 2017. Multifaceted impacts of the stony coral Porites astreoides on picoplankton abundance and community composition. *Limnology and Oceanography,* 62**,** 217-234.

MORRIS, R. M., CONNON, S. A., RAPPE, M., VERGIN, K. L., SIEBOLD, W. A., CARLSON, C. A. & GIOVANNONI, S. J. 2002. High cellular abundance of the SAR11 picoplankton clade in seawater. *Nature,* 420**,** 806-809.

MORRIS, R. M., VERGIN, K. L., CHO, J. C., RAPPE, M. S., CARLSON, C. A. & GIOVANNONI, S. J. 2005. Temporal and spatial response of bacterioplankton lineages to annual convective overturn at the Bermuda Atlantic Time-series Study site. *Limnology and Oceanography,* 50**,** 1687-1696.

PARSONS, R. J., BREITBART, M., LOMAS, M. W. & CARLSON, C. A. 2011a. Ocean time-series reveals recurring seasonal patterns of virioplankton dynamics in the northwestern Sargasso Sea. *ISME J,* 6**,** 273-84.

PARSONS, R. J., BREITBART, M., LOMAS, M. W. & CARLSON, C. A. 2011b. Ocean time-series reveals recurring seasonal patterns of virioplankton dynamics in the northwestern Sargasso Sea. *ISME J*.

PARSONS, R. J., NELSON, C. E., CARLSON, C. A., DENMAN, C. C., ANDERSSON, A. J., KLEDZIK, A. L., VERGIN, K. L., MCNALLY, S. P., TREUSCH, A. H. & GIOVANNONI, S. J. 2015. Marine bacterioplankton community turnover within seasonally hypoxic waters of a subtropical sound: Devil's Hole, Bermuda. *Environmental Microbiology,* 17**,** 3481-3499.

PORTER, K. G. & FEIG, Y. S. 1980. THE USE OF DAPI FOR IDENTIFYING AND COUNTING AQUATIC MICROFLORA. *Limnology and Oceanography,* 25**,** 943-948.

RICKER, W. E. 1973. Linear regressions in Fishery Research. *Journal of the Fisheries Research Board of Canada,* 30.

SIERACKI, M. E., VERITY, P. G. & STOECKER, D. K. 1993. Plankton Community Response to Sequential Silicate and Nitrate Depletion During the 1989 North Atlantic Spring Bloom. *Deep-Sea Research Part Ii-Topical Studies in Oceanography,* 40**,** 213-225.

TEIRA, E., REINTHALER, T., PERNTHALER, A., PERNTHALER, J. & HERNDL, G. J. 2004. Combining catalyzed reporter deposition-fluorescence in situ hybridization and microautoradiography to detect substrate utilization by bacteria and archaea in the deep ocean. *Applied and Environmental Microbiology,* 70**,** 4411-4414.

VAN KREVELEN, D. W. 1950. Graphical-Statistical Method for the Study of Structure and Reaction Processes of Coal. *Fuel,* 29**,** 228-269.

WRIGHT, S. W., JEFFREY, S. W., MANTOURA, F. C., LLEWELLYN, C. A., BJORNLAND, T., REPETA, D. AND WELSCHMEYER, N. 1991. Improved HPLC method for the analysis of chlorophylls and carotenoids from marine phytoplankton. *Marine Ecology Progress Series,* 77**,** 183-196.

ZHAO, Z., GONSIOR, M., LUEK, J., TIMKO, S., IANIRI, H., HERTKORN, N., SCHMITT-KOPPLIN, P., FANG, X. T., ZENG, Q. L., JIAO, N. Z. & CHEN, F. 2017. Picocyanobacteria and deep-ocean fluorescent dissolved organic matter share similar optical properties. *Nature Communications,* 8.

CHAPTER 3: The Role of Heterotrophic Bacteria and Archaea in the Transformation of Lignin in the Open Ocean

Abstract

The pelagic ocean receives terrigenous inputs of a range of organic compounds; however, the role that this terrigenous material plays in the ocean carbon cycle and biological pump is not entirely understood, and questions remain as to how oceanic cycles of terrigenous and autochthonous carbon interact. A significant portion of organic carbon that cannot be utilized by marine microbes in the epipelagic ocean escapes microbial remineralization to be sequestered in the deep ocean as refractory dissolved organic matter. Lignin, a 'model' terrigenous compound, is thought to be refractory in the open ocean unless chemically altered. However, in this study, incubation experiments performed using lignin-amended oligotrophic seawater from the Sargasso Sea exhibited bacteria and archaea growth that doubled compared to unamended control treatments. The increase in bacteria and archaea cell abundance in lignin-amended treatments coincided with a 21-25% decrease in absorbance (250 – 400 nm) of chromophoric dissolved organic matter (CDOM), suggesting that certain microbes may be capable of altering fractions of this ostensibly recalcitrant organic matter. Furthermore, the microbial response to the lignin-amended treatments appears to be taxon-specific. Two phyla of Archaea, Euryarchaeota and Thaumarchaeota exhibited an increase in abundance of 7 fold and 28 fold (from 2.42 x 10^6 cells L^{-1} to 1.72 x 10^7 cells L^{-1}, and from 1.60 x 10^6 cells L^{-1} to 4.54 x 10^7 cells L^{-1}, respectively), over four days of incubation in lignin-amended treatments. Additionally, an increase of 11 fold and 13 fold, (from 2.93 x 10^6 cells L^{-1} to 3.30 x 10^7 cells L^{-1}, and from 3.26 x 10^6 cells L^{-1} to 4.28 x 10^7 cells L^{-1}, respectively) was observed for abundance of these phyla in treatments containing lignin with added nitrogen and phosphorus, thus raising questions regarding primary and / or secondary responses to lignin degradation. Our findings indicate that marine bacteria and archaea play a role in the transformation of the optical properties of lignin in the open ocean and that they may serve as a potential sink for a portion of the lignin macromolecule.

Introduction

Dissolved organic matter (DOM) is an important component of many ocean biogeochemical cycles (Mopper et al., 2015, Hedges et al., 1997, Fasham et al., 2001) and can serve as a substrate for heterotrophic archaea and bacteria (Carlson et al., 2002, Cottrell and Kirchman, 2000).The majority of DOM in the open ocean is of marine origin (Carlson and Hansell, 2015, Koch et al., 2005); however, terrigenous inputs of compounds such as lignin may be important to the oceanic carbon cycle. Lignin, a cross-linked macromolecule, unique to woody vascular plants, has been used as a model compound and tracer of terrigenous carbon (Del Vecchio and Blough, 2004, Hernes and Benner, 2006). On the basis of measurements of lignin phenol concentrations, it has been shown that less than 2% of oceanic DOC is terrigenous (Hernes and Benner, 2006); yet, if estimates of annual riverine export to the ocean and atmospheric deposition of dissolved or water soluble organic carbon to the surface ocean are considered (~0.4 and ~0.65 Pg organic C, respectively), the concentrations of lignin phenols should be higher (Williams and Druffel, 1987, Hedges et al., 1997, Koch et al., 2005, Lavorivska et al.,

2016). This raises a number of questions about the transport and fate of terrigenous DOM in the open ocean.

Furthermore, a portion of DOM has been shown to be light-absorbing or chromophoric (CDOM), and is found ubiquitously throughout the global ocean. CDOM accounts for up to 50% of blue light absorption in the open ocean, thereby effectively regulating photosynthesis and influencing remote sensing algorithms used to predict primary production. Despite its impact on biogeochemical cycles, the composition and sources of CDOM in the open ocean remain largely unresolved. Dark microbial incubation studies have demonstrated that production of CDOM is positively correlated with an increase in bacterial cell abundance, providing evidence that CDOM is a byproduct of heterotrophic bacterial production (Nelson et al., 2004, Kinsey et al., 2017). The same studies also demonstrated that some fraction of CDOM is subsequently removed, presumably due to microbial remineralization. It is thought that the chemical composition and degradation rate of marine CDOM varies depending on the quality of the organic nutrient substrate available to bacterioplankton (Nelson et al., 2004). Lignin is also chromophoric, but its role in the pelagic CDOM pool is poorly understood. A number of studies have investigated the relationship between lignin and microbes in soil or riverine water, and suggest that some fraction of lignin is biologically available and that distinct microbial lineages under specific nutrient conditions are capable of degrading lignin (Hernes and Benner, 2003, Huang et al., 2013, Peng et al., 2008, Bugg et al., 2011). Additionally, recent genomics studies have shown a wide range of organisms with novel enzymes that have the potential to degrade lignin (Cragg et al., 2015, Janusz et al., 2017). However, the ability of microbial communities to utilize lignin in nutrient-depleted oceanic regions and the relationship to CDOM variability has not been fully investigated.

Here, we evaluate the response of the bacteria and archaea communities to lignin amended oligotrophic seawater from the Sargasso Sea to determine if specific lineages respond to lignin amended treatments and to assess whether terrigenous organic matter can serve as an intermediary in the production of autochthonous CDOM.

Methods and Materials

Sample collection

Samples were collected at the BATS site in the North Atlantic (31° 40’ N, 64° 10’ W) on board the *R/V Atlantic Explorer* in July, 2014. Water was collected from depths of 1 m and 60 m, using Niskin bottles on a rosette containing a conductivity, temperature and depth (CTD) sensor package. An inoculum of unfiltered “whole water” containing natural bacteria and archaea assemblages was added to grazer-diluted incubation media. Water samples for the incubation media were collected from 1 m depth, to ensure low background concentrations of CDOM as a result of photobleaching, low lignin concentrations due to photooxidation and low nutrients (Nelson et al., 2007, Hernes and Benner, 2006, Nelson et al., 2004). Seawater collected from 1 m depth was filtered through a 0.2 μm filter (Whatman Polycap AS) and 14-L aliquots were transferred into 20-L polycarbonate carboys (Nalgene, USA) that were pre-cleaned with 10% hydrochloric acid. Water for the inoculum was collected from a depth of 60 m (where

maximum bacterioplankton concentrations can typically be observed at BATS) (Bates and Johnson, 2016, Steinberg et al., 2001, Carlson and Ducklow, 1996), and 7 L of inoculum was added, unfiltered, to each carboy, thereby diluting the filtered surface seawater to 70% of the total volume (SI Table 1). This diluted seawater culture approach has been shown to alleviate grazing pressure by protistan grazers (Carlson et al., 2002, Carlson et al., 2004, Nelson et al., 2004). *In situ* concentrations of NO_3 and PO_4 were < 0.02 and < 0.03 μmol kg^{-1}, respectively, at both 1 m and 60 m depth (Steinberg et al., 2001); CDOM absorbance (325 nm) at 1 m was 0.075 m^{-1} and 0.155 m^{-1} at 60 m. Although *in situ* DOC concentrations were not measured on the cruise, TOC concentrations ranged from 67.1 μmol kg^{-1} at 60 m to 67.4 μmol kg^{-1} at the surface. Previous studies have indicated that DOC comprises the majority of TOC in the epipelagic zone at BATS and have evidenced DOC concentrations of ~68 μM from June to October (Carlson et al., 1998).

Nutrient amendments

Replicate incubations (n = 2) were performed in the dark and at the *in situ* temperature of the inoculum (23 °C). Seawater dilution cultures included unamended controls and treatments that included combination of organic and inorganic amendments (Table S1). The DOM amendments (shown in SI Table 1) included: 1) lignin (96% purity, alkali-extracted with low sulfonate content; Sigma Aldrich) (Lignin); 2) lignin with the addition of 1 μM ammonium chloride (99.998% trace metal basis; Sigma Aldrich) and 0.1 μM dipotassium phosphate (BioUltra anhydrous ≥ 99.0%; Sigma Aldrich) (LNP); or 3) glucose (D-(+)-Glucose ≥ 99.5% (Sigma Aldrich) with the addition of 1 μM ammonium chloride and 0.1 μM dipotassium phosphate (GNP). The inclusion of both GNP and LNP treatments in this study allowed for the direct comparison of microbial response to a model labile substrate compared with a complex terrigenous organic substrate. Commercial lignin was chosen according to previous work by Boyle, Blough et al., (2009). Concentrations of N and P were chosen to be similar to those used in previous work at the BATS site (Carlson et al., 2002). D-glucose was added to the carboys to obtain a final concentration of 10 μM C. The solution was prepared such that less than 20 mL of the aqueous glucose solution was added to the 20 L sample, and thus did not affect the ionic strength of the sample. A solution of lignin was prepared by the addition of solid lignin material to de-ionized water (MilliQ, Millipore, USA), with subsequent sonication and filtration (GF/F filters, Whatman, and a pre-rinsed 0.2 μm pore size track-etched polycarbonate filter, Whatman). The total organic carbon (TOC) content of the solution was determined according to Carlson et al. (2010) prior to inoculation and pipetted directly into the appropriate carboys to target a concentration of 10 μM C. Samples for bacteria and archaea cell abundance, DOC, CDOM, and fluorescent in situ hybridization (FISH) were drawn by spigot directly into sampling containers at discrete time intervals over a period of 35 days.

Determination of CDOM absorption coefficient

Changes in CDOM concentrations were determined by UV-Visible spectroscopy. Subsamples for each amendment were gravity filtered through a 0.2 μm filter (polycarbonate track-etched membrane filter; Whatman, Chicago, USA) that had been pre-flushed with 500 mL of de-ionized water and collected into muffled glass vials (I-

Chem, Thermo Scientific, MA, USA) fitted with PTFE-lined polypropylene caps. Samples were stored in the dark at 4 ºC until analysis. Absorbance measurements were made using a dual-beam spectrophotometer (Perkin Elmer Lambda-18), equipped with a photo-multiplier tube. Samples were analyzed in quartz cuvettes with a 10 cm pathlength and were blank corrected against de-ionized water. Blank-corrected spectra (250 to 700 nm) were reported as absorption coefficients (m^{-1}) using the equation:

$$a = 2.303A / l \quad (1)$$

where a is the absorption coefficient (m^{-1}), A is the absorbance and l is the pathlength (m). Absorbance values at discrete wavelengths in the near-UV spectrum (325 nm and 350 nm) were selected from individual spectra to measure changes in concentration and changes in CDOM components over time, particularly lignin (Hernes and Benner, 2003, Del Vecchio and Blough, 2004, Nelson et al., 2004).

Enumeration of Bacteria and Archaea cell abundance

Bacteria and archaea abundance samples (40 mL) were fixed with formalin (10% final concentration), and stored at -80 °C until slide preparation. Slides were prepared according to Parsons et al. (2015) and McNally et al. (2017.) Slides were then enumerated using an AX70 epifluorescence microscope (Olympus, Tokyo, Japan) under ultraviolet excitation at 1000X magnification. At least 500 cells per slide (10 fields) were counted for bacteria and archaea abundance.

Quantification of dissolved organic carbon

Dissolved organic carbon was sampled in duplicate and filtered through 0.7 μm pre-combusted glass fiber filters (Whatman, GF/F) into pre-combusted borosilicate glass vials (40 mL; I-Chem) fitted with acid-washed Teflon-lined caps and stored frozen at -20°C until analysis. All DOC samples were sent to the University of California for analysis. Samples were analyzed using high-temperature combustion on Shimadzu TOC-V analyzers, with slight modifications from the manufacturer model, as described in Carlson et al. (2010). In order to minimize the machine blanks, expansive conditioning of the combustion tube with repeated injections of low carbon water (LCW) as well as deep seawater was performed. A daily standardization of the system response was performed using a four-point standardization calibration curve of glucose solution in LCW. In-house surface and deep references were included in every analytical run in order to ensure comparability between sample sets. The in-house surface and deep references used in this study were collected from the Santa Barbara Channel in April 2014 and calibrated against consensus reference material (Hansell, 2005) and historical house reference materials. The average surface and deep reference values were 66.6 ± 0.9 and 38.0 ± 0.7, respectively. Further details of this method are described in Carlson et al. (1998) and (2010).

Enumeration of specific lineages by Fluorescence in situ Hybridization (FISH) and Catalyzed Reporter Deposition-FISH (CARD-FISH)

FISH was utilized to quantify the abundance of the major bacteria and archaea phylotypes present in the seawater. We followed the protocols described in Parsons et al.

(2015) and McNally et al. (2017) for all FISH and CARD-FISH. The FISH probes used for this study (Table S3) have previously been validated *in silico* for specificity using Probe Match on the Ribosomal Database Project (Cole et al., 2009) and TestProbe and Probebase on the SILVA website (Loy et al., 2007). The bacterial and archaeal groups quantified included the SAR11 clade (152R, 441R, 542R, 732R probes), *Alteromonas* spp. (AC137R), Flavobacteria II (CFB563R), Rhodobacteraceae (536R), SAR202 (103R, 311R), Euryarchaeota (Eury806), and Thaumarchaeota (Thaum537) (McNally et al., 2017).

Results

Bacteria and Archaea cell abundance

The cell abundance data show that in all treatments where lignin was added (Lignin or LNP), the microbial response was greater than that observed in the unamended Controls (Paired t-test for Control and Lignin ($p < 0.05$), and for Control and LNP ($p < 0.05$); Figure 1). The unamended Controls exhibited a 2.5 fold increase in bacteria and archaea cell abundance (from 1.875×10^8 cells $L^{-}1$ to 4.42×10^8 cells L^{-1}) between days 0 and 12. The treatments that were amended solely with commercial lignin showed an average increase in cell abundance of ~3 fold between days 0 and 5 (from 1.67×10^8 cells L^{-1} to 4.95×10^8 cells L^{-1}), after which the population remained relatively unchanged until day 12, when it increased by another 1.2 fold (to 6.59×10^8 cells L^{-1}). The treatments amended with lignin in addition to nitrogen and phosphorus (LNP) showed an average increase in cell abundance of 3 fold between days 0 and 5 (from 1.99×10^8 cells L^{-1} to 6.20×10^8 cells L^{-1}) and remained in stationary growth for the duration of the incubation. The glucose amendments with added nitrogen and phosphorus (GNP) demonstrated an increase in cell abundance (from 1.81×10^8 cells L^{-1} to 1.10×10^9 cells L^{-1}) between days 0 and 2, then approximated stationary growth through day 6 (at ~ 1.40×10^9 cells L^{-1}), after which cell densities declined through day 12.

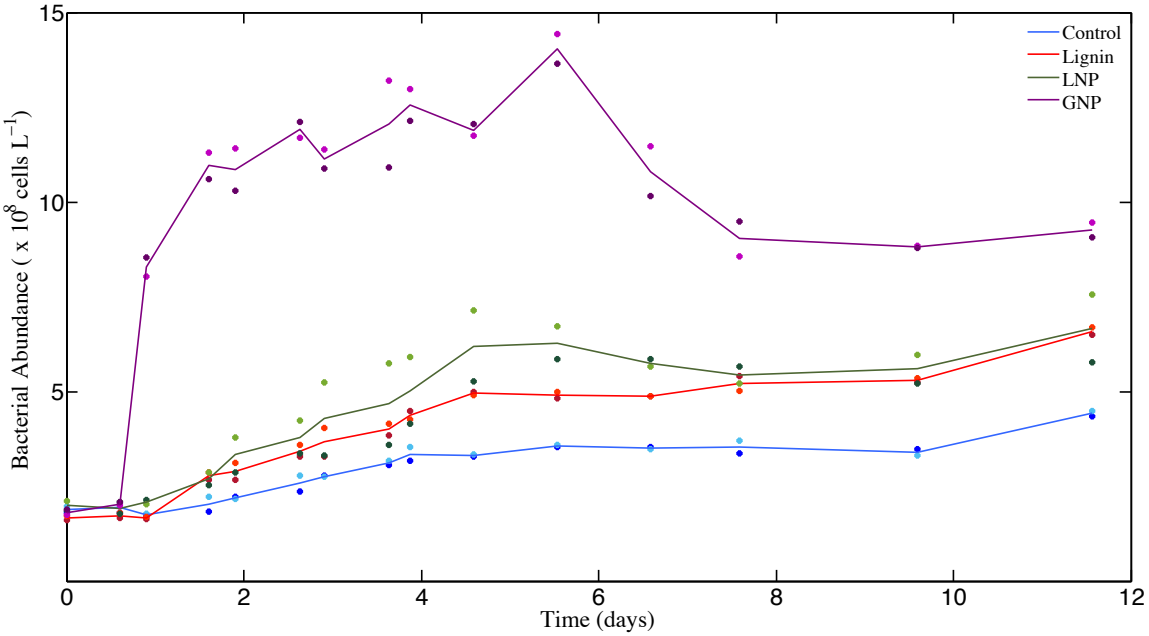

Figure 1. Bacterioplankton cell abundance (x 10^8 cells L^{-1}) over time (days). Solid lines represent the average of replicates for each of the four treatments: GNP, Lignin, LNP and un-amended controls. Individual datapoints, representing duplicates for each treatment are color-correlated with the plot of the respective mean.

Changes in CDOM absorbance

The absorbance of the unamended Control (absorption coefficient at 325 nm; m^{-1}) ranged from 0.098 m^{-1} at day 0 (T_0) to 0.134 m^{-1} at day 12 (T_{15}; Figure 2, top panel). In the GNP amendments, CDOM absorbance at 325 nm increased continuously over the first 3 days from 0.129 m^{-1} to 0.182 m^{-1}, then decreased to 0.123 m^{-1} by day 5 (T_9) (Figure 2, top panel) and remained relatively unchanged (paired t-test for T_9 and T_{14}, $p > 0.05$) for the remainder of the experiment (Figure 2). CDOM 325 nm absorption coefficients at the absorbance maximum in the GNP treatments were almost 70% higher than for Controls at the same time point. Both the Lignin and LNP amended samples exhibited a higher initial absorbance (between 250 – 450 nm) than the Controls at day 0 (T_0), due to the chromophoric nature of the amendments themselves (T_0 = 0.664 m^{-1} and 0.650 m^{-1}, respectively). Spectra (250-450 nm) of both Lignin and LNP amended samples (Figure 3, top and center panels, respectively) exhibited a discrete peak around 340 nm, attributed to the amendment of lignin, as well as a less pronounced shoulder between 260 – 280 nm. Both of these peaks decreased substantially between days 2 – 10, indicating a loss of absorbance at these wavelengths of approximately 30%, and resulting in spectra that resembled the shape of oceanic CDOM spectra (Figure 3, bottom panel). In both treatments, absorbance at 325 nm increased until day 2 (Figure 2, bottom panel), and then exhibited an almost 25% decrease in absorbance, falling below initial absorbance values (Figure 2, bottom panel). Both LNP and Lignin absorbance at 325 nm remained relatively unchanged from day 10 to 35 (paired t-tests, $p = 0.06$ and $p = 0.25$, respectively; Figure S1).

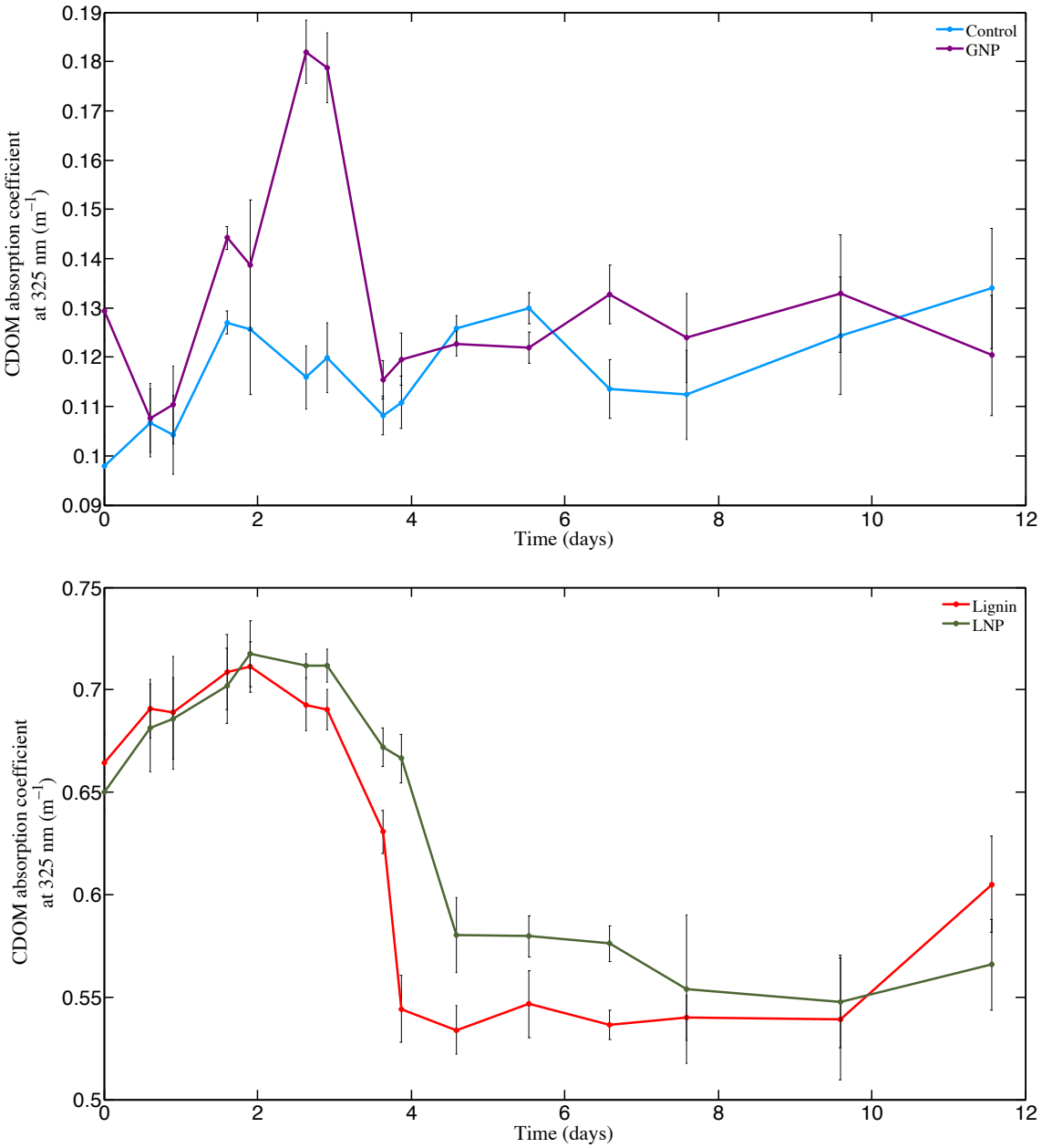

Figure 2. Changes in the CDOM absorption coefficient (m^{-1}) at 325 nm from day 0 through day 12 ($T_0 - T_{15}$) for (top panel) GNP (dark blue line with dots) and Control (light blue line with dots) and (bottom panel) Lignin and LNP treatments (red line and green line with dots, respectively).

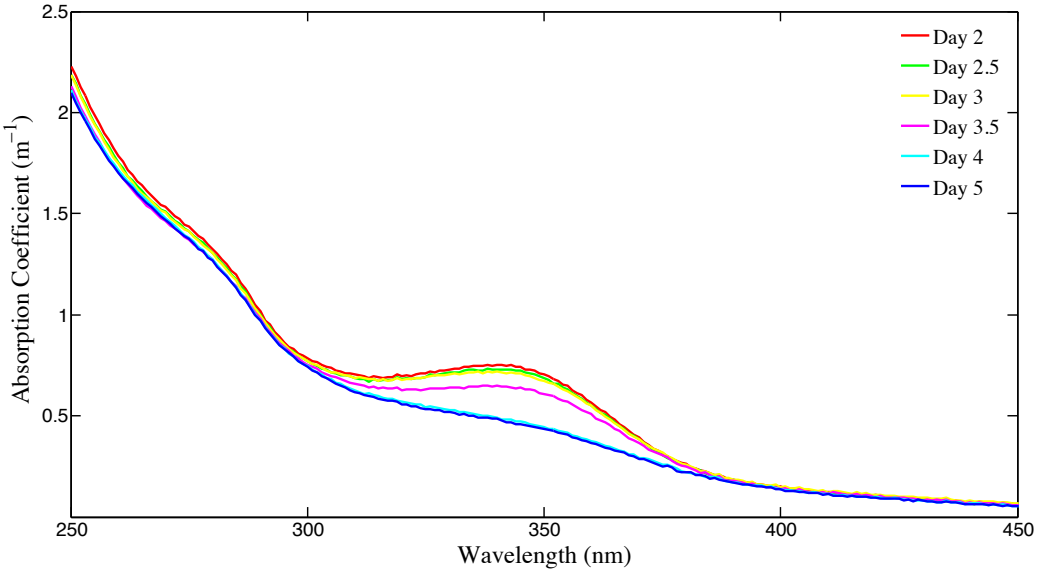
Day 2
Day 2.5
Day 3
Day 3.5
Day 4
Day 5
Absorption Coefficient (m^{-1})
Wavelength (nm)

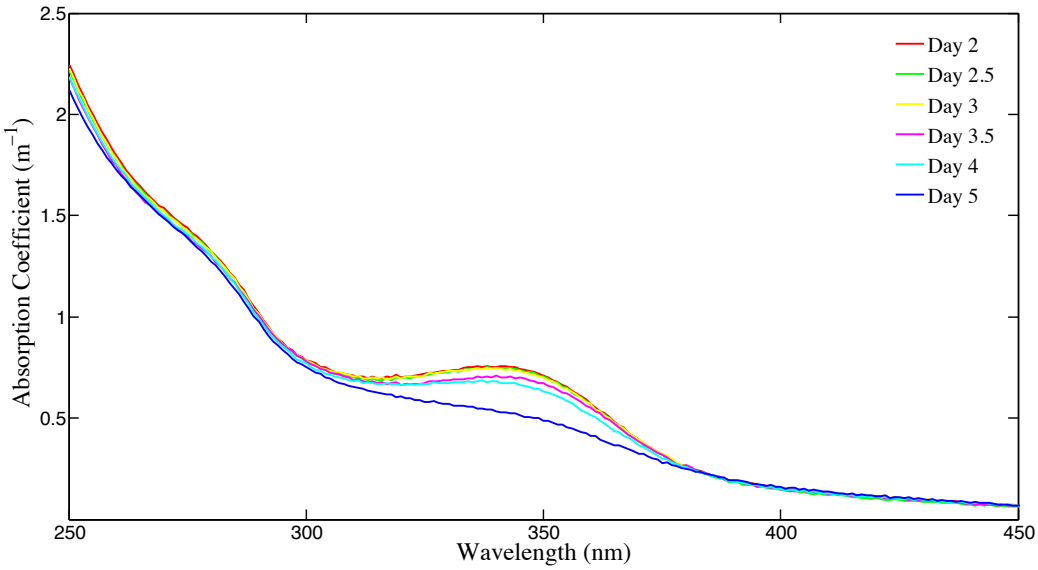
Day 2
Day 2.5
Day 3
Day 3.5
Day 4
Day 5
Absorption Coefficient (m^{-1})
Wavelength (nm)

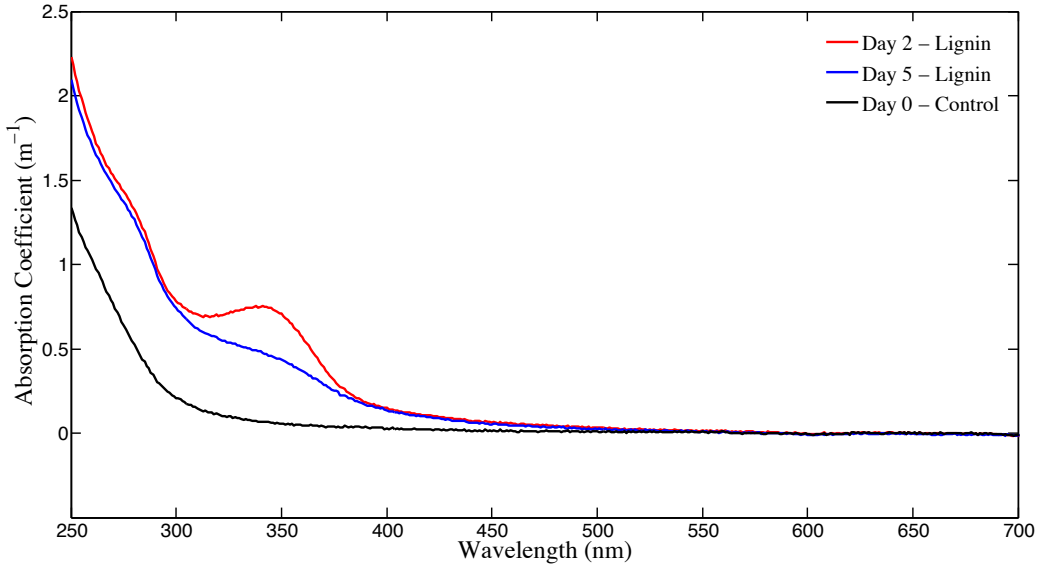
Day 2 – Lignin
Day 5 – Lignin
Day 0 – Control
Absorption Coefficient (m^{-1})
Wavelength (nm)

Figure 3. Top panel: CDOM absorption coefficient (m^{-1}) for the Lignin treatment (250 – 450 nm, for days 2 - 5 (T_4-T_9)). Center panel: CDOM absorption coefficient (m^{-1}) for the LNP treatment (250 – 450 nm, for days 2 - 5 (T_4-T_9)). Bottom panel: CDOM long-wavelength absorbance (250 – 700 nm; m^{-1}) for Lignin on days 2 and 5 (T_4 and T_9) and Control T_0 (day 0).

Dissolved organic carbon (DOC) utilization

DOC analysis confirmed an addition of ~10 µmol L^{-1} C to each of the Lignin, LNP, and GNP treatments, compared to the control at the time of inoculation (Control = 66.6 µmol L^{-1} C ± 1.2; Lignin = 78.2 µmol L^{-1} C ± 1.0; LNP = 78.2 µmol L^{-1} C ± 1.1; GNP = 77.6 µmol L^{-1} C ± 1.1.). There was no resolvable change in DOC throughout the incubation for either the unamended control or the LNP treatments. We observed a loss of ~ 4 µmol L^{-1} and 11 µmol L^{-1} in the Lignin and GNP treatments, respectively (Figure 4).

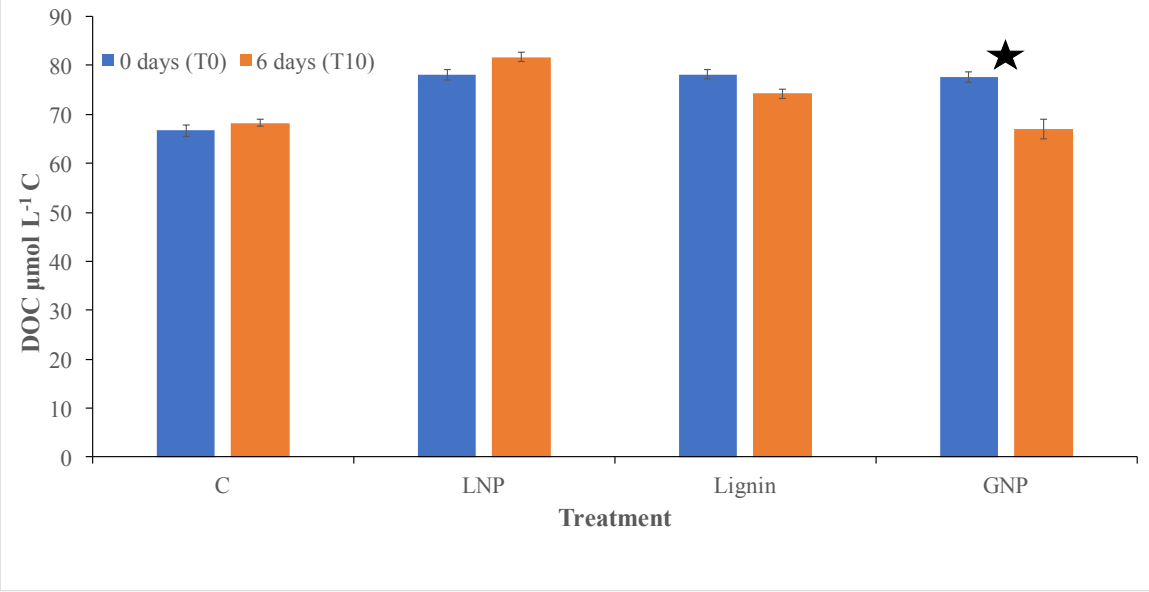

Figure 4. Dissolved organic carbon (DOC; µmol L^{-1} C) concentrations for all treatments and controls. DOC was measured at the initial time point (blue) and after 6 days (orange). Error is shown as standard deviation between replicate samples and treatments. The star indicates a significant change (two sample t-test assuming unequal variances) in DOC between the two time points.

Specific lineages measured using FISH and CARD-FISH

The initial microbial community (T_0) in all treatments was dominated by members of the SAR11 lineage, with cell abundances between 4.18 and 5.82 x 10^7 cells L^{-1}, while cell abundances of all other targeted groups were at least an order of magnitude lower (Figure Figure S2 A-D). In the unamended Control samples, SAR11 continued to increase throughout the incubation, reaching 1.61 x 10^8 cells L^{-1} by day 6 (T_{10}), with cell abundances still above 1 x 10^8 cells L^{-1} on day 10 (T_{13}; Figure 5, Figure S2 A). In

contrast, bacteria and archaea populations in the amended treatments shifted by day 4, and SAR11 abundance reached stasis, while other lineages increased (Figure S2 B-D). In the GNP treatments, *Alteromonas* spp increased from > 2 x 10^6 cells L^{-1} (T_0) to almost 9 x 10^8 cells L^{-1} by day 4, comprising 56.3% of the total microbial community (Figure 5B, Figure S2 B). The increase in *Alteromonas* was less pronounced in both lignin-amended samples (a net increase of 2.60 and 4.76 x 10^7 cells L^{-1}, respectively, compared to an increase of 8.87 x 10^8 cells L^{-1} in the GNP treatments), whereas Archaea became more pronounced in these treatments (Figure 5A, Figure S2 C-D). During days 0 through 4, the cell population of Thaumarchaeota increased from 1.60 x 10^6 cells L^{-1} to 4.54 x 10^7 cells L^{-1} (a factor of ~28) in the Lignin treatments and from 3.26 x 10^6 cells L^{-1} to 4.28 x 10^7 cells L^{-1} (a factor of ~13) in the LNP treatments. Over the same time period, Euryarchaeota increased from 2.42 x 10^6 cells L^{-1} to 1.72 x 10^7 cells L^{-1} (a factor of ~7) in the Lignin treatments and from 2.93 x 10^6 cells L^{-1} to 3.30 x 10^7 cells L^{-1} (a factor of ~11) in the LNP treatments (Figure 5A, Figure S2 C-D). In fact, Thaumarchaeota increased from 3.26 x 10^6 cells L^{-1} to 4.54 x 10^7 cells L^{-1} between days 0 and 4 (Figure S2 C). However, by day 6, Thaumarchaeota abunances in all lignin-amended treatments had decreased to approximately 2 x 10^7 cells L^{-1}. Euryarchaeota cell abundance decreased from 1.71 to 1.16 x 10^7 cells L^{-1} between days 4 and 6 in the Lignin treatments, and decreased from 3.30 x 10^7 cells L^{-1} to only 5.70 x 10^6 cells L^{-1} between days 4 and 6 in the LNP treatments (Figure S2 C-D). In the unamended Control treatments, the abundance of Thaumarchaeota and Euryarchaeota decreased by day 4 (a loss of 5.02 x 10^6 cells L^{-1} and 4.47 x 10^7 cells L^{-1}, respectively. Cell densities of Thaumarchaeota also decreased in the GNP treatments throughout the first 4 days (from 9.87 x 10^5 cells L^{-1} to 7.29 x 10^5 cells L^{-1}), while Euryarcheota cell abundances were low but exhibited an increase (from 8.65 x 10^5 cells L^{-1} to 1.41 x 10^6 cells L^{-1}) (Figure S2 A-B).

In addition to increases in Archaea, cell growth was observed for SAR202, which increased by between day 0 and day 4 for all amended samples (Figure 5, Figure S2 A-D). Cell densities of *Rhodobacteracea* in the unamended controls did not exceed an average of 1.55 x 10^7 cells L^{-1}; Figure 5A, but demonstrated a significant increase in cell abundance in all of the amended treatments (paired t-tests for growth between day 4 and 6 for each amendment, $p < 0.05$ for all tests; Figure S2 B-D). Cell growth was highest in the treatments with added inorganic nutrients (GNP = 1.30 x 10^8 cells L^{-1} and LNP = 1.08 x 10^8 cells L^{-1}, respectively, on day 6), whereas it only reached a maximum of 6.33 x 10^7 cells L^{-1} (on day 6) in the Lignin treatments. Notably, in all of the amended samples and the controls, the maximum growth for *Rhodobacteracea* did not occur until day 6. Additionally, growth of *Flavobacteriales* was investigated, but although it was detected at all time points for all treatments, in the lignin amended treatments, it reached a minimum on day 4, while like *Rhodobacteracea*, it reached a maximum on day 6.

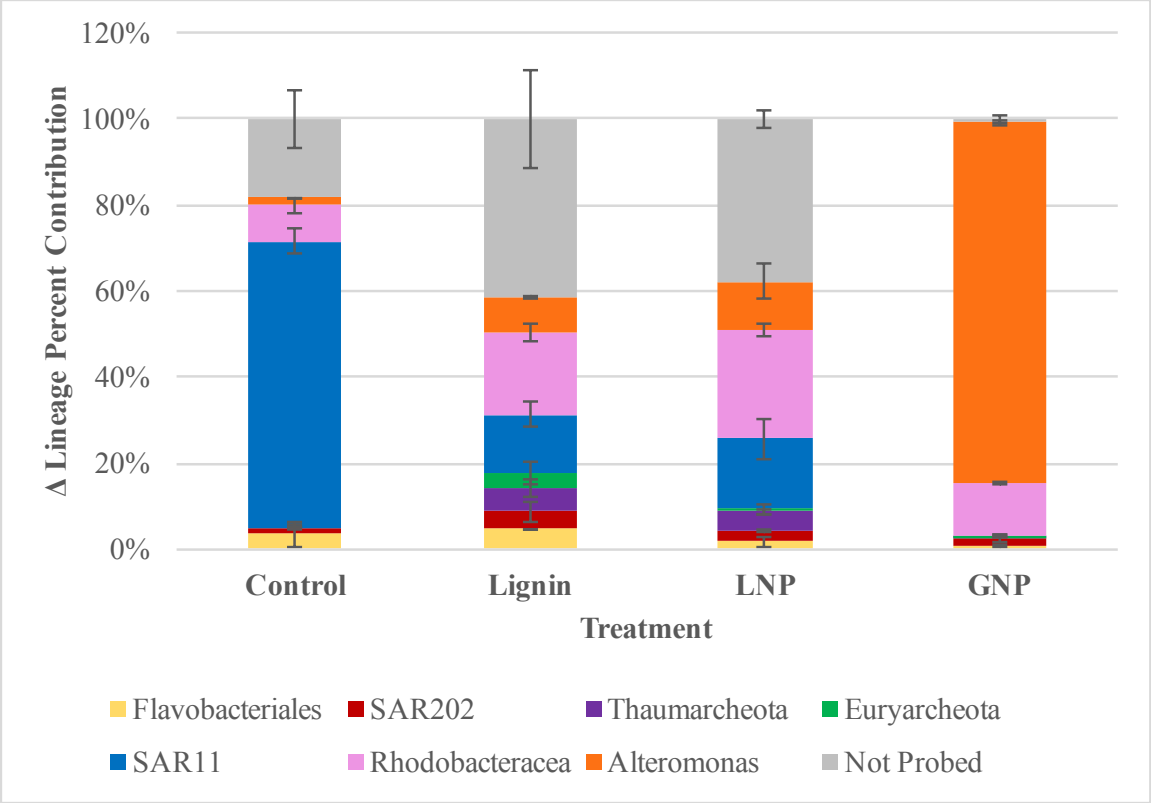
120%
100%
80%
60%
40%
20%
0%
Δ Lineage Percent Contribution
Control
Lignin
LNP
GNP
Treatment
Flavobacteriales
SAR202
Thaumarcheota
Euryarcheota
SAR11
Rhodobacteracea
Alteromonas
Not Probed

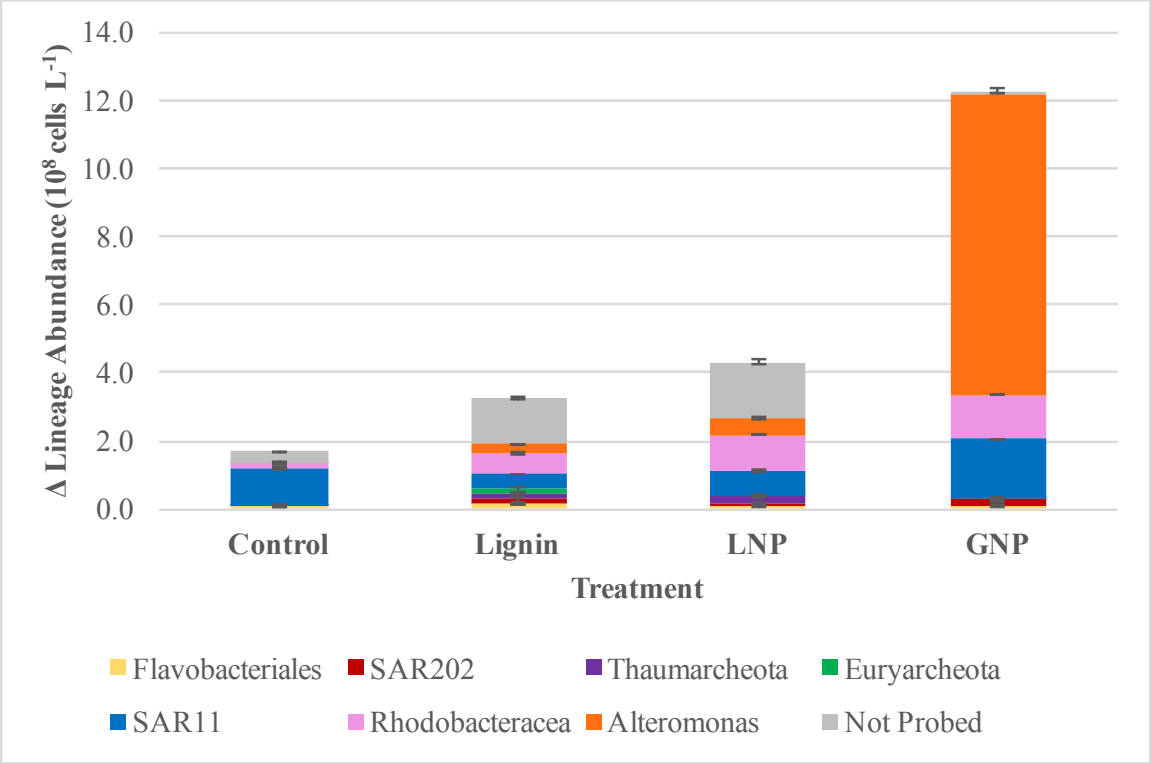
14.0
12.0
10.0
8.0
6.0
4.0
2.0
0.0
Δ Lineage Abundance (10^8 cells L^-1)
Control
Lignin
LNP
GNP
Treatment
Flavobacteriales
SAR202
Thaumarcheota
Euryarcheota
SAR11
Rhodobacteracea
Alteromonas
Not Probed

Figure 5. A) difference in percent contribution of specific lineages to the total prokaryote populations and B) difference in the cell abundance of targeted lineages in each of the four treatments (Control, GNP, Lignin, LNP) between days 0 and 6 (T_0 and T_{10}).

Discussion

Microbial growth and DOC utilization

The GNP amended treatments yielded the greatest growth response and coincident drawdown of DOC (Figures 4 and 5B) of all treatments, which is consistent with previous studies that have demonstrated that copiotrophic populations grow rapidly in the presence of a labile carbon source and available macronutrients (Carlson et al., 2002, Carlson et al., 2009, Nelson and Carlson, 2012, Carlson et al., 2004, Ewart et al., 2008, Goldberg et al., 2011). Microbial cell growth was also evidenced in the Lignin and LNP treatments (Figure 1), which suggests that some marine heterotrophs were able to utilize a portion of the added lignin; however, the question of which components of the lignin molecule were used remains unresolved. Unlike the GNP amendments, where DOC drawdown accounted for all of the added organic carbon, no significant DOC drawdown was observed in the Lignin or LNP amendments (Figure 4). However, DOC removal in the Lignin treatment was greater than that observed in the unamended control (Student's t-test, $p = 0.174$), where DOC removal was also not resolved. As the DOC measurements were not resolvable below the micromolar level, we cannot say definitively whether DOC was utilized in the Lignin and LNP treatments. However, the lignin amended dark incubations revealed greater prokaryote growth compared to the unamended controls, suggesting that marine heterotrophs were able to utilize a portion of the DOM in the lignin amended treatments to support anabolism. A such, we utilized CDOM measurements to further investigate changes in DOM.

Changes in CDOM absorbance

The microbial growth over the first few days, coincident with an increase in CDOM absorption at 325 nm in all amended samples (Figures 1 and 2), is consistent with the idea that as organic matter is remineralized by microbes, chromophoric byproducts are produced, either through direct release or by transformation of organic matter to a molecular structure with enhanced chromophoric properties (Stedmon and Nelson, 2015). While CDOM production in the GNP amendments was followed by a decrease in the 325 nm absorption coefficient to levels similar to those at T_0, (Figure 2, top panel; SI Table 2), the CDOM absorbance at 325 nm in the Lignin and LNP amendments decreased to values 20% lower than the T_0 values (Figure 2, bottom panel), further suggesting an alteration of chromophoric organic matter in the lignin amended treatments. Nevertheless, the final CDOM values between 250 – 450 nm in the Lignin and LNP treatments remained well above those of the unamended control (Figure 3), suggesting that portions of the lignin remained unaltered in these treatments. Absorbance measurements alone do not conclusively prove that microbial remineralization of the amended carbon took place in the incubated samples; however, a decrease in CDOM absorbance coincident with an increase in some lineages of bacteria and archaea in the lignin amended treatments does suggest that these microbes altered the chromophoric components of lignin throughout the incubation. Thaumarchaeota and Euryarchaeota, in

particular, reached maximum cell abundances in the Lignin and LNP treatments in conjunction with minimum CDOM 325 nm values (Figures 2 and 5). Specifically, there was a coinciding decrease in spectral absorbance at the lignin excitation maxima (~340 nm) (Figure 2, bottom panel; Figure 3, top panel and middle panel) as Thaumarchaeota cell abundance increased (Figure S2 C-D). The more pronounced growth of Euryarchaeota in the LNP treatment than in the Lignin treatment (2.91×10^7 cells L^{-1} vs. 1.27×10^7 cells $L^{-1,}$ respectively; Figure S2 C-D) may indicate the additional requirements of nitrogen and phosphorus for cell growth of this lineage. Furthermore, metagenomic analysis has revealed that Marine Group II Euryarcheota have protein degradation pathways (Orsi et al., 2016, Iverson et al., 2012) and may have a role in DON transformation.

The featureless absorption spectrum of CDOM in natural waters, which exhibits an exponential increase in absorbance with decreasing wavelength, has been the subject of much discussion, as it has been shown that this spectrum cannot be the result of the superposition of spectra of individual chromophores (Blough and Del Vecchio, 2002a, Del Vecchio and Blough, 2002, Del Vecchio and Blough, 2004), and it has been suggested that chemical alteration of chromophores must occur to produce the CDOM spectrum. Del Vecchio and Blough (2004, 2002) proposed that charge-transfer complexes formed from the partial oxidation of lignin precursors were responsible for the absorbance spectra in laboratory experiments using dissolved humic substances and that these complexes would be found in natural waters, where donor-acceptor complexes arise. Upon initial amendment of the incubations with lignin, a distinct absorbance peak was observed at ~340 nm (which is not observed in monthly *in situ* CDOM measurements at BATS), along with a broad "shoulder" between 265-280 nm (Figure 3, top and middle panels). However, as absorbance was measured over time, the enhanced absorbance at these wavelengths gradually decreased, resulting in a spectrum which more closely resembled the shape of the featureless 'textbook' CDOM spectrum, as described by Blough and Del Vecchio (2002b) and Nelson and Siegel (2002) (Figure 3, bottom panel). The timing of this CDOM transformation coincided with an increase in cell abundance and could indicate that microbes may play a previously unknown role in creating the charge-transfer complexes proposed to govern CDOM absorbance.

Taxon-specific microbial response

The taxa targeted by the probes used in this study have been found within the North Atlantic Subtropical Gyre, which is dominated by the oligotrophic alphaproteobacterium, SAR11, representing ~40% of the prokaryotic community in the euphotic zone (Morris et al., 2002b, Morris et al., 2002a). In the amended incubations, the absolute cell abundance of SAR11 was relatively constant over time (Figure S2 C-D), while several other lineages increased. Members of the SAR202 clade of marine bacteria exhibited a maximum increase in cell abundance (Figure 5, Figure S2 C-D) in the amended treatments at the same time when CDOM decreased. SAR202 have been estimated to account for ~30% of all bathypelagic plankton (Morris et al., 2004, Varela et al., 2008) and studies have shown that multiple SAR202 clade genomes encode families of enzymes such as flavin-dependent monooxygenases, enolases and ring-hydroxylating dioxygenases, that may allow for the degradation of recalcitrant organic matter (Landry et al, 2017; Liu et al.

submitted). As such, the ability of SAR202 to degrade lignin warrants further study. While maximum cell abundance was reached on day 4 for most of the targeted lineages, the copiotrophic alphaproteobacterium *Rhodobacteracea* exhibited maximum growth on day 6 in all treatments (Figure S2 A-D). The maxima for *Rhodobacteracea* occurred after CDOM had already decreased and therefore, it remains unclear if members of this lineage were consuming lignin directly or if they were utilizing byproducts of its remineralization. Members of *Rhodobacteracea* have been shown to comprise approximately 5% of the total bacterioplankton community within the surface 300 m of the Sargasso Sea (Parsons et al., 2011). However, in this study, *Rhodobacteracea* comprised up to 13% of the population in the Lignin amendment and 17% of the total population in the LNP amendment. The maximum cell abundance of *Rhodobacteracea* in the LNP treatments was almost double that in the Lignin treatments (Figure 5), and was comparable to the maximum observed for *Rhodobacteracea* in the GNP treatment (Figure 5). This presents the possibility that *Rhodobacteracea* growth was influenced by added N and P.

It is interesting to note that *Alteromonas* exhibited higher cell abundances in the LNP than the Lignin treatment (Figure 5 and S2 C-D), as *Alteromonas* is a copiotrophic organism, and has been shown to outcompete other species in the presence of labile carbon substrates, especially when nitrogen and phosphorus are not limited. Additionally, the added N and P in the LNP amended samples could account for the fact that *Alteromonas* cell abundance was almost double that in the Lignin treatment. Several possible mechanisms could account for its growth in the lignin amended samples. It is possible that *Alteromonas* was able to utilize the DOM that was originally present in the seawater before the carbon substrate was added. Conversely, labile breakdown products could have been generated by the degradation of lignin by other lineages, which *Alteromonas* was then able to utilize. Alternately, *Alteromonas* may be able to directly utilize a portion of the lignin macromolecule.

The growth of Thaumarchaeota in both lignin amended treatments is of particular interest, as this lineage is known for its demonstrated ability to oxidize ammonia and as such is largely known as a chemoautotroph (Konneke et al., 2005, Walker et al., 2010). However, it has also been shown to take up amino acids, and genes linked to the utilization of organic carbon have been identified in the same lineage of marine Archaea as that identified in our study, thus revealing the potential mixotrophic nature of this lineage (Varela et al., 2011, Hallam et al., 2006, Pester et al., 2011). It has been reported that approximately 60% of Archaea in samples collected from the Mediterranean and Pacific, including Marine GI Crenarchaeota-1 and Crenarchaeota-2, could uptake dissolved amino acids (Ouverney and Fuhrman, 2000). This study concluded that a portion of Crenarchaeota are heterotrophic and coexist with bacteria. Furthermore, a 2006 study of Crenarchaeota in the North Atlantic also demonstrated their ability to uptake amino acids, with certain lineages actively incorporating D- and L- aspartic acid (Teira et al., 2006). Notably, while the Crenarchaeota phylum has since been divided, creating the new Thaumarchaeota phylum, the oligonucleotide probe used by both Varela et al. (2011) and Teira et al. (2006) to identify Crenarchaeota (Cren537 [5 -

TGACCACTTGAGGTGCTG-3']) is the same as was used in the present study to detect Thaumarchaeota.

Proposed mechanisms of lignin degradation by Bacteria and Archaea
As a component of cell walls in vascular plants, lignin serves to protect plants from pathogens and is therefore naturally resistant to degradation from many types of microbes. The complex nature of the cross-linked lignin macromolecule, comprising of three phenolic monomers, creates a natural hindrance to radical decoupling and therefore can impede microbial degradation of the compound. While enzymatic breakdown of lignin has not previously been demonstrated for oceanic microbes, particularly archaea, two species of bacteria have been found to degrade lignin in marine pulp mill effluent (Gonzales et al., 1997), and there are groups of soil-associated bacteria, as well as many fungi (Tien and Kirk, 1984, Glenn and Gold, 1985, Glenn et al., 1983, Gong et al., 2014) that use peroxidases and laccases (Cragg et al., 2015) to degrade lignin. Although fungi typically utilize heme-based lignin peroxidase (LiP) or manganese peroxidase (MnP) to depolymerize lignin, the mechanisms for microbial degradation of lignin are less clear (Brown et al., 2011, Brown and Chang, 2014). It is interesting to note that archaeal ammonia monooxygenases belong to a family of copper-containing membrane-bound monooxygenases (CuMMOs) (Pester et al., 2011) and the ability of these enzymes to oxidize lignin into phenolic breakdown products has not yet been investigated.

Conclusions

This study provides evidence that transformation of terrigenous DOM in dark incubations by marine heterotrophs is taxon-specific, with some marine lineages of bacteria and archaea altering what were previously thought to be biologically recalcitrant carbon sources, on a timescale of days. Furthermore, these results indicate that in addition to the photochemical interactions speculated as being responsible for the distinct CDOM absorbance spectrum, that biologically-driven alterations of chromophores may occur. Additionally, this study demonstrates a clear growth response to added lignin by multiple bacteria and archaea lineages, including Thaumarchaeota, warranting further investigation as to whether this is a primary response consistent with previous evidence that Thaumarcheota is mixotrophic, or a secondary response to reduced remineralization byproducts of other organisms. These results also provide further insight into the mechanisms by which cycles of terrigenous and autochthonous DOM in the pelagic ocean are inter-connected. The subsequent *in situ* production of CDOM in lignin-amended incubations of marine heterotrophs suggests a cycle in which terrigenous and autochthonous CDOM are linked, with specific lineages of bacteria and archaea capable of transforming portions of lignin and then producing autochthonous CDOM. Because up to 25% of lignin remains undegraded by photolysis, and lignin has been detected in the bathypelagic region of the North Atlantic, questions remain about the role of microbial degradation in the deep ocean. It is increasingly evident that the chemical composition and optical properties of DOM are linked to microbial community composition, and that these factors play a large role in determining the lability and fate of organic carbon in the ocean. It is by better understanding these links that a more comprehensive view of DOM cycling in the ocean can be achieved.

Acknowledgements

We would like to thank Ellie Halewood and Keri Opalk for their valuable contributions and assistance with DOC analysis, as well as Dr. Rod Johnson and BATS technicians for facilitating at-sea sample collection and the captain and crew of the R/V Atlantic Explorer. This study was supported with funding from the Canadian Associates of BIOS (CABIOS), as well as from Simons Foundation International's BIOS-SCOPE program. Additionally, travel support was granted by Future Ocean.

References

BATES, N. R. & JOHNSON, R. J. 2016. Bermuda Atlantic Time Series (BATS) Bottle Data. http://www.bats.bios.edu/ Bermuda Institute of Ocean Sciences.

BLOUGH, N. V. & DEL VECCHIO, R. 2002a. *In:* HANSELL, D. & CARLSON, C. (eds.) *Biogeochemistry of Marine Dissolved Organic Matter.* San Diego: Academic Press.

BLOUGH, N. V. & DEL VECCHIO, R. 2002b. Chromophoric DOM in the Coastal Environment. *In:* HANSELL, D. A. C., C. (ed.) *Biogeochemistry of Marine Dissolved Organic Matter.* Academic Press.

BOYLE, E. S., GUERRIERO, N., THIALLET, A., DEL VECCHIO, R. & BLOUGH, N. V. 2009. Optical Properties of Humic Substances and CDOM: Relation to Structure. *Environmental Science & Technology,* 43**,** 2262-2268.

BROWN, M. E. & CHANG, M. C. Y. 2014. Exploring bacterial lignin degradation. *Current Opinion in Chemical Biology,* 19**,** 1-7.

BROWN, M. E., WALKER, M. C., NAKASHIGE, T. G. & CHANG, M. C. 2011. Discovery and Characterization of Heme Enzymes from Unsequenced Bacteria: Application to Microbial Lignin Degradation. *Journal of the American Chemical Society,* 133**,** 18006-9.

BUGG, T. D. H., AHMAD, M., HARDIMAN, E. M. & RAHMANPOUR, R. 2011. Pathways for degradation of lignin in bacteria and fungi. *Natural Product Reports,* 28**,** 1883-1896.

CARLSON, C. & HANSELL, D. 2015. DOC Sources, Sinks, Reactivity, and Budgets. *In:* HANSELL, D. & CARLSON, C. (eds.) *Biogeochemistry of Marine Dissolved Organic Matter, 2nd Edition.* USA: Academic Press.

CARLSON, C. A. & DUCKLOW, H. W. 1996. Growth of bacterioplankton and consumption of dissolved organic carbon in the Sargasso Sea. *Aquatic Microbial Ecology,* 10**,** 69-85.

CARLSON, C. A., DUCKLOW, H. W., HANSELL, D. A. & SMITH, W. O. 1998. Organic carbon partitioning during spring phytoplankton blooms in the Ross Sea polynya and the Sargasso Sea. *Limnology and Oceanography,* 43**,** 375-386.

CARLSON, C. A., GIOVANNONI, S. J., HANSELL, D. A., GOLDBERG, S. J., PARSONS, R., OTERO, M. P., VERGIN, K. & WHEELER, B. R. 2002. Effect of nutrient amendments on bacterioplankton production, community structure,

and DOC utilization in the northwestern Sargasso Sea. *Aquatic Microbial Ecology,* 30**,** 19-36.

CARLSON, C. A., GIOVANNONI, S. J., HANSELL, D. A., GOLDBERG, S. J., PARSONS, R. & VERGIN, K. 2004. Interactions among dissolved organic carbon, microbial processes, and community structure in the mesopelagic zone of the northwestern Sargasso Sea. *Limnology and Oceanography,* 49**,** 1073-1083.

CARLSON, C. A., HANSELL, D. A., NELSON, N. B., SIEGEL, D. A., SMETHIE, W. M., KHATIWALA, S., MEYERS, M. M. & HALEWOOD, E. 2010. Dissolved organic carbon export and subsequent remineralization in the mesopelagic and bathypelagic realms of the North Atlantic basin. *Deep-Sea Research Part Ii-Topical Studies in Oceanography,* 57**,** 1433-1445.

CARLSON, C. A., MORRIS, R., PARSONS, R., GIOVANNONI, S. J. & VERGIN, K. 2009. Seasonal dynamics of SAR11 populations in the euphotic and mesopelagic zones of the northwestern Sargasso Sea. *ISME Journal,* 3**,** 283-295.

COLE, J. R., WANG, Q., CARDENAS, E., FISH, J., CHAI, B., FARRIS, R. J., KULAM-SYED-MOHIDEEN, A. S., MCGARRELL, D. M., MARSH, T., GARRITY, G. M. & TIEDJE, J. M. 2009. The Ribosomal Database Project: improved alignments and new tools for rRNA analysis. *Nucleic Acids Research,* 37**,** D141-D145.

COTTRELL, M. T. & KIRCHMAN, D. L. 2000. Natural assemblages of marine proteobacteria and members of the Cytophaga-Flavobacter cluster consuming low and high molecular weight dissolved organic matter. *Applied and Environmental Microbiology,* 66**,** 1692-1697.

CRAGG, S. M., BECKHAM, G. T., BRUCE, N. C., BUGG, T. D. H., DISTEL, D. L., DUPREE, P., ETXABE, A. G., GOODELL, B. S., JELLISON, J., MCGEEHAN, J. E., MCQUEEN-MASON, S. J., SCHNORR, K., WALTON, P. H., WATTS, J. E. M. & ZIMMER, M. 2015. Lignocellulose degradation mechanisms across the Tree of Life. *Current Opinion in Chemical Biology,* 29**,** 108-119.

DEL VECCHIO, R. & BLOUGH, N. V. 2002. Photobleaching of chromophoric dissolved organic matter in natural waters: kinetics and modeling. *Marine Chemistry,* 78**,** 231-253.

DEL VECCHIO, R. & BLOUGH, N. V. 2004. On the origin of the optical properties of humic substances. *Environmental Science & Technology,* 38**,** 3885-3891.

EWART, C. S., MEYERS, M. K., WALLNER, E. R., MCGILLICUDDY, D. J. & CARLSON, C. A. 2008. Microbial dynamics in cyclonic and anticyclonic mode-water eddies in the northwestern Sargasso Sea. *Deep-Sea Research Part Ii-Topical Studies in Oceanography,* 55**,** 1334-1347.

FASHAM, M. J. R., BALINO, B. M., BOWLES, M. C., ANDERSON, R., ARCHER, D., BATHMANN, U., BOYD, P., BUESSELER, K., BURKILL, P., BYCHKOV, A., CARLSON, C., CHEN, C. T. A., DONEY, S., DUCKLOW, H., EMERSON, S., FEELY, R., FELDMAN, G., GARCON, V., HANSELL, D., HANSON, R., HARRISON, P., HONJO, S., JEANDEL, C., KARL, D., LE BORGNE, R., LIU, K. K., LOCHTE, K., LOUANCHI, F., LOWRY, R., MICHAELS, A., MONFRAY, P., MURRAY, J., OSCHLIES, A., PLATT, T., PRIDDLE, J., QUINONES, R., RUIZ-PINO, D., SAINO, T., SAKSHAUG, E., SHIMMIELD, G., SMITH, S., SMITH, W., TAKAHASHI, T., TREGUER, P., WALLACE, D.,

WANNINKHOF, R., WATSON, A., WILLEBRAND, J. & WONG, C. S. 2001. A new vision of ocean biogeochemistry after a decade of the Joint Global Ocean Flux Study (JGOFS). *Ambio*, 4-31.

GLENN, J. K. & GOLD, M. H. 1985. Purification and Chracterization of an Extracellular Mn(II)-Dependent Peroxidase from the Lignin-Degrading Basidomycete, *Phanerochaete Chrysosporium*. *Archives of Biochemistry and Biophysics,* 242, 329-341.

GLENN, J. K., MORGAN, M. A., MAYFIELD, M. B., KUWAHARA, M. & GOLD, M. H. 1983. AN EXTRACELLULAR H2O2-REQUIRING ENZYME PREPARATION INVOLVED IN LIGNIN BIODEGRADATION BY THE WHITE ROT BASIDIOMYCETE PHANEROCHAETE-CHRYSOSPORIUM. *Biochemical and Biophysical Research Communications,* 114, 1077-1083.

GOLDBERG, S. J., CARLSON, C. A., BRZEZINSKI, M., NELSON, N. B. & SIEGEL, D. A. 2011. Systematic removal of neutral sugars within dissolved organic matter across ocean basins. *Geophysical Research Letters,* 38.

GONG, G., WOO, H. M., UM, Y. & PARK, T. H. 2014. Lignin utilization by Bacillus sp. associated with the growth enhancement and the molecular weight distribution change of lignin. *New Biotechnology,* 31, S102-S102.

GONZALES, J. M., MAYER, F., MORAN, M. A., HODSON, R. E. & WHITMAN, W. B. 1997. *Microbulbifer hydrolyticus* gen. nov., sp. nov., and *Marinobacterium georgiense* gen. nov., sp. nov., Two Marine Bacteria from a Lignin-Rich Pulp Mill Waste Enrichment Community. *International Journal of Systematic Bacteriology,* 47, 369-376.

HALLAM, S. J., MINCER, T. J., SCHLEPER, C., PRESTON, C. M., ROBERTS, K., RICHARDSON, P. M. & DELONG, E. F. 2006. Pathways of carbon assimilation and ammonia oxidation suggested by environmental genomic analyses of marine crenarchaeota. *PLoS Biology*.

HANSELL, D. 2005. Dissolved organic carbon reference material program. *EOS Trans. Amer. Geophys. Union,* 86, 318.

HEDGES, J. I., KEIL, R. G. & BENNER, R. 1997. What happens to terrestrial organic matter in the ocean? *Organic Geochemistry,* 27, 195-212.

HERNES, P. J. & BENNER, R. 2003. Photochemical and microbial degradation of dissolved lignin phenols: Implications for the fate of terrigenous dissolved organic matter in marine environments. *Journal of Geophysical Research-Oceans,* 108.

HERNES, P. J. & BENNER, R. 2006. Terrigenous organic matter sources and reactivity in the North Atlantic Ocean and a comparison to the Arctic and Pacific oceans. *Marine Chemistry,* 100, 66-79.

HUANG, X. F., SANTHANAM, N., BADRI, D. V., HUNTER, W. J., MANTER, D. K., DECKER, S. R., VIVANCO, J. M. & REARDON, K. F. 2013. Isolation and characterization of lignin-degrading bacteria from rainforest soils. *Biotechnol Bioeng,* 110, 1616-26.

IVERSON, V., MORRIS, R. M., FRAZAR, C. D., BERTHIAUME, C. T., MORALES, R. L. & ARMBRUST, E. V. 2012. Untangling genomes from metagenomes: revealing an uncultured class of marine Euryarchaeota. *Science,* 335, 587-590.

JANUSZ, G., PAWLIK, A., SULEJ, J., ŚWIDERSKA-BUREK, U., JAROSZ-WILKOŁAZKA, A. & PASZCZYŃSKI, A. 2017. Lignin degradation:

microorganisms, enzymes involved, genomes analysis and evolution. *FEMS Microbiology Reviews,* 41**,** 941-962.
KINSEY, J., CORRADINO, G., ZIERVOGEL, K., SCHNETZER, A. & OSBURN, C. 2017. Formation of Chromophoric Dissolved Organic Matter by Bacterial Degradation of Phytoplankton-Derived Aggregates. *Frontiers in Marine Science,* 4:430.
KOCH, B. P., WITT, M. R., ENGBRODT, R., DITTMAR, T. & KATTNER, G. 2005. Molecular formulae of marine and terrigenous dissolved organic matter detected by electrospray ionization Fourier transform ion cyclotron resonance mass spectrometry. *Geochimica Et Cosmochimica Acta,* 69**,** 3299-3308.
KONNEKE, M., A.E., B., DE LA TORRE, J. R., WALKER, C. B., WATERBURY, J. B. & STAHL, D. A. 2005. Isolation of an autotrophic ammonia-oxidizing marine archaeon. *Nature,* 437**,** 543-546.
LAVORIVSKA, L., BOYER, E. W. & DEWALLE, D. R. 2016. Atmospheric deposition of organic carbon via precipitation. *Atmospheric Environment,* 146**,** 153-163.
LOY, A., MAIXNER, F., WAGNER, M. & HORN, M. 2007. probeBase - an online resource for rRNA-targeted oligonucleotide probes: new features 2007. *Nucleic Acids Research,* 35**,** D800-D804.
MCNALLY, S. P., PARSONS, R. J., SANTORO, A. E. & APPRILL, A. 2017. Multifaceted impacts of the stony coral Porites astreoides on picoplankton abundance and community composition. *Limnology and Oceanography,* 62**,** 217-234.
MOPPER, K., KIEBER, D. J. & STUBBINS, A. 2015. Marine Photochemistry of Organic Matter. *In:* HANSELL, D. & CARLSON, C. (eds.) *Biogeochemistry of Dissolved Organic Matter, 2nd Edition.* San Diego: Academic Press.
MORRIS, R. M., CONNON, S. A., RAPPE, M., VERGIN, K. L., SIEBOLD, W. A., CARLSON, C. A. & GIOVANNONI, S. J. 2002a. High cellular abundance of the SAR11 picoplankton clade in seawater. *Nature,* 420**,** 806-809.
MORRIS, R. M., RAPPE, M., E., U., CONNON, S. A. & GIOVANNONI, S. J. 2004. Prevalence of the Chloroflexi-related SAR202 bacterioplankton cluster throughout the mesopelagic zone and deep ocean. *Applied and Environmental Microbiology,* 70**,** 2836-2842.
MORRIS, R. M., RAPPE, M. S., CONNON, S. A., VERGIN, K. L., SIEBOLD, W. A., CARLSON, C. A. & GIOVANNONI, S. J. 2002b. SAR11 clade dominates ocean surface bacterioplankton communities. *Nature,* 420**,** 806-810.
NELSON, C. E. & CARLSON, C. A. 2012. Tracking differential incorporation of dissolved organic carbon types among diverse lineages of Sargasso Sea bacterioplankton. *Environmental Microbiology,* 14**,** 1500-1516.
NELSON, N. B., CARLSON, C. A. & STEINBERG, D. K. 2004. Production of chromophoric dissolved organic matter by Sargasso Sea microbes. *Marine Chemistry,* 89**,** 273-287.
NELSON, N. B. & SIEGEL, D. A. 2002. Chromophoric DOM in the Open Ocean. *In:* HANSELL, D. A. C., C. (ed.) *Biogeochemistry of Marine Dissolved Organic Matter.* Academic Press.
NELSON, N. B., SIEGEL, D. A., CARLSON, C. A., SWAN, C., SMETHIE, W. M. & KHATIWALA, S. 2007. Hydrography of chromophoric dissolved organic matter

in the North Atlantic. *Deep-Sea Research Part I-Oceanographic Research Papers,* 54**,** 710-731.

ORSI, W. D., SMITH, J. M., LIU, S., LIU, Z., SAKAMOTO, C. M., WILKEN, S., POIRIER, C., RICHARDS, T. A., KEELING, P. J., WORDEN, A. Z. & SANTORO, A. E. 2016. Diverse, uncultivated bacteria and archaea underlying the cycling of dissolved protein in the ocean. *ISME J,* 10**,** 2158-73.

OUVERNEY, C. & FUHRMAN, J. 2000. Marine Planktonic Archaea Take Up Amino Acids. *Applied and Environmental Microbiology,* 66**,** 4829-4833.

PARSONS, R. J., BREITBART, M., LOMAS, M. W. & CARLSON, C. A. 2011. Ocean time-series reveals recurring seasonal patterns of virioplankton dynamics in the northwestern Sargasso Sea. *The ISME Journal,* 2011**,** 1-12.

PARSONS, R. J., NELSON, C. E., CARLSON, C. A., DENMAN, C. C., ANDERSSON, A. J., KLEDZIK, A. L., VERGIN, K. L., MCNALLY, S. P., TREUSCH, A. H. & GIOVANNONI, S. J. 2015. Marine bacterioplankton community turnover within seasonally hypoxic waters of a subtropical sound: Devil's Hole, Bermuda. *Environmental Microbiology,* 17**,** 3481-3499.

PENG, R. H., XIONG, A. S., XUE, Y., FU, X. Y., GAO, F., ZHAO, W., TIAN, Y. S. & YAO, Q. H. 2008. Microbial biodegradation of polyaromatic hydrocarbons. *FEMS Microbiol Rev,* 32**,** 927-55.

PESTER, M., SCHLEPER, C. & WAGNER, M. 2011. The Thaumarchaeota: an emrging view of their phylogeny and ecophysiology. *Current Opinion in Microiology,* 14**,** 300-306.

PORTER, K. G. & FEIG, Y. S. 1980. THE USE OF DAPI FOR IDENTIFYING AND COUNTING AQUATIC MICROFLORA. *Limnology and Oceanography,* 25**,** 943-948.

STEDMON, C. A. & NELSON, N. B. 2015. The Optical Properties of DOM in the Ocean. *In:* HANSELL, D. A. C., C. (ed.) *Bioegeochemistry of Marine Dissolved Organic Matter* San Diego: Academic Press.

STEINBERG, D. K., CARLSON, C. A., BATES, N., JOHNSON R. J., F., M. A. & KNAP, A. H. 2001. Overview of the US JGOFS Bermuda Atlantic Time-series Study (BATS): a decade-scale look at ocean biology and biogeochemistry. *deep-Sea Research II,* 48**,** 1405-1447.

TEIRA, E., VAN AKEN, H., VETH, C. & HERNDL, G. J. 2006. Archaeal uptake of enantiomeric amino acids in the meso- and bathypelagic waters of the North Atlantic. *Limnology and Oceanography,* 51**,** 60-69.

TIEN, M. & KIRK, T. 1984. Lignin-Degrading Enzyme from *Phanerochaete Chrysosporium*: Purification, Characterization, and Catalytic Properties of a Unique H2O2-Requiring Oxygenase. *Proceedings of the National Academy of Sciences of the United States of America,* 81**,** 2280-2284.

VARELA, M. M., VAN AKEN, H. M. & HERNDL, G. J. 2008. Abundance and activity of Chloroflexi-type SAR202 bacterioplankton in the meso- and bathypleagic waters of the (sub)tropical Atlantic. *Environmental Microbiology,* 10**,** 1903-1911.

VARELA, M. M., VAN AKEN, H. M., SINTES, E., REINTHALER, T. & HERNDL, G. J. 2011. Contribution of Crenarchaeota and Bacteria to autotrophy in the North Atlantic interior. *Environmental Microbiology,* 13**,** 1524-1533.

WAGGONER, D. C., CHEN, H. M., WILLOUGHBY, A. S. & HATCHER, P. G. 2015. Formation of black carbon-like and alicyclic aliphatic compounds by hydroxyl radical initiated degradation of lignin. *Organic Geochemistry,* 82**,** 69-76.

WALKER, C. B., JR, D. L. T., MG, K., H, U., N, P., DJ, A., C, B.-A., PS, C., PP, C., A, G., J, H., M, H., EA, K., M, K., M, S., TJ, L., T, L., W, M.-H., LA, S.-S., D, L., SM, S., AC, R., G, M. & DA., S. 2010. Nitrosopumilus maritimus genome reveals unique mechanisms for nitrification and autotrophy in globally distributed marine crenarchaea. *Proceedings of the National Academy of Sciences of the United States of America,* 107**,** 8818-23.

WILLIAMS, P. M. & DRUFFEL, E. R. M. 1987. RADIOCARBON IN DISSOLVED ORGANIC-MATTER IN THE CENTRAL NORTH PACIFIC-OCEAN. *Nature,* 330**,** 246-248.

Supplemental Information for Chapter 3

Sample #	Sample ID	Depth and Sample Mix Ratio	Amendments
1a and 1b	C1; C2	70:30 mix of 0.2 μm filtered 1 m seawater and unfiltered water from 60 m.	Unamended control
2a and 2b	L1; L2	70:30 mix of 0.2 μm filtered 1 m seawater and unfiltered water from 60 m.	Lignin (10 μmol L^{-1} carbon)
3a and 3b	LNP1; LNP2	70:30 mix of 0.2 μm filtered 1 m seawater and unfiltered water from 60 m.	Lignin (10 μmol L^{-1} carbon) Ammonium chloride (1 μmol L^{-1}) Dipotassium phosphate (0.1 μmol L^{-1})
4a and 4b	GNP1; GNP2	70:30 mix of 0.2 μm filtered 1 m seawater and unfiltered water from 60 m.	Glucose (10 μmol L^{-1} carbon), Ammonium chloride (1 μmol L^{-1}) Dipotassium phosphate (0.1 μmol L^{-1})

Table S1. A description of the samples, their identification, the composition of seawater used and how each incubation was amended.

Table S2. Bacterioplankton abundance (Cells mL^{-1}) averages and standard deviation for all time points (with time also indicated in days). Averages were calculated from replicate counts (n = 10).

Time Point	T0	T1	T2	T3	T4	T5	T6	T7
Days	0.0	0.6	0.9	1.6	1.91	2.63	2.91	3.63
Average								
C1	1.79E+05	1.80E+05	1.71E+05	1.82E+05	2.23E+05	2.36E+05	2.79E+05	3.07E+05
C2	1.96E+05	2.09E+05	1.77E+05	2.23E+05	2.16E+05	2.79E+05	2.74E+05	3.16E+05
L1	1.62E+05	1.65E+05	1.63E+05	2.68E+05	2.68E+05	3.28E+05	3.29E+05	3.84E+05
L2	1.72E+05	1.79E+05	1.69E+05	2.86E+05	3.12E+05	3.58E+05	4.03E+05	4.16E+05
LNP1	1.87E+05	1.78E+05	2.14E+05	2.53E+05	2.87E+05	3.36E+05	3.32E+05	3.59E+05
LNP2	2.10E+05	2.07E+05	2.02E+05	2.85E+05	3.79E+05	4.23E+05	5.23E+05	5.75E+05
GNP1	1.74E+05	1.99E+05	8.03E+05	1.13E+06	1.14E+06	1.17E+06	1.14E+06	1.32E+06
GNP2	1.88E+05	2.07E+05	8.53E+05	1.06E+06	1.03E+06	1.21E+06	1.09E+06	1.09E+06
Std Dev								
C1	1.07E+04	1.43E+04	1.87E+04	2.36E+04	2.09E+04	2.30E+04	4.27E+04	4.62E+04
C2	2.08E+04	1.73E+04	2.08E+04	2.10E+04	1.94E+04	2.71E+04	3.90E+04	4.06E+04
L1	1.49E+04	1.29E+04	1.48E+04	2.30E+04	3.78E+04	2.88E+04	2.71E+04	4.93E+04
L2	1.51E+04	1.53E+04	2.28E+04	4.77E+04	3.87E+04	2.44E+04	4.44E+04	6.36E+04
LNP1	1.81E+04	1.59E+04	2.97E+04	2.17E+04	2.80E+04	2.54E+04	2.86E+04	4.36E+04
LNP2	1.41E+04	2.01E+04	1.62E+04	2.93E+04	4.07E+04	4.98E+04	4.04E+04	5.47E+04
GNP1	1.37E+04	1.83E+04	7.12E+04	1.25E+05	1.39E+05	1.04E+05	1.52E+05	1.81E+05
GNP2	1.43E+04	1.88E+04	1.10E+05	6.68E+04	1.01E+05	1.83E+05	1.73E+05	1.04E+05

Time Point	T8	T9	T10	T11	T12	T13	T14	T15
Days	3.87	4.59	5.54	6.59	7.59	9.59	11.56	34.56
Average								
C1	3.18E+05	3.27E+05	3.54E+05	3.55E+05	3.38E+05	3.48E+05	4.35E+05	4.51E+05
C2	3.52E+05	3.33E+05	3.58E+05	3.48E+05	3.71E+05	3.30E+05	4.49E+05	4.31E+05
L1	4.50E+05	4.99E+05	4.82E+05	4.86E+05	5.41E+05	5.24E+05	6.48E+05	5.43E+05
L2	4.26E+05	4.91E+05	4.99E+05	4.88E+05	5.00E+05	5.35E+05	6.70E+05	5.81E+05
LNP1	4.14E+05	5.26E+05	5.84E+05	5.85E+05	5.66E+05	5.22E+05	5.78E+05	4.07E+05
LNP2	5.91E+05	7.13E+05	6.72E+05	5.65E+05	5.20E+05	5.96E+05	7.55E+05	4.53E+05
GNP1	1.30E+06	1.17E+06	1.44E+06	1.15E+06	8.57E+05	8.85E+05	9.46E+05	1.02E+06
GNP2	1.21E+06	1.21E+06	1.37E+06	1.01E+06	9.48E+05	8.79E+05	9.08E+05	9.18E+05
Std Dev								
C1	3.53E+04	2.89E+04	3.72E+04	4.87E+04	1.63E+04	5.62E+04	4.74E+04	4.81E+04
C2	4.61E+04	2.18E+04	3.06E+04	4.03E+04	3.79E+04	2.86E+04	5.28E+04	3.54E+04
L1	4.29E+04	6.67E+04	4.89E+04	9.66E+04	6.28E+04	4.42E+04	8.18E+04	3.47E+04
L2	3.83E+04	3.72E+04	9.10E+04	5.25E+04	6.78E+04	6.40E+04	5.86E+04	3.17E+04
LNP1	5.77E+04	4.98E+04	5.35E+04	6.43E+04	9.15E+04	5.66E+04	8.04E+04	4.53E+04
LNP2	4.09E+04	6.69E+04	1.03E+05	1.05E+05	9.71E+04	8.23E+04	1.10E+05	6.57E+04
GNP1	1.12E+05	1.35E+05	1.83E+05	1.29E+05	1.02E+05	1.77E+05	7.95E+04	1.25E+05
GNP2	1.02E+05	1.18E+05	2.23E+05	1.04E+05	1.29E+05	1.17E+05	9.39E+04	7.97E+04

Hybridization Solutions:
Set 001*: 0.9 M NaCl, 20 mM Tris/HCl pH 7.4, 35% formamide 0.01%, and SDS in 3.58 mL of Millipore de-ionized water.*

Set 002*: 0.9 M NaCl, 20 mM Tris/HCl pH 7.4, 15% formamide and 0.01% SDS in 7.58 mL of Millipore de-ionized water.*

Hybridization washes:
Set 001*: 70 mM NaCl, 20 mM Tris/HCl pH 7.4, 15% formamide and 0.01% SDS in 934 mL of Millipore de-ionized water.*
Set 002*: 150 mM NaCl, 20 mM Tris/HCl pH 7.4, 5 mM EDTA and 0.01% SDS in 894 mL of Millipore de-ionized water.*

Table S3. Table showing probes used for FISH (normal) and **CARD-FISH (bold)** in this project including their sequences, target species including class level and what % of hits are the target species according to the SILVA and RDP databases. Additional information on the % formamide used in the hybridization solution, the hybridization temperature (°C), the NaCl concentration (M) in the wash solution and the wash temperature (°C) are also included.

Probe Name	DNA Sequence 5' to 3'	Target (Class Level)	SILVA (RDP) Probe Hit %Target/Total	% Formamide	Hybridization Temperature °C	NaCl Concentration M	Wash Temperature °C
338F[1]	TGAGGATGCCCTCCGTCG	Non Specific	0.0 (0.0)	15-35	37	0.07-0.15	50-55
536R-Cy3[2]	CAACGCTAACCCCCTCCG	*Rhodobacteraceae* (Family)	99.7 (99.1)	35	37	0.07	52
AC137-Cy3[3]	TGTTATCCCCCTCGCAAA	*Alteromonas* (Genus)	91.4 (95.6)	35	37	0.07	52
CFB563-Cy3[4]	GGACCCTTTAAACCCAAT	*Flavobacteriales* (Order)	97.7 (97.5)	20	46	0.225	48
152R-Cy3[1]	ATTAGCACAAGTTTCCYCGTGT	SAR11	98.7 (99.1)	15	37	0.15	55
441R-Cy3[1]	TACAGTCATTTTCTTCCCCGAC	(Family)	99.8 (99.6)				
542R-Cy3[1]	TCCGAACTACGCTAGGTC	Peligibacter	99.9 (99.7)				
732R-Cy3[1]	GTCAGTAATGATCCAGAAAGYTG	(Genus)	99.9 (99.8)				
103R-Cy3[5]	GTTACTCAGCCGTCTGCC	SAR202		35	37	0.07	57.5
311R-Cy3[5]	TGTCTCAGTCCCCCTCTG	Chloroflexi (Phylum)	72.7 (96.0) 60.9 (87.7) 72.7 (84.7)				
Cren-537[6]	**TGACCACTTGAGGTGCTG**	***Thaumarcaheota* (Phylum)**	**99.9 (99.9)**	**20**	**35**	**0.145**	**37**
Eury-806[6]	**CACAGCGTTTACACCTAG**	***Euryarchaeota* (Phylum)**	**99.4 (99.3)**	**20**	**35**	**0.145**	**37**

[1] Morris et al. 2002 [2] Parsons et al. 2011 [3] Parsons et al. 2015 [4]Weller et al. 2000 [5]Morris et al. 2005 [6]Teira et al. 2004; Herndl et al. 2005

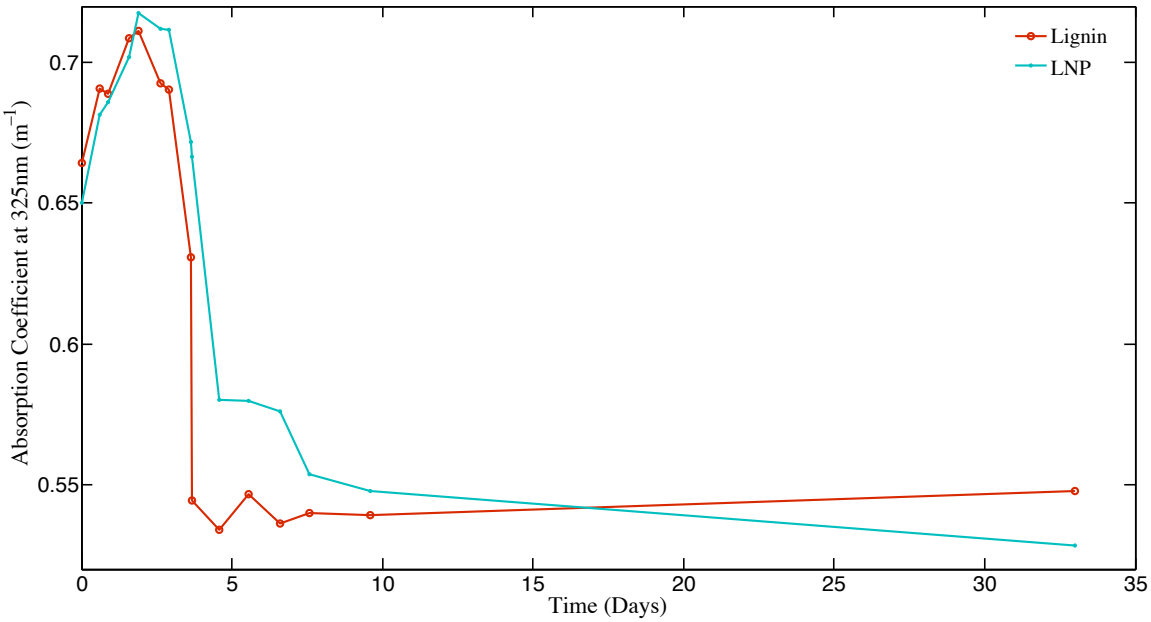

Figure S1. Changes in the CDOM absorption coefficient (m^{-1}) at 325 nm for LNP (blue line with dots) and Lignin treatments (orange line with circles) over time, for the full 35 day incubation.

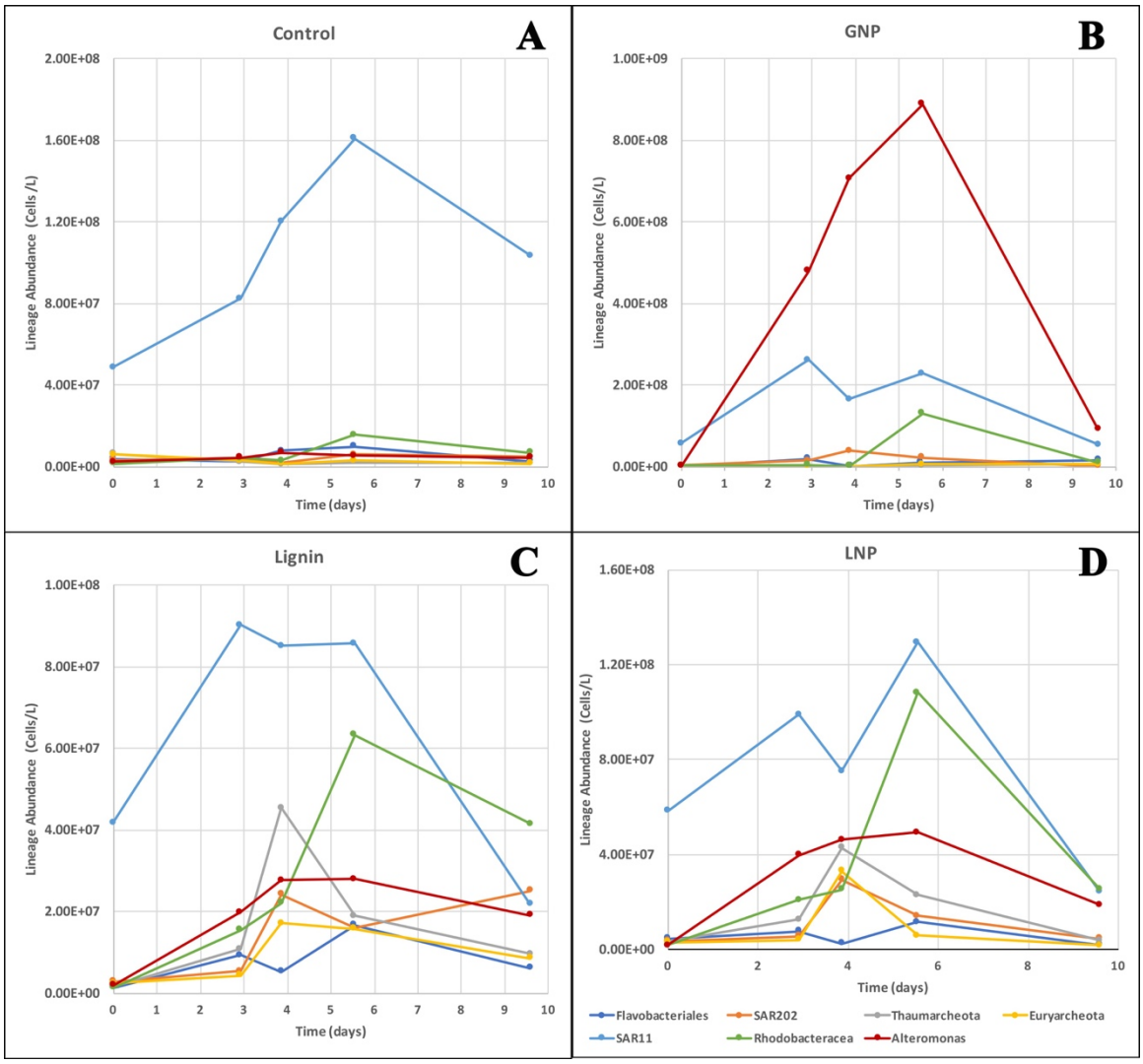

Figure S2. Changes in the absolute cell abundance (cells L^{-1}) of targeted groups using FISH and CARD-FISH (Flavobacteriales, SAR202, Thaumarchaeota, Euryarchaeota, SAR11, Rhodobacteracea and *Alteromonas*) in each of the four treatments A) Control B) GNP C) Lignin and D) LNP, between days 0 and 10. Please note the change in the scale of the Y axis between treatments. See Figure 1 for total prokaryotic cell counts.

CHAPTER 4: *Prochlorococcus* is Linked to the Production of Chromophoric Dissolved Organic Matter in the North Atlantic Subtropical Gyre

Abstract

Chromophoric dissolved organic matter (CDOM) accounts for over 50% of blue light absorption in the ocean, impacting many ocean processes including photosynthesis, but its sources in pelagic waters remain unclear. A lack of strong correlation between CDOM and chlorophyll *a* over the seasonal blooming cycle has led to the suggestion that autotrophs do not play a significant role in the production of open ocean CDOM. However, studies have demonstrated the *in vitro* production of CDOM by cultured phytoplankton, including picocyanobacteria. Although 25% of annual primary production in the Sargasso Sea has been attributed to *Prochlorococcus*, its relationship to *in situ* CDOM has not been investigated. Here, we demonstrate a significant correlation between CDOM and *Prochlorococcus* abundance ($R = 0.58$; $p < 0.01$) in the North Atlantic subtropical gyre, using a ten-year dataset of measurements collected from the Bermuda Atlantic Time-series Study (BATS) site (31° 40' N, 64° 10' W). The data indicate that the CDOM subsurface maximum observed at BATS is linked to *Prochlorococcus* abundances. Additionally, signatures of other marine autotrophs and heterotrophs indicated no significant correlations with CDOM for the CDOM maximum or deep chlorophyll maximum. Furthermore, we found that total virioplankton abundance was significantly correlated with both CDOM and *Prochlorococcus* at the depth of the CDOM maxmimum ($R = 0.73$ and 0.65, respectively, $p < 0.01$). These findings suggest that *Prochlorococcus*, along with viruses, may play a vital role in the accumulation of CDOM in the open ocean and highlight a previously unknown source of CDOM in the subtropical North Atlantic. As *Prochlorococcus* abundances are predicted to increase by 29% by the end of the 21st century, this could have substantial implications for future CDOM concentrations in the global oceans and could influence algorithms for satellite prediction of primary production.

Significance Statement

CDOM plays an important role in a wide range of ocean processes. It effectively regulates light available for photochemistry and photosynthesis and influences satellite observations of ocean color. Therefore, a thorough understanding of CDOM sources and cycling in the open ocean is critical for global ocean primary productivity and photochemical assessments using remote sensing. Autotrophic sources of ocean CDOM have been deemphasized due to a weak correlation with chlorophyll *a*. However, chlorophyll *a*-based biomass is often decoupled from primary production. Furthermore, despite the fact that *Prochlorococcus* is the most abundant photosynthetic organism on earth, its role in oceanic CDOM cycling has never been investigated. Here, we demonstrate a significant correlation between CDOM and *Prochlorococcus* in the open ocean and reveal a possible new role of *Prochlorococcus* in the global carbon cycle.

Introduction

The light absorbing, or chromophoric fraction of dissolved organic matter (CDOM) effectively regulates the underwater light field and influences numerous biogeochemical processes (Blough and Del Vecchio, 2002, Nelson and Siegel, 2002, Nelson and Siegel, 2013). In the subtropical gyres, CDOM influences ocean color-based estimates of primary production from satellite (Siegel et al., 2005, Maritorena and Siegel, 2005); therefore, tracking the sources and sinks of CDOM in the open ocean is critical to our understanding of carbon cycling in the surface ocean. CDOM in the pelagic euphotic zone is considered largely autochthonous (Nelson and Siegel, 2002, Stedmon and Nelson, 2015, Nelson et al., 2004, Nelson et al., 1998) due to low levels of allochthonous terrigenous markers such as lignin (Hernes and Benner, 2006, Hernes and Benner, 2002, Hedges et al., 1997, Blough and Del Vecchio, 2002). A direct link between CDOM accumulation and autotrophic biomass in the open ocean has been discounted due to a weak correlation with chlorophyll *a*, and research has therefore focused on heterotrophic sources of CDOM. The hypothesis that a portion of the oceanic CDOM pool is a byproduct of heterotrophic microbial remineralization of organic matter is supported by qualitative evaluations of depth profiles of bacterial abundance and bacterial production rates (Nelson et al., 2004, Nelson et al., 2014, Goldberg et al., 2010, Carlson et al., 2009, Nelson et al., 1998, Nelson and Siegel, 2013), as well as direct measurements of CDOM production in microbial seawater culture experiments (Nelson et al., 2004). However, *in vitro* production of CDOM in axenic cultures of marine eukaryotic microphytoplankton has also been demonstrated. Romera-Castillo et al. (2010) found that four phytoplankton species (*Chaetoceros*, *Skeletonema*, *Prorocentrum*, and *Micromonas*) produced DOM that exhibited both protein-like and humic-like fluorescence signatures, indicating the potential for marine diatoms, dinoflagellates and green algae to contribute to the ocean CDOM pool. The strong correlation found between total algal biomass and marine humic-like CDOM fluorescence ($R^2 = 0.78$, $p < 0.01$) is in contrast with *in situ* findings; however, Romera-Castillo et al. suggest that both UV irradiation and bacterial sources of CDOM could obscure the phytoplankton-derived CDOM signature in natural waters. Two species of picocyanobacteria, *Synechococcus* and *Prochlorococcus*, have also been found to produce CDOM in axenic cultures. Zhao et al. (2017) demonstrated that these species produced CDOM *in vitro* that resembled fluorescent compounds found in the North Atlantic, further suggesting a role for marine autotrophs in CDOM production. They also found that CDOM production in cultures of *Synechococccus* was expediated by viral lytic infection (Zhao et al., 2019, Zhao et al., 2017). However, the relationship between CDOM and picocyanobacteria has not been explored using *in situ* data, despite the fact that *Prochlorococcus* is the most abundant photosynthetic organism on Earth (Biller et al., 2015). In this study, we utilize data from the longest running time-series of CDOM absorption measurements and phytoplankton pigments, as well as picocyanobacteria numerical abundance, at a range of depths throughout the euphotic and upper mesopelagic zones to investigate the contribution of marine autotrophs to CDOM production in the North Atlantic subtropical gyre.

Results and Discussion

Characterization of the CDOM cycle at BATS

Monthly time series measurements of the absorption coefficient (m^{-1}) of CDOM at 325 nm (CDOM-325; the standard wavelength used for open ocean CDOM measurements. (Nelson and Siegel, 2002)) were collected from June 2006 – 2015 at 12 discrete depths between 1 and 250 m (Fig. 1; depths listed in Table 1). While the data show that CDOM is maintained at a minimum in the surface 20 – 50 m, due to solar bleaching (Nelson and Siegel, 2002), a maximum in CDOM-325 absorbance is regularly observed between 60 – 100 m during summer and autumn (July-October; SI Fig. 1). Deep convective mixing homogenizes the subsurface CDOM maximum in the late winter and no increase in CDOM-325 is evident during the spring phytoplankton bloom (Fig. 1).

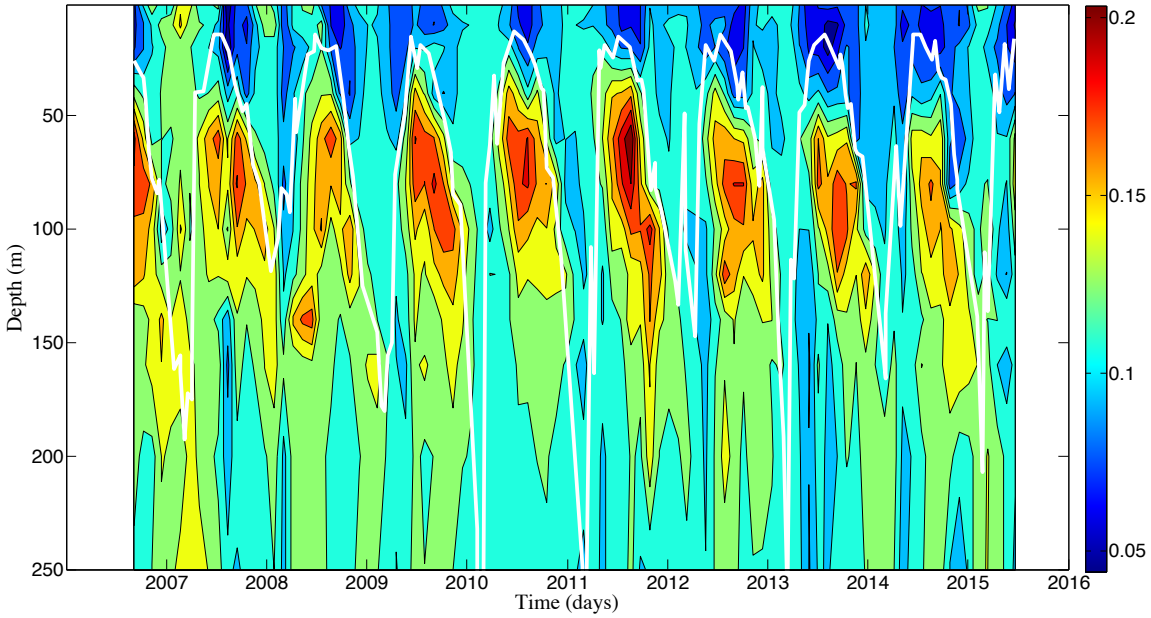

Figure 1. CDOM-325 time-series of monthly samples at 12 discrete depths between 1 and 250 m at BATS between June 2006 and June 2015. The CDOM absorption coefficient at 325 nm (m^{-1}) is shown on the color bar; the mixed layer depth (MLD) is shown as a solid white line (Matlab v. 2014b; Mathworks) and was obtained using the parameter *Sigma-t*, equivalent to a 0.2°C temperature change, according to Sprintall and Tomczak (1992).

Correlations between CDOM and measures of biological processes

To determine links between parameters related to autochthonous processes and CDOM accumulation in the euphotic zone, pairwise comparisons of CDOM-325 and 7 indicators of autotrophic and heterotrophic activity (chlorophyll *a* and chlorophyll *b* concentrations, *Prochlorococcus*, *Synechococcus* and total bacterioplankton cell abundances, as well as net primary production (NPP) and bacterial production (BP) rates) were performed at discrete depths throughout the time series record at BATS. Model II regression was used for the comparisons, and the Pearson's correlation coefficients (R), along with 95% confidence intervals (see *Methods*) were used to explore significant correlations between CDOM-325 and each of the 7 aforementioned parameters associated with autotrophic and heterotrophic processes. Correlations were investigated at 12 regularly-sampled depths from the surface to 250 m (8 regularly sampled depths from surface to 140 m for NPP

and BP; Table 1). Additionally, each parameter was averaged over the depths of 60, 80 and 100 m (the typical depth range of the CDOM maximum) and compared with CDOM values averaged over the same range.

Chl_a

Depth	1	10	20	40	60	80	100	**CDOM Max**	120	140	160	200	250
m	0.0002	0.0002	0.0001	0.0002	-0.0003	0.0003	0.0003	-0.0004	0.0003	0.0002	-0.0003	-0.0004	-0.0004
b	0.0714	0.0698	0.0801	0.0866	0.1871	0.0650	0.0651	0.2238	0.0934	0.1091	0.1415	0.1283	0.1228
sm	0.0000	0.0000	0.0000	0.0000	0.0000	0.0000	0.0000	0.0001	0.0000	0.0000	0.0000	0.0001	0.0001
sb	0.0032	0.0030	0.0025	0.0046	0.0083	0.0114	0.0107	0.0130	0.0067	0.0035	0.0027	0.0017	0.0016
r	0.5703	0.5996	0.5073	0.0628	-0.1563	0.0548	0.1073	**-0.0312**	0.0139	0.1850	-0.1078	-0.1226	-0.0831
p	0.0000	0.0000	0.0000	0.5456	0.1304	0.5979	0.3007	**0.7644**	0.8938	0.0726	0.2982	0.2364	0.4234

Chl_b

Depth	1	10	20	40	60	80	100	**CDOM Max**	120	140	160	200	250
m	0.0015	0.0015	0.0012	0.0011	-0.0011	0.0006	0.0005	0.0009	0.0004	0.0004	0.0006	-0.0016	-0.0019
b	0.0778	0.0758	0.0813	0.0938	0.1648	0.1022	0.0975	0.0895	0.1082	0.1131	0.1171	0.1286	0.1238
sm	0.0002	0.0002	0.0001	0.0002	0.0002	0.0001	0.0001	0.0001	0.0000	0.0001	0.0001	0.0002	0.0003
sb	0.0032	0.0029	0.0026	0.0040	0.0062	0.0064	0.0050	0.0064	0.0037	0.0028	0.0025	0.0019	0.0017
r	0.4354	0.5257	0.4802	0.0600	-0.0454	0.2800	0.5457	**0.4129**	0.4725	0.2964	0.0361	-0.0648	-0.0239
p	0.0000	0.0000	0.0000	0.5765	0.6727	0.0079	0.0000	**0.0001**	0.0000	0.0048	0.7369	0.5463	0.8243

Prochlorococcus

Depth	1	10	20	40	60	80	100	**CDOM Max**	120	140	160	200	250
m	0.0000	0.0000	0.0000	0.0000	0.0000	0.0000	0.0000	0.0000	0.0000	0.0000	0.0000	0.0000	0.0000
b	0.0674	0.0654	0.0730	0.1438	0.0785	0.0837	0.0952	0.0841	0.1126	0.1192	0.1205	0.1201	0.1179
sm	0.0000	0.0000	0.0000	0.0000	0.0000	0.0000	0.0000	0.0000	0.0000	0.0000	0.0000	0.0000	0.0000
sb	0.0048	0.0048	0.0042	0.0052	0.0065	0.0067	0.0060	0.0056	0.0039	0.0023	0.0020	0.0016	0.0016
r	0.2180	0.1964	0.0855	-0.0376	0.4889	0.4748	0.3102	**0.5767**	0.1772	0.3148	0.1932	0.0631	0.0050
p	0.0338	0.0565	0.4100	0.7178	0.0000	0.0000	0.0022	**0.0000**	0.0857	0.0019	0.0607	0.5437	0.9613

Synchococcus

Depth	1	10	20	40	60	80	100	**CDOM Max**	120	140	160	200	250
m	0.0000	0.0000	0.0000	0.0000	0.0000	0.0000	0.0000	0.0000	0.0000	0.0000	0.0000	0.0000	0.0000
b	0.0648	0.0761	0.0740	0.0842	0.1720	0.1795	0.1585	0.1709	0.1459	0.1218	0.1348	0.1260	0.1172
sm	0.0000	0.0000	0.0000	0.0000	0.0000	0.0000	0.0000	0.0000	0.0000	0.0000	0.0000	0.0000	0.0000
sb	0.0047	0.0035	0.0037	0.0046	0.0070	0.0048	0.0032	0.0043	0.0028	0.0026	0.0022	0.0016	0.0015
r	0.3188	0.2933	0.2556	0.1749	-0.0157	-0.5531	-0.5430	**-0.5040**	-0.2630	0.0314	-0.0591	-0.1558	0.2075
p	0.0016	0.0039	0.0124	0.0900	0.8798	0.0000	0.0000	**0.0000**	0.0100	0.7629	0.5697	0.1316	0.0436

Bacterioplankton Abundance

Depth	1	10	20	40	60	80	100	**CDOM Max**	120	140	160	200	250
m	-0.0170	-0.0151	0.0136	0.0147	0.0194	0.0225	-0.0217	0.0213	-0.0167	-0.0167	-0.0154	-0.0159	-0.0211
b	0.1947	0.1816	0.0168	0.0255	0.0196	0.0147	0.2453	0.0207	0.2007	0.1861	0.1674	0.1567	0.1593
sm	0.0023	0.0022	0.0018	0.0016	0.0023	0.0032	0.0030	0.0029	0.0018	0.0020	0.0016	0.0019	0.0026
sb	0.0136	0.0129	0.0112	0.0098	0.0141	0.0182	0.0151	0.0163	0.0076	0.0072	0.0046	0.0044	0.0051
r	-0.1195	-0.0140	0.1456	0.4513	0.3293	0.0714	-0.1269	**0.1322**	-0.4351	-0.3025	-0.4664	-0.3153	-0.2967
p	0.2486	0.8927	0.1592	0.0000	0.0011	0.4918	0.2203	**0.2014**	0.0000	0.0029	0.0000	0.0019	0.0035

NPP

Depth	1	10	20	40	60	80	100	**CDOM Max**	120	140
m	0.0051	0.0053	0.0075	0.0143	0.0175	-0.0326	-0.0581	0.0212	0.0703	0.0051
b	0.0679	0.0664	0.0776	0.0791	0.0959	0.1762	0.1512	0.0846	0.1242	0.0679
sm	0.0006	0.0006	0.0011	0.0018	0.0023	0.0047	0.0084	0.0028	0.0094	0.0006
sb	0.0043	0.0040	0.0056	0.0078	0.0070	0.0066	0.0036	0.0077	0.0023	0.0043
r	0.3469	0.3984	0.0894	0.2458	0.1758	-0.0135	-0.0338	**0.1809**	0.1640	0.3469
p	0.0006	0.0001	0.3889	0.0163	0.0885	0.8969	0.7452	**0.0793**	0.1123	0.0006

BP

Depth	1	10	20	40	60	80	100	**CDOM Max**	120	140
m	0.1262	0.1313	0.1550	0.1762	0.3296	0.6323	0.5591	0.2763	-0.6599	0.1262
b	0.0813	0.0870	0.0998	0.1147	0.1107	0.1099	0.1169	0.1144	0.1444	0.0813
sm	0.0223	0.0235	0.0216	0.0273	0.0532	0.1039	0.0965	0.0442	0.1105	0.0223
sb	0.0049	0.0039	0.0038	0.0057	0.0066	0.0061	0.0042	0.0055	0.0036	0.0049
r	0.0496	0.0201	0.4096	0.2655	0.2047	0.1766	0.0913	**0.2180**	-0.1447	0.0496
p	0.6997	0.8759	0.0009	0.0354	0.1076	0.1661	0.4766	**0.0861**	0.2579	0.6997

Table 1. Reduced major axis model II regression of 7 indicators of biological processes for 12 standard depths sampled monthly at BATS (8 standard depths for NPP and BP). 'CDOM Max' refers to the values calculated using the average values for depths 60 – 100 m. The slope of the regression line and y-intercept are given by *m* and *b*, respectively. Standard deviation of these two components is given as *sm* and *sb*, respectively. The Pearson's product moment and the p-values are indicated by *r* and *p,* respectively, where $p < 0.05$ is considered statistically significant.

The decoupling of in-situ CDOM and chlorophyll

A significant positive correlation was observed between CDOM-325 and chlorophyll (R = 0.57 and 0.44 for *a* and *b*, respectively, $p < 0.001$) at the surface, with similar significant values throughout the top 20 m (SI Fig. 7; Table 1). However, while no significant correlations were found below 20 m for Chl *a* (SI Fig. 7, Table 1), significant positive correlations were found between CDOM and chlorophyll *b* at 100 and 120 m (R = 0.55 and 0.47, respectively, $p < 0.001$; Table 1), and a weak but significant correlation was observed at 80 m (R = 0.28, p = 0.008). The 60 – 100 m average of Chl *b* was also significantly correlated with CDOM-325 (R = 0.41, $p < 0.001$, Table 1). The statistical correlation between CDOM and chlorophyll (*a* and *b*) in surface waters is likely because they all exhibit a minimum in the top 20 meters during the summer months. However, the mechanisms driving these minima are fundamentally different for CDOM than for the phytopigments. The autotrophs that produce chlorophyll bloom in the spring, upon supply of nutrients to surface waters through deep winter mixing, and decline upon water column stratification in summer, when phytopigments become photoacclimated to high light concentrations (Hansell, 2002, Lomas and Moran, 2011, Steinberg et al., 2001, Nelson and Siegel, 2013). However, this increase in solar radiation cleaves covalent bonds in CDOM molecules and results in a 'bleaching' or loss of chromophoric activity in surface CDOM-325. Despite the loss of surface CDOM in summer, levels of DOC remain relatively constant at ~ 68 μM C from June through October in the Sargasso Sea (Carlson et al., 1998). It is therefore likely that correlations between CDOM and chlorophyll pigments in surface waters are coincidental and not indicative of the production of CDOM by autotrophs.

Significant correlations were also found between CDOM and chlorophyll *b* at 100 m (R = 0.46; $p < 0.01$; Table 1). Additionally, the link between CDOM-325 and other marker pigments was examined (SI Figure 7) and a significant correlation also existed between CDOM-325 and carotenes at 100 m (R = 0.48, $p < 0.01$). The correlation between carotenes and chlorophyll *b* at this depth was strong (R = 0.82; $p < 0.01$), suggesting that these pigments are indicative of the same autotrophic group – such as green algae (Beale, 2009), which contains chlorophyll *b* and has been reported to produce CDOM *in vitro* (Romera-Castillo et al., 2010). There was also a lack of a significant correlation with prasinoxanthin at these depths (SI Fig 7), suggesting the absence of prasinophytes (Foss, 1984). Green algae at BATS proliferate in deeper parts of the euphotic zone, below diatoms, cyanobacteria and prymnesiophytes (Steinberg et al., 2001, Bidigare, 1990), which could explain why their pigments are not correlated with CDOM at depths shallower than 100 m. The chemical composition and nutrient content of phytoplankton-derived DOM varies widely amongst different species (Becker et al., 2014, Nelson and Carlson, 2012, Wear, 2015), suggesting that CDOM produced by specific groups may have varying bioavailability to microbial heterotrophs, thus creating a decoupling between phytoplankton abundance and CDOM absorbance.

The relationship between production and CDOM

Due to photoadaptation, chlorophyll *a* concentration is decoupled from biomass in oligotropic systems within deep euphotic zones. The deep chlorophyll *a* maximum is vertically separated from biomass and the primary production maximum by 50+ m at

BATS, and as a result, the two parameters are not correlated at the DCM (SI Fig. 2). As such, the relationship between CDOM and the rate of net primary production (NPP) was also investigated. A slight but significant positive correlation was found between NPP and CDOM-325 at 1, 20 and 60 m (R = 0.35 0.40, and 0.25, respectively, $p < 0.05$), but not at 80 – 100 m (SI Fig. 3; Table 1). The lack of correlation found between chlorophyll *a* and CDOM in previous studies, in conjunction with the observed increase of CDOM in dark incubations of natural microbial assemblages in seawater (Nelson et al., 2004, Steinberg et al., 2004) has led to the hypothesis that CDOM production in the open ocean is largely a result of chromophoric byproducts, released through heterotrophic bacterioplankton remineralization of organic matter (Nelson et al., 1998). However, although CDOM and heterotrophic bacterial abundance both exhibit a maximum at BATS during the late summer, these occur at different depths, and the two time series are distinctly different (SI Fig. 4). There is a slight but significant correlation between CDOM-325 and bacterial production at 40 and 60 m (R = 0.41 and 0.27, respectively, $p < 0.05$; SI Fig. 5; Table 1), the typical depths of the local bacterioplankton maximum in summer/fall months. A similar correlation was observed between CDOM-325 and total bacterioplankton abundance at the same depths (R = 0.45 and 0.33, respectively, $p < 0.001$; Table 1). This supports the heterotrophic production of CDOM evidenced *in vitro* in previous studies (Steinberg et al., 2004, Nelson et al., 2004), but the lack of correlation between either BP or bacterial abundance at 80 or 100 m suggests removal processes, and potentially other important sources of CDOM.

The relationship between CDOM and picocyanobacteria

While the above measures of autotrophic activity revealed some significant correlations with CDOM-325, no parameter was significantly correlated throughout the entire time series with the CDOM maxima (ca. 60 – 100 m). However, when performing the analysis for a subset of the time-series record, when the water column was stratified and the CDOM maximum had fully developted, CDOM at 80 m was found to be strongly correlated with both chlorophyll *a* and *b* (R = 0.87 and R = 0.84, respectively, $p < 0.01$ both (August and September, averaged; Fig. 2). This significance was not found for any other months. However, this could be due to the fact that divinyl chlorophyll *a* and *b*, which are indicative of *Prochlorococcus*, co-elute with chlorophyll *a* and *b*, respectively, using the BATS method of HPLC-based pigment analysis. Additionally, this means that the significant correlation between CDOM and chlorophyll *b* at 100 and 120 m may actually be indicative of *Prochlorococcus* rather than green algae.

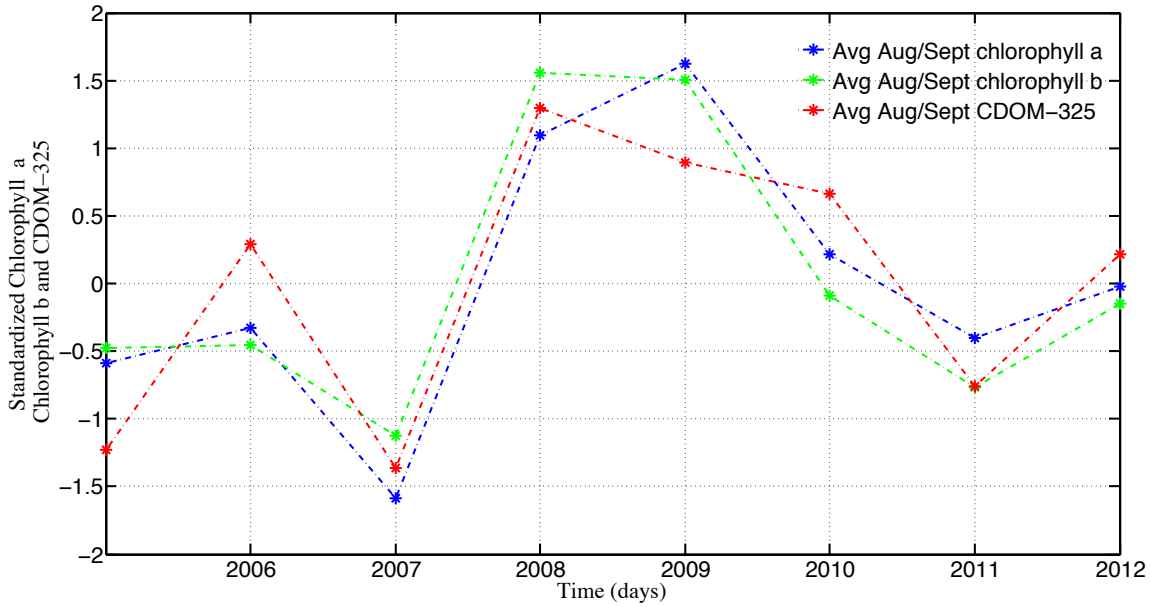

Figure 2. Standardized average August/September values for chlorophyll *a* (blue line), chlorophyll *b* (green line) and CDOM-325 (red line) at 80 m for 2005 – 2012. A Pearson's correlation yields values of $R = 0.87$ and $R = 0.84$ for chlorophyll *a* and *b*, respectively, with CDOM-325. *P*-values are less than 0.01 for both correlations. Note that due to the HPLC method used, these chlorophyll values also include the concentrations of divinyl chlorophyll *a* and *b*, respectively.

Although divinyl chlorophyll and phycoerythrin are not individually quantified as part of the BATS suite of analyses, *Prochlorococcus* and *Synechococcus* are enumerated with flow cytometry on a monthly basis. The *Synechococcus* time-series is characterized by a seasonal maximum throughout the euphotic zone, coinciding with the spring bloom (SI Fig. 6); however, *Synechococcus* cell abundance is at no time directly positively correlated with CDOM-325. However, cross-correlation analysis was used (*SI Methods*) to determine if there were significant correlations given a time lag, thus indicating the possibility of a delayed cause and effect relationship between *Synechococcus* and CDOM at 60 – 100 m. The results of this analysis revealed that the significant negative direct correlation ($R = -0.50$; $p < 0.01$) between the two variables becomes positively correlated ($R = 0.47$; $p < 0.05$) by introducing a time-lag of 6 months (Fig. 3), reiterating the seasonality of the two parameters. Although significant, it is unlikely that these correlations are indicative of a causal relationship between *Synechococcus* abundance and CDOM. *Synechococcus* has been shown to exhibit growth rates on the order of 0 – 2 day^{-1} in the Sargasso Sea (Parsons et al., 2011), while studies of CDOM production in natural assemblages of Sargasso Sea water showed that autochthonous CDOM generally persisted in the water column for 2 – 3 days, with some cases of up to 50 days. There is no known mechanism by which a *Synechococcus* bloom and subsequent decrease in cell abundance can lead to the production of CDOM 6 months later. It is more likely that the correlation is due to a seasonal offset between the spring bloom and the subsurface CDOM maximum in the late summer and early autumn and does not suggest a causal relationship. While we cannot rule out the possibility that CDOM production by *Synechococcus* is taking place (Zhao et al., 2017), our analyses do not reveal an obvious

causative relationship between *Synechococcus* biomass variability and accumulation of CDOM at BATS. These data suggest that CDOM production and accumulation is decoupled from *Synechococcus* abundance in the water column in the North Atlantic Subtropical Gyre (Fig. 3; Table 1).

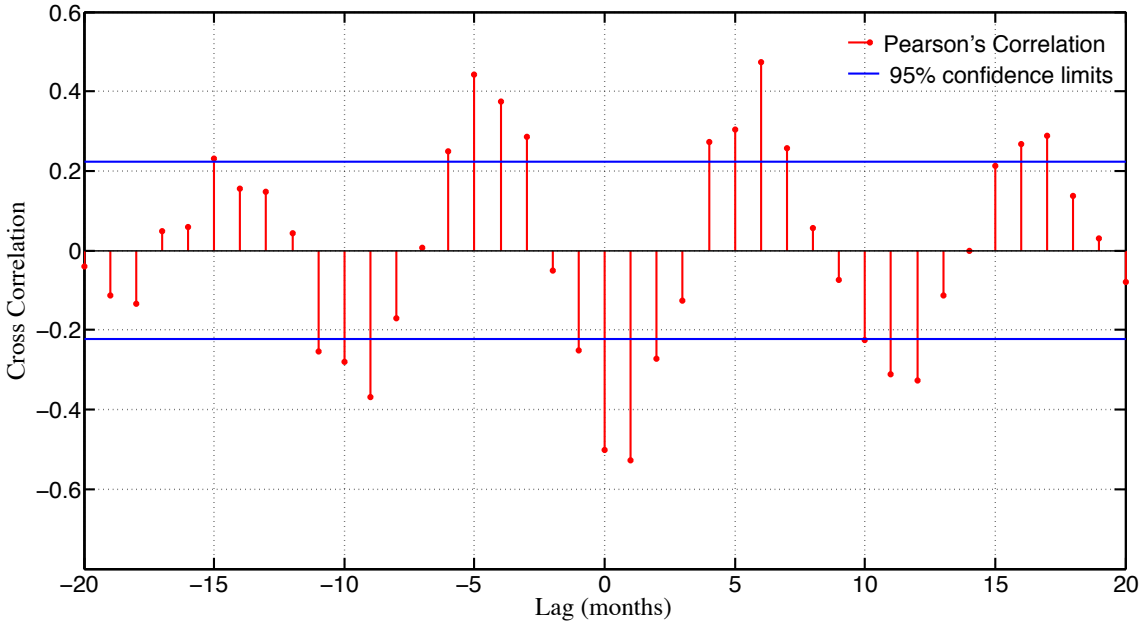

Figure 3. The cross-correlation function of CDOM-325 (80 m) and *Synechococcus* (80 m). *R*-values are shown as red bars and 95 % confidence limits are shown as blue lines (Matlab v. 2014b; Mathworks).

In contrast, an analysis of *Prochlorococcus* abundance and CDOM-325 over time shows that both variables exhibited annual maxima during the late summer at depths between 60 – 100 m, with the *Prochlorococcus* maximum coinciding with that of CDOM-325 (Fig. 4). Although specific ecotypes of *Prochlorococcus* are not differentiated in the monthly measurements at BATS, both high-light and low-light *Prochlorococcus* ecotypes have been shown to exist in the North Atlantic Subtropical Gyre, with the high-light ecotype proliferating during the same season and at the depths (Biller et al., 2015, Malmstrom, 2010, DuRand, 2001) at which subsurface CDOM accumulates. A significant correlation was found between CDOM-325 and *Prochlorococcus* between 60 – 100 m during summer stratified periods throughout the BATS record (Pearson's Correlation, $R = 0.58$; $p < 0.01$; Figure 5; Table 1), suggesting a strong potential link between *Prochlorococcus* cell abundance and CDOM absorbance at BATS.

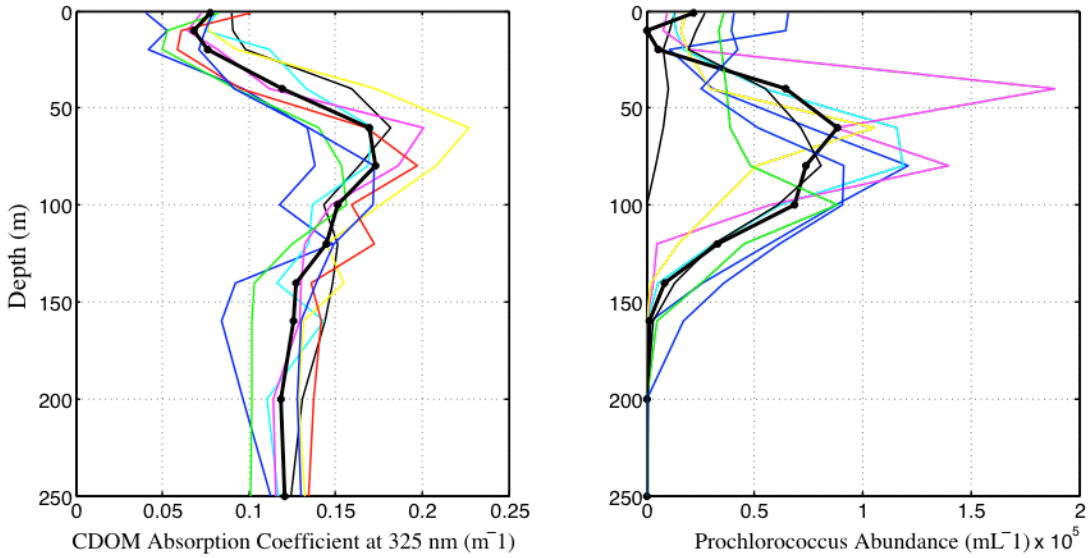

Figure 4. August depth profiles for CDOM-325 (left panel) and *Prochlorococcus* abundance (right panel), measured at BATS between 2006 and 2015. The mean of each profile is shown as a thick black line (Matlab v. 2014b; Mathworks).

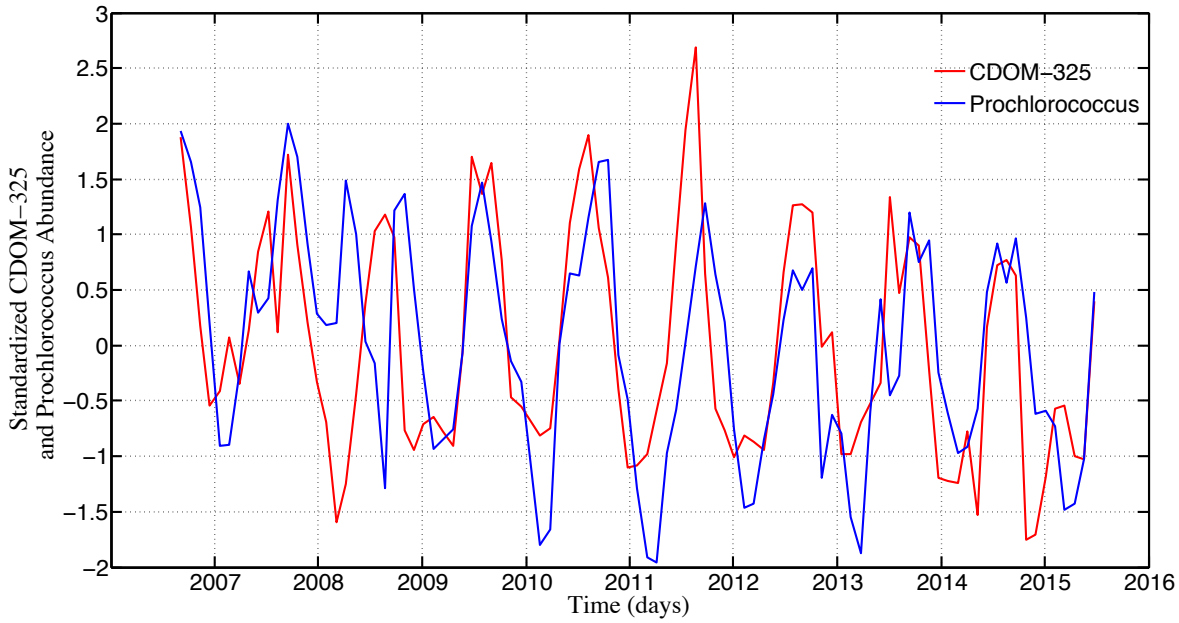

Figure 5. Time series of CDOM-325 (m^{-1}) and *Prochlorococcus* abundance (cells mL^{-1}), averaged between 60 and 100 m at BATS from 2006 to 2015. Both parameters are shown as unitless, standardized values (Matlab v. 2014b; Mathworks).

Discrepancy between Prochlorococcus and Synechococcus-produced CDOM

The seasonal profile of *Prochlorococcus* at BATS, along with the strong direct correlation with CDOM-325 (Fig. 5, SI Fig. 6), indicates that this genus is linked to the

production of the seasonal CDOM subsurface maximum. This is supported by the findings of Zhao et. al (2017), who demonstrated the production of CDOM in axenic cultures of *Prochlorococcus*. However, Zhao also showed the production of CDOM in axenic cultures of *Synechococcus*; therefore, the question remains as to why *in situ* CDOM is correlated with *Prochlorococcus* but not *Synechococcus*. A previous study showed that the chemical composition of *Synechococcus*-produced DOM differs from that of *Prochlorococcus,* and that DOM from high-light strains of *Prochlorococcus*, in particular, exhibited the least similarity with *Synechococcus* DOM (similarity of 6-14%) (Becker et al., 2014). However, this study did not indicate the specific molecular formulas or even functional groups comprising the DOM.

In the present study, the molecular composition of DOM extracted from axenic cultures of both *Prochlorococcus* and *Synechococcus* was analyzed using electrospray ionization (ESI) coupled with Fourier transform ion cyclotron resonance mass spectrometry (FT-ICR-MS) and revealed differences in the DOM exuded from each phytoplankton species. *Prochlorococcus* DOM obtained using solid phase extraction (SPE-DOM; details in *Methods*) was dominated by formulas containing only carbon, hydrogen, and oxygen (CHO, 67% of assignments), followed by nitrogen containing formulas (CHNO, 26% of assignments), and sulfur containing formulas (CHOS, 8% of assignments). *Synechococcus* SPE-DOM was dominated by CHNO formulas (49% of assignments), followed by CHO formulas (37% of assignments), and CHOS formulas (13% of assignments). Only 37% of the assigned molecular formulas were found in both *Synechococcus* and *Prochlorococcus* SPE-DOM, but it should be noted that these assigned formulas may not represent identical compounds, due to potentially high numbers of isomers for each molecular formula. The CHO, CHNO, and CHOS compounds that were common between *Synechococcus* and *Prochlorococcus* SPE-DOM represent a pool of aliphatic DOM with intensity weighted average (wt) O/C_{wt} ratios ranging from 0.3 to 0.4 and H/C_{wt} ratios ranging from 1.2 to 1.7 (Fig. 7, SI Table 2), similar to a freshwater algal extract (Zhang, 2014).

There were far more CHO formulas unique to *Prochlorococcus* SPE-DOM (704 formulas) than to *Synechococcus* SPE-DOM (54 formulas), and these *Prochlorococcus* CHO formulas occupied a wide range of van Krevelen (Van Krevelen, 1950) space (O/C from ~0.1 to 0.6 and H/C from ~1 to 2; Fig. 7; *Methods*). Thus, unique *Prochlorococcus* CHO formulas had the largest range of molecular characteristics with weighted double bond equivalent (DBE_{wt}) averaging from 6 ± 5, the intensity-weighted modified aromaticity index (AI_{mod_wt}) averaging 0.15 ± 0.17, and COS averaging -1 ± 0.5 (SI Table 2). CHNO formulas unique to *Prochlorococcus* SPE-DOM had similar O/C_{wt} ratios to common formulas but were more saturated (H/C_{wt} ~1.6 for *Prochlorococcus* CHNO formulas versus H/C_{wt} ~1.2 for common CHNO formulas) (SI Table 3). On the other hand, CHNO formulas unique to *Synechococcus* SPE-DOM had similar H/C_{wt} ratio to common formulas but were more slightly more oxygenated (O/C_{wt} ~0.5 for *Synechococcus* CHNO formulas versus ~0.4 for common formulas) (SI Table 2). While less common than CHO and CHNO assignments, *Prochlorococcus* SPE-DOM also had the highest abundance of CHOS formula assignments (210 formulas from *Prochlorococcus* SPE-DOM versus 94 formulas from *Synechococcus* SPE-DOM).

However, it is not currently possible to definitively predict interactions between DOM and microbes (Kujawinski, 2011, Kujawinski, 2016). Therefore, we can only hypothesize that, although SPE is not 100% efficient and not all compounds ionize using ESI, the different molecular compositions of *Synechococcus* and *Prochlorococcus* SPE-DOM may contribute to the fact that CDOM at BATS is correlated with *Prochlorococcus* but not *Synechococcus*.

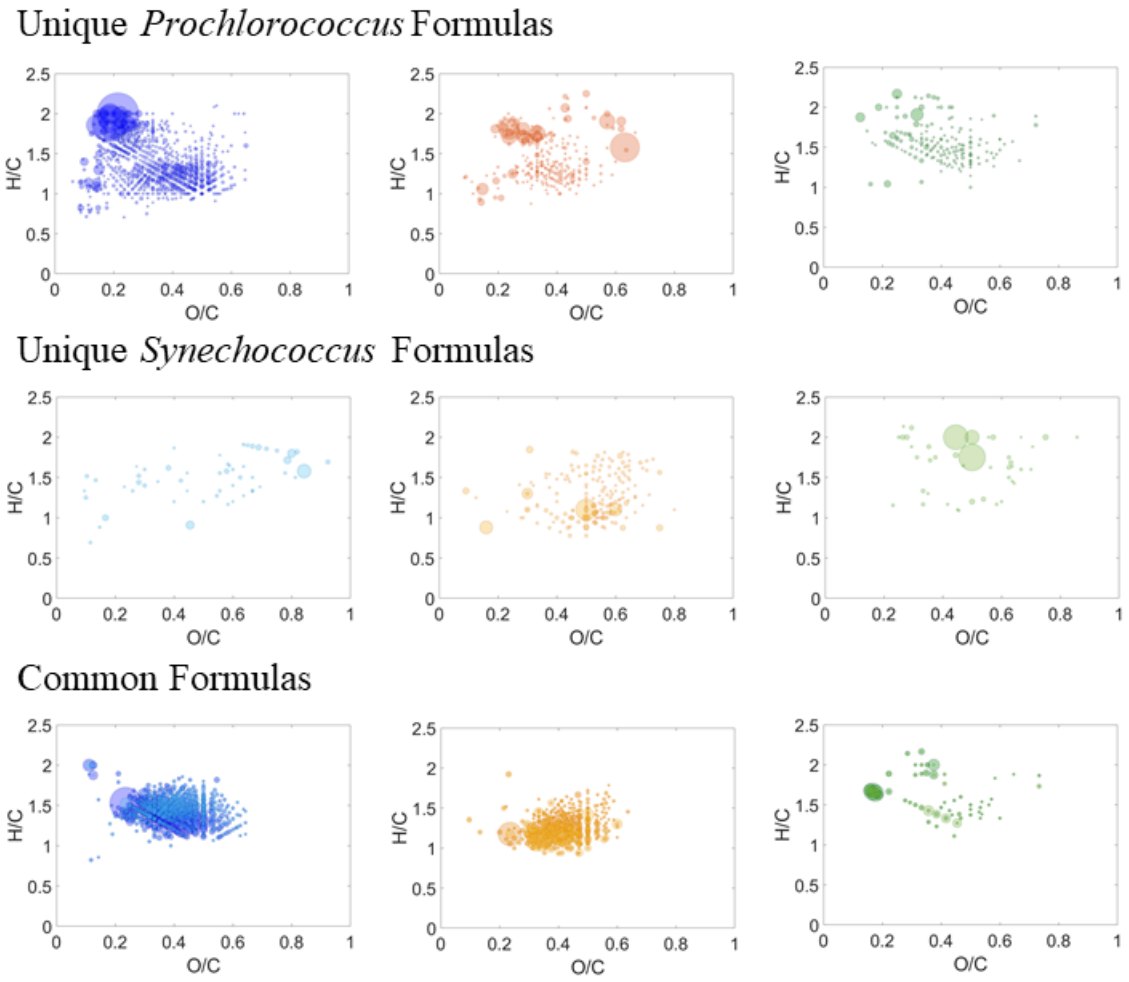

Figure 7. Van Krevelen diagrams (hydrogen to carbon, H/C, versus oxygen to carbon, O/C, ratios) of assigned molecular formulas in algal SPE-DOM where blue dots contain only carbon, hydrogen and oxygen (CHO, left panels), orange dots contain CHO + nitrogen (CHNO, center panels), and green dots contain CHO + sulfur (CHOS, right panels). In the top row are formulas that were unique to *Prochlorococcus* SPE-DOM, in the center row are formulas that were unique to *Synechococcus* SPE-DOM, and in the bottom row are formulas that were commonly found in both *Prochlorococcus* SPE-DOM and *Synechococcus* SPE-DOM. The size of the dots indicates relative abundance.

Alternatively, the lack of direct relationship between *Synechococcus* and CDOM may be explained by physical processes. *Synechococcus* can form aggregates (Lomas and Moran, 2011, Amacher et al., 2013, Deng, 2015), thus providing a possible mechanism for rapid sinking and escape from remineralization at the site of the *Synecococcus* biomass and production maximum. Additionally, analysis of the chemical composition of *Synechococcus*-derived DOM using ultra-high resolution mass spectrometry and nuclear magnetic resonance in a 2017 study revealed an enhanced abundance of nitrogen-containing groups that the authors thought to be microbial resistant phycocyanobilin metabolites (Zhao et al., 2017). Sediment trap-derived fluxes of particulate organic carbon (POC) and Thorium-234 measurements from BATS have been shown to correlate with depth-integrated abundance of *Synechococcus* (Brew, 2009). Therefore, another explanation for the lack of correlation with CDOM is that *Synechococcus* cells are exported out of the euphotic zone before lysis and subsequent CDOM release can occur. While *Prochlorococcus* abundance in the trap study was not similarly correlated, recent research has demonstrated the presence of *Prochlorococcus* in sediment traps at BATS and suggested that this genus is under-represented in traps, as compared to the water column (Amacher et al., 2013). While it was once thought that *Prochlorococcus* accounted for less than 0.2% of POC flux at BATS due to its small size (De Martini, 2017), recent studies have demonstrated that *Prochlorococcus* cells can account for up to 20% of POC flux, as measured in sediment traps, and are thought to comprise ~33% of autotrophic POC biomass (Lomas and Moran, 2011). In fact, sinking fluxes of *Prochlorococcus* cells in summer months are ca. 5 times larger than those of *Synechococcus* (Brew, 2009), indicating that export alone cannot explain the lack of correlation between *Synechococcus* and CDOM in the euphotic zone.

Viral lysis of Prochlorococcus may facilitate the production of CDOM

Parsons et al. (2011) revealed a strong correlation between *Prochlorococcus* and total virioplankton abundance between 60 – 100 m at BATS ($R = 0.66$; $p < 0.01$) that was strikingly similar to the correlation found in the present study between *Prochlorococcus* and CDOM (80 m: $R = 0.65$; $p < 0.01$; Avg 60 – 80 m: $R = 0.58$, $p < 0.01$). Upon reanalysis of the coincident data sets, we found a significant positive relationship between CDOM-325 (m^{-1}) and virioplankton abundance (cells mL^{-1}) at 80 m, the depth of the local CDOM maximum at BATS ($R = 0.73$; $p < 0.01$; Fig. 8).

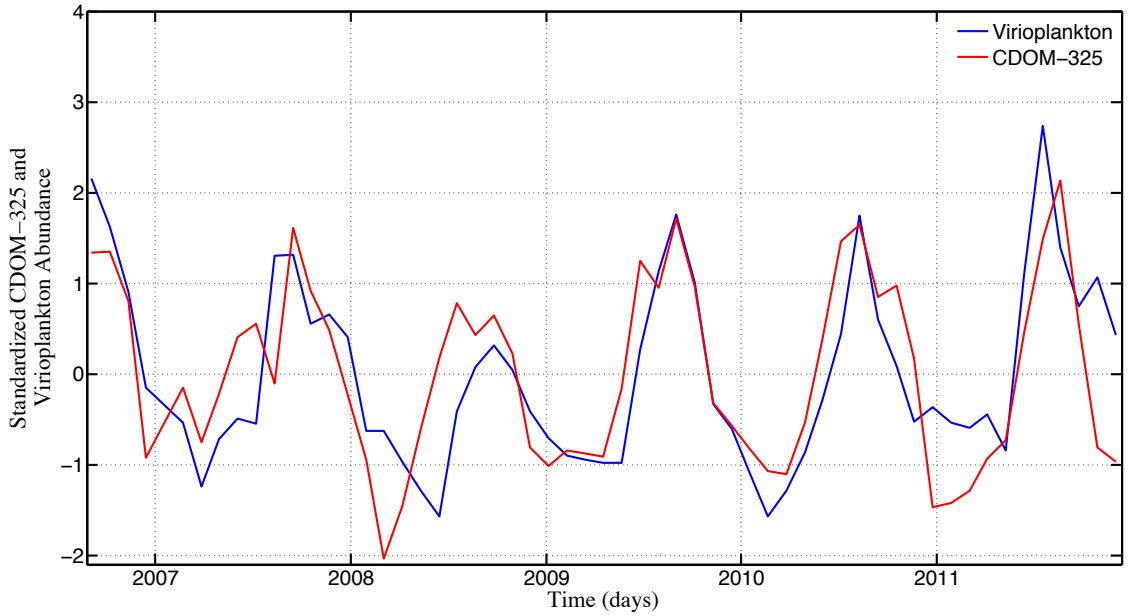

Figure 8. Standardized CDOM-325 (m^{-1}) and virioplankton abundance (cells mL^{-1}) at 60-100 m, from June 2006 – Dec 2011. Although CDOM data at BATS extended until mid-2016 for this study, virioplankton abundance was not routinely measured during this period.

As CDOM is operationally defined as that organic matter which is able to pass through a 0.2 µm filter, a preliminary test was implemented to determine if the notably small (< 30 KDa) virus cells themselves were chromophoric and responsible for the strong correlation with CDOM. CDOM absorbance was measured over the serial dilution of viral concentrates, and no relationship was observed with CDOM absorbance over increasing concentrations of viral-like particles (SI *Methods*; SI Fig. 7, SI Table 3), confirming that virus particles themselves are not chromophoric. While virus particles themselves do not appear to produce a resolvable CDOM signature, it is possible that subsequent remineralization of lysate may be important in CDOM production. Previous *in vitro* studies have shown a decrease in picocyanobacteria abundance and a shift to CDOM-like absorption, corresponding to an increase of virioplankton abundance in culture and subsequent infection of host cells (Zhao et al., 2017, Balch, 2007). However, while these *in vitro* studies were carried out using axenic cultures of *Synechococcus*, the high *in situ* ratio of virioplankton cells to *Synechococcus* (> 1000:1 between July - December) (Parsons et al., 2011) in the open ocean suggests that any infection of these bacterioplankton is masked by the total signal of viruses. In contrast, the ratio of virioplankton to *Prochlorococcus* abundance at BATS for the same time period was on average < 100:1 (Parsons et al., 2011). While the exact mechanism remains unresolved, the strong covariation between CDOM, the *Prochlorococcus* maximum and virioplankton maximum indicates a relationship that deserves further study. Though other mechanisms such as microzooplankton grazing of *Prochlorococcus* are also likely to contribute to the release of CDOM, it has been shown that in mid-latitude regions and oligotrophic waters, viral lysis contributes to phytoplankton mortality more than grazers (Mojika, 2016).

Additionally, the contribution of *Prochlorococcus* vesicles, which have been shown to contain organic carbon (Biller, 2014), to the CDOM pool has not been investigated and may constitute another mechanism by which CDOM is correlated to *Prochlorococcus* cell abundance. The lack of strong correlation between CDOM and other genera of both marine autotrophs and heterotrophs suggests that although these organisms may produce CDOM *in situ*, it is rapidly degraded, re-processed or escapes the microbial loop. However, the significant positive correlation between CDOM and both *Prochlorococcus* and virioplankton abundance is compelling and suggests that they may be interlinked. Although the exact mechanisms for *in situ* CDOM production and accumulation in the open ocean remain unproven, we propose a hypothesis whereby the magnitude of the *Prochlorococcus* summer bloom and the tight coupling with virioplankton abundance, combined with the fact that waters are highly stratified during this period, is the reason that *Prochlorococcus*-derived CDOM persists and accumulates to form a local maximum. Additionally, a study by Zhao et al. (2019) revealed that seawater incubations innoculated with the viral lysate of picocyanobacteria developed a stable DOM pool upon microbial processing of the amended organic matter. This presents the possibility that the CDOM-325 maximum observed at BATS could be the result of microbially-transformed viral lysate of *Prochloroccocus*. Further research should be undertaken to test this theory and to determine definitively if the viral lysis of *Prochlorococcus* drives CDOM variability in the open ocean.

While *Synechococcus* was not directly correlated with the local CDOM maximum observed seasonally in the upper water column at BATS, it may play an important role in other ocean basins. According to Yang et al. (Yang, 2010), virioplankton abundance in the southern oceans and Pacific is driven largely by *Synechococcus*, indicating the possibility that CDOM in these regions is governed more by *Synechococcus* than *Prochlorococcus*. Additionally, *Synechococcus* may play a role in the deep ocean CDOM pool. Natural water samples collected at depths > 4500 m at BATS have shown fluorescence signatures comparable to those produced by *Synechococcus* in culture (Zhao et al., 2017). This supports the notion that while *Prochlorococcus* may contribute to the CDOM pool in the euphotic zone, *Synechococcus*, in the form of sinking aggregates or zooplankton fecal pellets, may leach CDOM, thus transporting it to the deep ocean. This reveals the possibility for CDOM measurements to be used as an indicator of ocean carbon flux from the euphotic zone to the deep ocean and could allow for a better understanding of deep carbon sequestration and better constraint of the global carbon cycle.

Conclusions

The results of this study suggest that in addition to heterotrophic processes, the accumulation of CDOM in the open ocean is linked to the autotrophic production of *Prochlorococcus*. Our work reveals that there is a significant positive correlation between CDOM absorbance and *Prochlorococcus* abundance in the euphotic zone at BATS, suggesting that the seasonal accumulation of CDOM in the upper water column of the North Atlantic Subtropical Gyre is at least partly controlled by seasonal *Prochlorococcus* dynamics. The covariation of the CDOM and virioplankton maxima is also intriguing and allows us to pose a hypothesis that viral / host interactions, which are coincident with the

CDOM maximum, may contribute to the accumulated CDOM absorbance. *Prochlorococcus* plays an invaluable role in many ocean processes – estimates show that the genera accounts for 8.5 % of global carbon fixation (4 Gt C y^{-1}) (Flombaum, 2013, Biller et al., 2015), with estimates of up to 80% contribution to primary production in some oligotrophic ocean regions (Fernandez-Pinos, 2015). As such, this possible new role of *Prochlorococcus* in open ocean biogeochemistry may have important implications for the estimation of primary production using remote sensing and could enable a more comprehensive understanding of ocean carbon cycling.

Methods

Samples were collected monthly at the Bermuda Atlantic Time Series (BATS) site (31 40° N, 64 10° W) between July 2006 and June 2016 onboard the R/V Atlantic Explorer.

CDOM

Seawater was filtered directly from Niskin bottles (General Oceanics) mounted on a steel rosette affixed with a conductivity, temperature and depth (CTD) sensor package (Seabird SBE 9/11 Plus). Samples were filtered through a 0.2 μm capsule filter (Whatman Polycap 75 AS) and collected in muffled amber glass vials (I-Chem) with Polytetrafluoroethylene-lined caps. Samples were stored in the dark at 4°C until analysis. Samples were analyzed in 10 cm quartz cuvettes, using a dual-beam spectrophotometer (Perkin Elmer Lambda 18), equipped with deuterium and tungsten lamps. A slit width of 2 nm was selected and absorbance was measured in 1 nm wavelength increments from 250-750 nm. De-ionized water (Milli-Q, Millipore) was used for instrument blanks and spectra were corrected for baseline offsets according to Green and Blough (1994). Absorbance values were converted to the parameter "absorption coefficient" $_a$cdom (m^{-1}), which is obtained by multiplying the absorbance values by *e* (2.303) and dividing by the cell path length. A wavelength of 325 nm was nominally chosen to best represent CDOM absorbance in the open ocean, as per Nelson and Siegel (2002).

Ancillary BATS Data

High-performance liquid chromatography (HPLC) phytopigment analysis and flow-cytometry (FCM) enumeration of picoplankton were carried out as part of the BATS Study. Detailed methods for these measurements can be found on the BATS website (www.bats.bios.edu), as well as in Lomas and Moran (2011) and Ondrusek et al. (1991). The methods are outlined in the Supplementary Information.

Collection and Solid Phase Extraction (SPE) of DOM

Synechococcus and *Prochlorococcus* cultures were grown using established procedures and filtered to collect DOM as described in detail in Zhao et al. (Zhao et al., 2017). All samples were acidified to pH 2 using formic acid (Sigma Aldrich) for an established solid-phase extraction (SPE) procedure (Dittmar, 2008) using Agilent Bond Elut PPL cartridges. Samples were drawn through clean Teflon tubing and connected to PPL cartridges at a flow rate of ~4 mL/min until sample solutions had passed through the cartridges. After extraction, cartridges were rinsed with 0.1% formic acid water (Sigma Aldrich), dried under N_2, and eluted with 10 mL pure methanol (LC-MS Chromasolv,

Sigma Aldrich). Methanol extracts were stored at -20 °C prior to mass spectrometric analysis.

Ultrahigh Resolution Mass Spectrometry

We used ultrahigh resolution mass spectrometry to characterize the molecular composition of *Prochlorococcus* and *Synechococcus* SPE-DOM using a Bruker Solarix 12 Tesla Fourier transform (FT) ion cyclotron resonance (ICR) mass spectrometer housed at Helmholtz Zentrum, Munich, Germany. Ionization was achieved using negative ion mode electrospray ionization (ESI) with an electrospray voltage of –3.6 kV. Samples were infused at a flow rate of 120 µL h^{-1} and 500 scans were averaged. The resolution (>500,000 at *m/z* 400) and the mass error (<0.2 ppm) were sufficiently precise to compute exact molecular formulae (Koch BP, 2007, Herzsprung P, 2014) based on the following atomic numbers: $^{12}C_{0-\infty}$, $^{1}H_{0-\infty}$, $^{16}O_{0-30}$, $^{14}N_{0-10}$ and $^{32}S_{0-2}$, as well as the ^{13}C and ^{34}S isotopologues (Herzsprung P, 2014, Koch BP, 2007). Van Krevelen or elemental diagrams were used to visualize the chemical space FT-ICR MS data by plotting assigned molecular formulas according to their hydrogen to carbon (H/C) and oxygen to carbon (O/C) ratios (Van Krevelen, 1950). A number of parameters were calculated to gain information based on assigned molecular formulas. For instance, double bond equivalents (DBE), or the number of unsaturations plus rings in a molecule, were determined for assigned molecular formulas according to the equation below (Koch BP, 2016, Koch BP, 2006).

$$DBE = 1 + C - O - S - \tfrac{1}{2}(N + H) \quad (1)$$

An additional parameter, the modified aromaticity index (AI_{mod}), or the DBE to carbon ratio, was introduced to be indicative or aromatic structures in DOM when AI_{mod} is greater than 0.5 according to the following equation (7, 8).

$$AI_{mod} = DBE/C = (1 + C - O - S - \tfrac{1}{2}(N + H))/(C - O - N - S) \quad (2)$$

For compounds containing only carbon, hydrogen, and oxygen (CHO) the average carbon oxidation state (COS) was approximated by

$$COS = (2O - H)/C \quad (3)$$

where a formula with COS less than or equal to 0 is reduced and that greater than 0 is oxidized (Kroll JH, 2011).

Statistical Analyses and Data Visualization

Significant correlations between routine measurements of biological processes at BATS and CDOM-325 were tested using reduced major axis (or geometric mean) model II regression, using Matlab code provided by Ed Peltzer at MBARI, available at https://www.mbari.org/index-of-downloadable-files/, with standard deviation calculated according to Ricker (1973). *R*-values with *p*-values < 0.05, corresponding to 95% confidence, were considered statistically significant. Cross correlations were calculated using the fast Fourier transform-based cross correlation theorem, such that $f * g = \mathscr{F}[\overline{F}(\nu)\,\overline{G}(\nu)]$, where $f * g$ is the cross correlation of $f(t)$ and $g(t)$ and $\mathscr{F}$ is the Fourier transform applied to each column of data. The number of degrees of displacement of the first dataset relative to the second, or 'lags', was set to 20 (months), with the center lag set equal to zero. Cross correlation plots included 95% confidence boundaries. Further details on the methods of statistical analysis performed in this study are discussed in the Supplementary Information. All statistical analyses and plots were generated using Matlab (version 2014b; Mathworks)

References

AMACHER, J., NEUER, S. & LOMAS, M. 2013. DNA-based molecular fingerprinting of eukaryotic protists and cyanobacteria contributing to sinking particle flux at the Bermuda Atlantic time-series study. *Deep-Sea Research Part Ii-Topical Studies in Oceanography,* 93**,** 71-83.

BALCH, W. M., VAUGHN, J.M., GOES, J.I., NOVOTNY, J.F., DRAPEAU, D.T., BOOTH, E.S., VINING, C.L. 2007. Bio-optical consequences of viral infection of phytoplankton: 1 Experiments with the cyanobacterium, *Synechococcus* sp. *Limnology and Oceanography,* 52**,** 727-738.

BEALE, S. I. 2009. Biosynthesis of Chlorophylls and Hemes. *In:* HARRIS, E., STERN, D., AND WITMAN, G. (ed.) *The Chlamydomonas Sourcebook.* Academic Press.

BECKER, J. W., BERUBE, P. M., FOLLETT, C. L., WATERBURY, J. B., CHISHOLM, S. W., DELONG, E. F. & REPETA, D. J. 2014. Closely related phytoplankton species produce similar suites of dissolved organic matter. *Frontiers in Microbiology,* 5.

BIDIGARE, R. R., MARRA, J., DICKEY, T.D., ITURRIAGA, R., BAKER, K.S., SMITH, R.C., PAK, H. 1990. Evidence for phytoplankton succession and chromatic adaptation in the Sargasso Sea during spring 1985. . *Marine Ecology Progress Series 60,* 113-122.

BILLER, S. J., BERUBE, P. M., LINDELL, D. & CHISHOLM, S. W. 2015. Prochlorococcus: the structure and function of collective diversity. *Nature Reviews Microbiology,* 13**,** 13-27.

BILLER, S. J., SCHUBOTZ, F., ROGGENSACK, S.E., THOMPSON, A.W., SUMMONS, R.E., CHISHOLM, S.W. 2014. Bacterial Vesicles in Marine Ecosystems. *Science,* 343**,** 183-186.

BLOUGH, N. V. & DEL VECCHIO, R. 2002. Chromophoric DOM in the Coastal Environment. *In:* HANSELL, D. A. C., C. (ed.) *Biogeochemistry of Marine Dissolved Organic Matter.* Academic Press.

BREW, H. S., MORAN, S. B., LOMAS, M. W., BURD, A. B 2009. Plankton Community Composition, Organic Carbon and Thorium-234 Particle Size Distributions, and Particle Export in the Sargasso Sea. *Journal of Marine Research,* 67**,** 845-868.

CARLSON, C. A., DUCKLOW, H. W., HANSELL, D. A. & SMITH, W. O. 1998. Organic carbon partitioning during spring phytoplankton blooms in the Ross Sea polynya and the Sargasso Sea. *Limnology and Oceanography,* 43**,** 375-386.

CARLSON, C. A., MORRIS, R., PARSONS, R., TREUSCH, A. H., GIOVANNONI, S. J. & VERGIN, K. 2009. Seasonal dynamics of SAR11 populations in the euphotic and mesopelagic zones of the northwestern Sargasso Sea. *Isme Journal,* 3**,** 283-295.

DE MARTINI, F., NEUER, S., HAMILL, D., ROBIDART, J., LOMAS, M. 2017. Clade and Strain Specific Contributions of *Synechococcus* and *Prochlorococcus* to Carbon Export in the Sargasso Sea. *Limnology and Oceanography*.

DENG, W., MONKS, L., NEUER, S. 2015. Effects of Clay Minerals on the Aggregation and Subsequent Settling of Marine *Synechococcus*. *Limnology and Oceanography,* 60**,** 805-816.

DITTMAR, T., KOCH, B., HERTKORN, N., KATTNER, G. 2008. A simple and efficient method for the solid-phase extraction of dissolved organic matter (SPE-DOM) from seawater. . *Limnology and Oceanography Methods,* 6**,** 230-235.

DURAND, M., OLSEN, R., CHISHOM, S. 2001. Phtyoplankton Population Dynamics at the Bermuda Atlantic Time-series Study Station in the Sargasso Sea. *Deep Sea Research Part II,* 48**,** 1983-2003.

FERNANDEZ-PINOS, M., CASADO, M., CABALLERO, G., ZINSER, E., DACHS, J., PINA, B. 2015. Clade-Specific Quantitative Analysis of Photosynthetic Expression in Prochlorococcus. *Plos One*.

FLOMBAUM, P. E. A. 2013. Present adn future global distributions of the marine Cyanobacteria Prochlorococcus and Synechococcus. *Proceedings of the National Academy of Sciences of the United States of America,* 110**,** 9824-9829.

FOSS, P., GUILLARD, R.R.L., LIAAEN-JENSEN, S. 1984. Prasinoxanthin - a chemosystematic marker for algae. *Phytochemistry,* 23**,** 1629-1633.

GOLDBERG, S. J., CARLSON, C. A., BOCK, B., NELSON, N. B. & SIEGEL, D. A. 2010. Meridional variability in dissolved organic matter stocks and diagenetic state within the euphotic and mesopelagic zone of the North Atlantic subtropical gyre. *Marine Chemistry,* 119**,** 9-21.

GREEN, S. A. & BLOUGH, N. V. 1994. OPTICAL-ABSORPTION AND FLUORESCENCE PROPERTIES OF CHROMOPHORIC DISSOLVED ORGANIC-MATTER IN NATURAL-WATERS. *Limnology and Oceanography,* 39**,** 1903-1916.

HANSELL, D. 2002. DOC in the Global Ocean Carbon Cycle. *In:* HANSELL, D. A. C., C. (ed.) *Biogeochemistry of Marine Dissolved Organic Matter.* Academic Press.

HEDGES, J. I., KEIL, R. G. & BENNER, R. 1997. What happens to terrestrial organic matter in the ocean? *Organic Geochemistry,* 27**,** 195-212.

HERNES, P. J. & BENNER, R. 2002. Transport and diagenesis of dissolved and particulate terrigenous organic matter in the North Pacific Ocean. *Deep-Sea Research Part I-Oceanographic Research Papers,* 49**,** 2119-2132.

HERNES, P. J. & BENNER, R. 2006. Terrigenous organic matter sources and reactivity in the North Atlantic Ocean and a comparison to the Arctic and Pacific oceans. *Marine Chemistry,* 100**,** 66-79.

HERZSPRUNG P, E. A. 2014. Understanding molecular formula assignment of Fourier transform ion cyclotron resonance mass spectrometry data of natural organic matter from a chemical point of view. *Analytical and Bioanalytical Chemistry,* 406**,** 7977-7987.

KOCH BP, D. T. 2006. From mass to structure: An aromaticity index for high-resolution mass data of natural organic matter. *Rapid Communications in Mass Spectrometry,* 20**,** 926-932.

KOCH BP, D. T. 2016. Erratum: From mass to structure: An aromaticity index for high-resolution mass data of natural organic matter *Rapid Communications in Mass Spectrometry,* 30**,** 250.

KOCH BP, D. T., WITT M, KATTNER G 2007. Fundamentals of Molecular Formula Assignment to Ultrahigh Resolution Mass Data of Natural Organic Matter. *Analytical Chemistry,* 79**,** 1758-1763.

KROLL JH, E. A. 2011. Carbon oxidation state as a metric for describing the chemistry of atmospheric organic aerosol. *Nature Chemistry,* 3**,** 133-139.

KUJAWINSKI, E. B. 2011. The impact of microbial metabolism on marine dissolved organic matter: Insights from analytical chemistry and microbiology. *Annual Review of Marine Science,* 3**,** 567-599.

KUJAWINSKI, E. B., LONGNECKER, K., BAROTT, K.L., WEBER, R.J.M., SOULE KIDO, M.C. 2016. Microbial community structure affects marine dissolved organic matter composition. *Frontiers in Marine Science,* 3.

LOMAS, M. W. & MORAN, S. B. 2011. Evidence for aggregation and export of cyanobacteria and nano-eukaryotes from the Sargasso Sea euphotic zone. *Biogeosciences,* 8**,** 203-216.

MALMSTROM, R. R., COE, A., KETTLER, G.C., MARTINY, A.C., FRIAS-LOPEZ, J., ZINSER, E.R., CHISHOLM, S.W. 2010. Temporal dynamics of P*rochlorococcus* ecotypes in the Atlantic and Pacific oceans. *The ISME Journal,* 4**,** 1252-1264.

MARITORENA, S. & SIEGEL, D. A. 2005. Consistent merging of satellite ocean color data sets using a bio-optical model. *Remote Sensing of Environment,* 94**,** 429-440.

MOJIKA, K. D. A., HUISMAN, J., WILHELM, S.W., BRUSSAARD, C.P.D 2016. Latitudinal variation in virus-induced mortaility of phytoplankton across the North Atlantic Ocean. *The ISME Journal,* 10**,** 500-513.

NELSON, C. E. & CARLSON, C. A. 2012. Tracking differential incorporation of dissolved organic carbon types among diverse lineages of Sargasso Sea bacterioplankton. *Environmental Microbiology,* 14**,** 1500-1516.

NELSON, C. E., CARLSON, C. A., EWART, C. S. & HALEWOOD, E. R. 2014. Community differentiation and population enrichment of Sargasso Sea bacterioplankton in the euphotic zone of a mesoscale mode-water eddy. *Environmental Microbiology,* 16**,** 871-887.

NELSON, N. B., CARLSON, C. A. & STEINBERG, D. K. 2004. Production of chromophoric dissolved organic matter by Sargasso Sea microbes. *Marine Chemistry,* 89**,** 273-287.

NELSON, N. B. & SIEGEL, D. A. 2002. Chromophoric DOM in the Open Ocean. *In:* HANSELL, D. & CARLSON, C. (eds.) *Biogeochemistry of Marine Dissolved Organic Matter.* Academic Press.

NELSON, N. B. & SIEGEL, D. A. 2013. The Global Distribution and Dynamics of Chromophoric Dissolved Organic Matter. *Annual Review of Marine Science***,** 447-76.

NELSON, N. B., SIEGEL, D. A. & MICHAELS, A. F. 1998. Seasonal dynamics of colored dissolved material in the Sargasso Sea. *Deep-Sea Research Part I-Oceanographic Research Papers,* 45**,** 931-957.

ONDRUSEK, M. E., BIDIGARE, R. R., SWEET, S. T., DEFREITAS, D. A. & BROOKS, J. M. 1991. DISTRIBUTION OF PHYTOPLANKTON PIGMENTS IN THE NORTH PACIFIC-OCEAN IN RELATION TO PHYSICAL AND OPTICAL VARIABILITY. *Deep-Sea Research Part a-Oceanographic Research Papers,* 38**,** 243-266.

PARSONS, R. J., BREITBART, M., LOMAS, M. W. & CARLSON, C. A. 2011. Ocean time-series reveals recurring seasonal patterns of virioplankton dynamics in the northwestern Sargasso Sea. *The ISME Journal,* 2011**,** 1-12.

RICKER, W. E. 1973. Linear regressions in Fishery Research. *Journal of the Fisheries Research Board of Canada,* 30.

ROMERA-CASTILLO, C., SARMENTO, H., ALVAREZ-SALGADO, X. A., GASOL, J. M. & MARRASE, C. 2010. Production of chromophoric dissolved organic matter by marine phytoplankton (vol 55, pg 446, 2010). *Limnology and Oceanography,* 55**,** 1466-1466.

SIEGEL, D. A., MARITORENA, S., NELSON, N. B., BEHRENFELD, M. J. & MCCLAIN, C. R. 2005. Colored dissolved organic matter and its influence on the satellite-based characterization of the ocean biosphere. *Geophysical Research Letters,* 32.

SPRINTALL, J., TOMCZAK, M. 1992. Evidence of the barrier layer in the surface layer of the tropics. *Journal of Geophysical Research,* 97**,** 7305-7316.

STEDMON, C. A. & NELSON, N. B. 2015. The Optical Properties of DOM in the Ocean. *In:* HANSELL, D. A. C., C. (ed.) *Bioegeochemistry of Marine Dissolved Organic Matter* San Diego: Academic Press.

STEINBERG, D. K., CARLSON, C. A., BATES, N., JOHNSON R. J., F., M. A. & KNAP, A. H. 2001. Overview of the US JGOFS Bermuda Atlantic Time-series Study (BATS): a decade-scale look at ocean biology and biogeochemistry. *deep-Sea Research II,* 48**,** 1405-1447.

STEINBERG, D. K., NELSON, N. B., CARLSON, C. A. & PRUSAK, A. C. 2004. Production of chromophoric dissolved organic matter (CDOM) in the open ocean by zooplankton and the colonial cyanobacterium Trichodesmium spp. *Marine Ecology Progress Series,* 267**,** 45-56.

VAN KREVELEN, D. W. 1950. Graphical-Statistical Method for the Study of Structure and Reaction Processes of Coal. *Fuel,* 29**,** 228-269.

WEAR, E. K., CARLSON, C.A.,WINDECKER, L.A., BRZEZINKSI, M.A. 2015. Roles of diatom nutrient stress and species identity in determining the short-and-long-term bioavailability of diatom exudates to bacterioplankton. *Marine Chemistry,* 177**,** 335-348.

YANG, Y., MOTEGI, C., YOKOKAWA, T., NAGATA, T. 2010. Large-scale distribution patterns of virioplankton in the upper ocean. *Aquatic Microbial Ecology,* 60**,** 233-246.

ZHANG, F., HARIR, M., MORITZ, F., ZHANG, J., WITTING, M., WU, Y., SCHMITT-KOPPLIN, P., FEKETE, A., GASPAR, A., HERTKORN, N. 2014. Molecular and structural characterization of dissolved organic matter during and post cyanobacterial bloom in Taihuby combination of NMR spectroscopy and FTICR mass spectrometery. *Water Research,* 57**,** 280-94.

ZHAO, Z., GONSIOR, M., LUEK, J., TIMKO, S., IANIRI, H., HERTKORN, N., SCHMITT-KOPPLIN, P., FANG, X. T., ZENG, Q. L., JIAO, N. Z. & CHEN, F. 2017. Picocyanobacteria and deep-ocean fluorescent dissolved organic matter share similar optical properties. *Nature Communications,* 8.

ZHAO, Z., GONSIOR, M., SCHMITT-KOPPLIN, P., ZHAN, Y., ZHANG, R., JIAO, N. & CHEN, F. 2019. Microbial transformation of virus-induced dissolved organic

matter from picocyanobcteria: coupling of bacterial diversity and DOM chemodiversity. *The ISME Journal*.

Supplemental Information for Chapter 4

Methods

High Performance Liquid Chromatography (HPLC) Pigments Identification and Quantification

To obtain pigment samples, 4 liters of seawater were collected directly from niskin bottles (General Oceanics; Miami, USA) affixed to a rosette equipped with a conductivity, temperature and depth (CTD) sensor package (Seabird SBE 9/11 Plus) into pre-cleaned polycarbonate bottles (Nalgene) and were immediately filtered at a pressure of ≤ 5 inches Hg, through 0.7 μm, 47 mm glass fiber filters (Whatman, GF/F; Chicago, USA). The filters were then placed into aluminum foil and flash frozen in liquid nitrogen. Samples were subsequently stored at -80°C until analysis. Samples were analyzed by the Bermuda Atlantic Time-series Study (BATS) lab, according to methods outlined in Bidigare (1991) and Wright et al (1991) . For analysis, samples were extracted overnight at -20 °C in 5 mL of acetone (ACS grade; Fisher Scientific) and then an additional 5 mL of acetone was added to each sample. The HPLC system (Agilent 1100 Series with a Waters Spherisorb ODS2 silica-based reversed phased C_{18} column) was equilibrated with a primary solvent mixture (80:20, v:v, methanol: 0.5M ammonium acetate, aq., pH 7.2; Sigma HPLC grade > 99.99% purity) at a flow rate of 1 mL/min. A continuous gradient of 3 eluents was used (in decreasing order of polarity) consisting of the primary solvent mixture (Eluent A), 90:10 v:v acetonitrile:water (Eluent B; Sigma HPLC grade > 99.99% purity) and ethyl acetate (Eluent C; Sigma HPLC grade > 99.99% purity). A 1 mL aliquot of each sample was combined with 400 μL of de-ionized water, agitated and placed in the dark for 5 min. A sample volume of 200 μL was injected into the sample loop. Retention times and visible spectrum, referenced to certified standards (DHI Labs, Denmark) were used to determine the identity and concentration of pigments in each sample.

Picocyanobacteria Enumeration

Samples for picoplankton enumeration by flow cytometry (FCM) were collected, unfiltered, directly from Niskin bottles, into sterile 2.0 mL cryogenic vials (Thermo Scientific) and immediately fixed with paraformaldehyde (0.5% final volume; reagent grade; Sigma Aldrich). Samples were refrigerated for 1-2 hours and then stored in liquid nitrogen or at -80°C until analysis. A Becton Dickinson Influx cell sorter (BD Biosciences, NJ, USA) was used for the FCM analysis (ex = 488 nm; bandpass filters = 692 ± 20 nm and 580 ± 15 nm for chlorophyll *a* and phycoerythrin, respectively). 0.53 μm and 2.88 μm sized beads were used to perform daily calibrations (Spherotech Inc, USA). *Synechococcus* and *Prochlorococcus* were distinguished by size and whether phycoerythrin fluorescence was observed. Cell abundances were calculated using the volume analyzed method of Sieracki, Verity et al. (1993).

Virioplankton Dilution Experiment

Twenty liters of surface water was collected from Niskin bottles aboard the R/V Atlantic Explorer in June 2018 (cruise AE1819). Water samples were filtered through a 0.2 μm polycarbonate filter (Whatman, Chicago USA), concentrated using tangential flow filtration (TFF) with a 30 kDa cutoff to 500 mL to create viral lysate. The < 30 kDa

permeate was also retained. A four-point dilution series was created using the following ratios of lysate to permeate: A) 100% lysate; B) 50% lysate : 50% permeate; C) 25% lysate : 75% permeate; and D) 100% permeate. Samples were counted using epifluorescent microscopy to determine virioplankton abundance, according to the methods outlined in Parsons et al. (2011) and were analyzed using a Liquid Waveguide 50-cm spectrophotometer (World Precision Industries; FL, USA) to determine CDOM absorption coefficient (m^{-1}). A 35 salinity NaCl solution (Sigma NaCl, extra pure, combusted for 5 h at 450 °C) was used as the absorbance blank.

Statistical Analyses

Changes in the frequency domain of time series spectra were analyzed by generating evolutionary power spectra using the Lomb-Scargle algorithm for un-evenly spaced time-series data as follows:

$$P_x(\omega) = \frac{1}{2\sigma}\left\{\frac{\left[\sum_j (y_j-\bar{y})\cos\omega(t_j-\tau)\right]^2}{\sum_j \cos^2\omega(t_j-\tau)} + \frac{\left[\sum_j (y_j-\bar{y})\sin\omega(t_j-\tau)\right]}{\sum_j \sin^2\omega(t_j-\tau)}\right\}$$

where N is the number of data points for y(t), ω is the angular frequency (2πf), τ is an offset that allows $P_x\omega$ (the periodogram) to be independent of uneven time spacing and

$$\bar{y} = \frac{1}{N}\sum_{i=1}^{N} y_i$$

and

$$s^2 = \frac{1}{N-1}\sum_{i=1}^{N} (y_i-\bar{y})^2$$

are the mean and variance of the dataset, respectively. To observe the power spectra for all measured depths simultaneously, a '3D' Lomb-Scargle periodogram was compiled for 1 – 250 m depth by creating a filled contour plot with frequency ($days^{-1}$) on the x-axis, depth (m) on the y-axis and the unitless power intensity on the z-axis. Frequencies at statistically significant power intensities were converted to periods ($t = \omega^{-1}$).

Figures

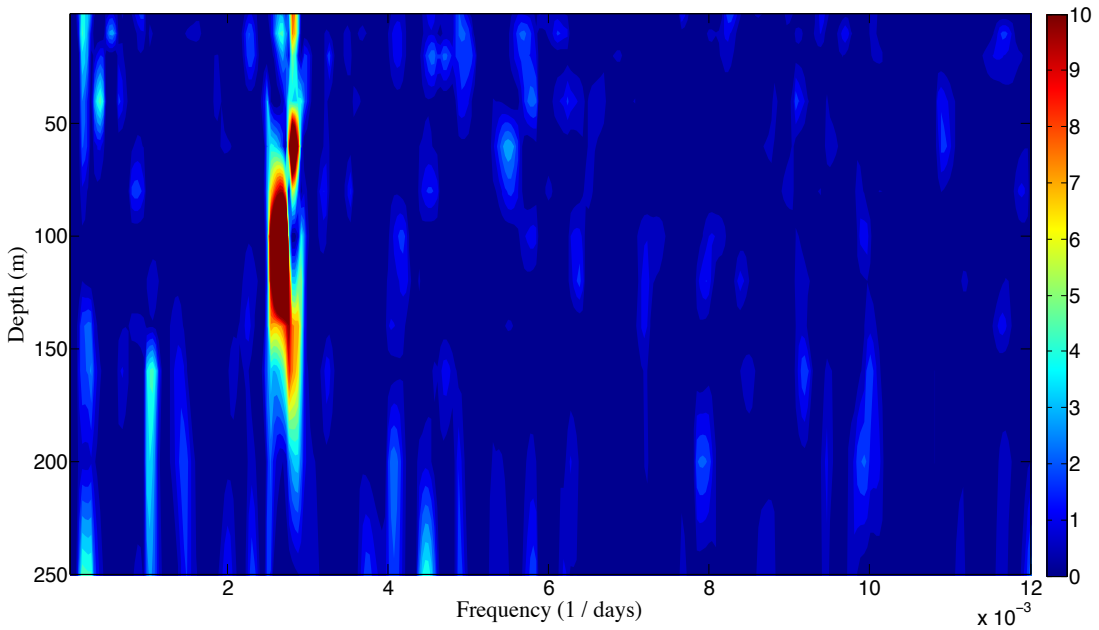

SI Figure 1. A Lomb-Scargle power spectrum for un-interpolated CDOM-325 data at each of 12 standard depths at BATS. Power intensity P_x is shown on the c axis and power intensities above 8 are within the 95% confidence interval. The x axis shows the frequency ($days^{-1}$), which is the inverse of the period.

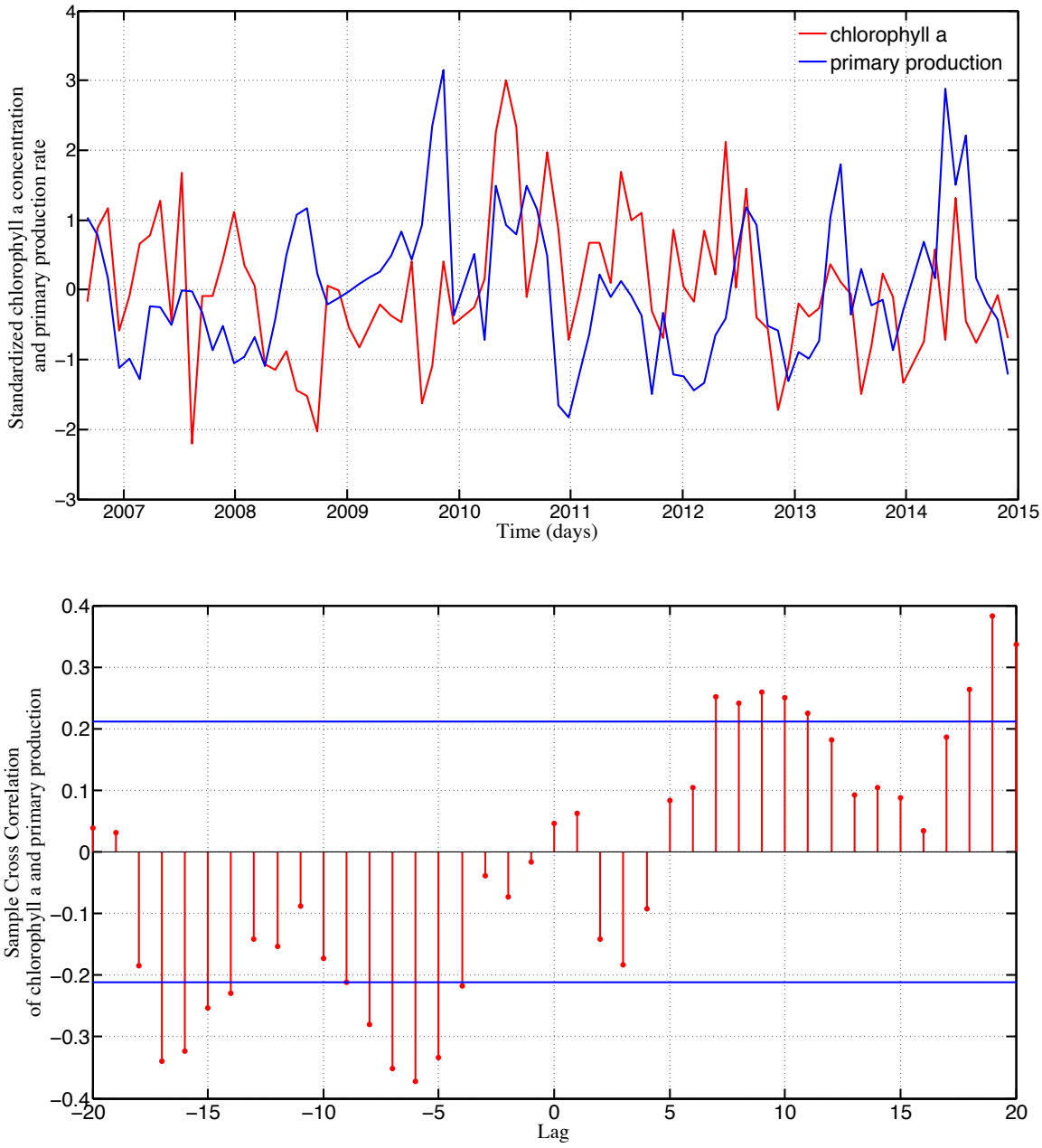

SI Figure 2. Top panel: Chlorophyll *a* (ng/kg; red line) and rate of primary production (mg C m^{-3} d^{-1}; blue line) at 80 m vs. time (days). Bottom panel: cross-correlation function of chlorophyll *a* and primary production at 80 m, with a time lag from 0 – 20 months. Red lines indicate the *R* value of the Pearson's correlation and blue lines indicate the 95% confidence interval.

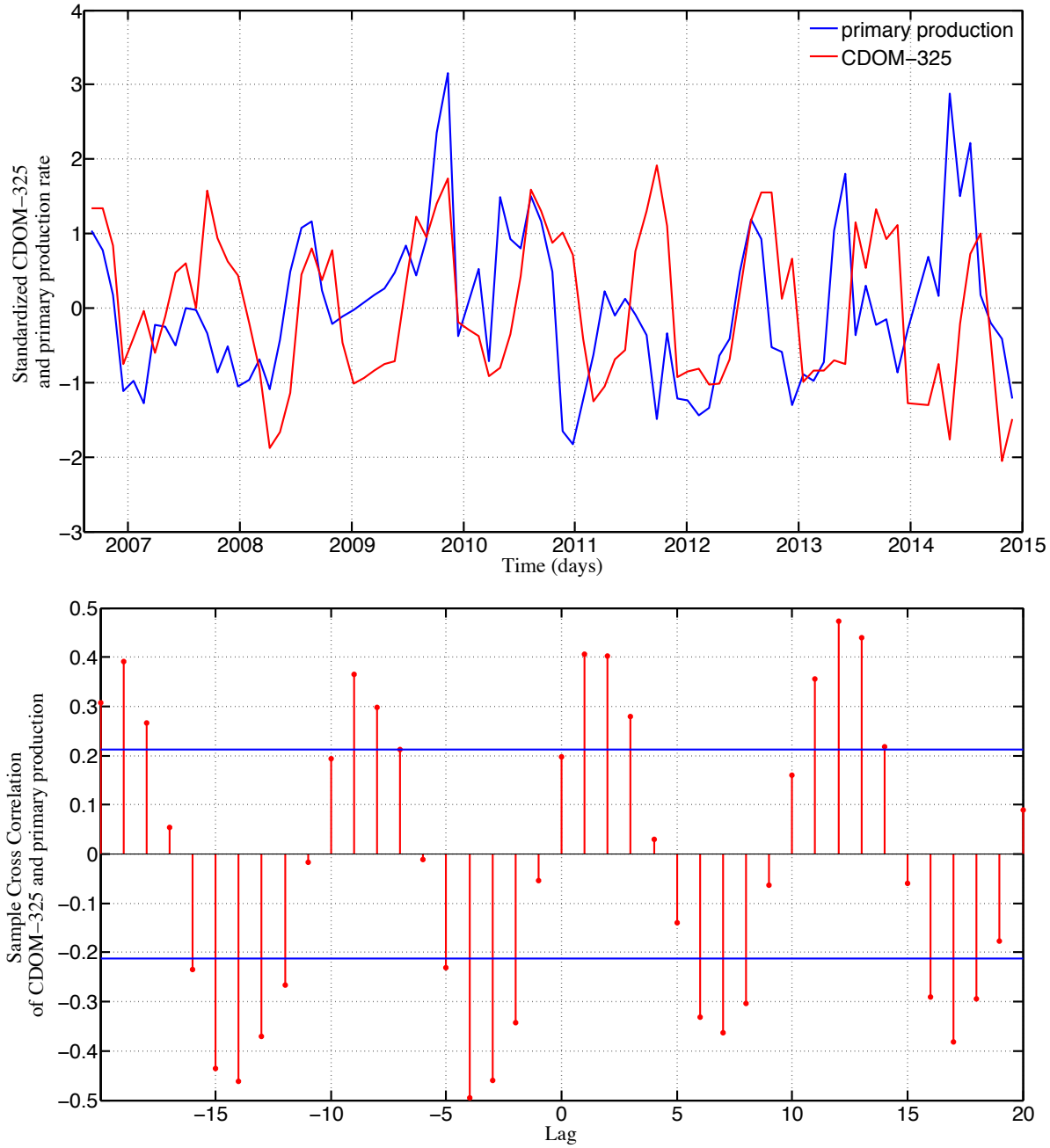

SI Figure 3. Top panel: CDOM-325 (m^{-1}; red line) and rate of primary production (mg C m^{-3} d^{-1}; blue line) at 60 - 100 m vs. time (days). Bottom panel: cross-correlation function of CDOM-325 and primary production, with a time lag from 0 – 20 months. Red lines indicate the *R* value of the Pearson's correlation and blue lines indicate the 95% confidence interval.

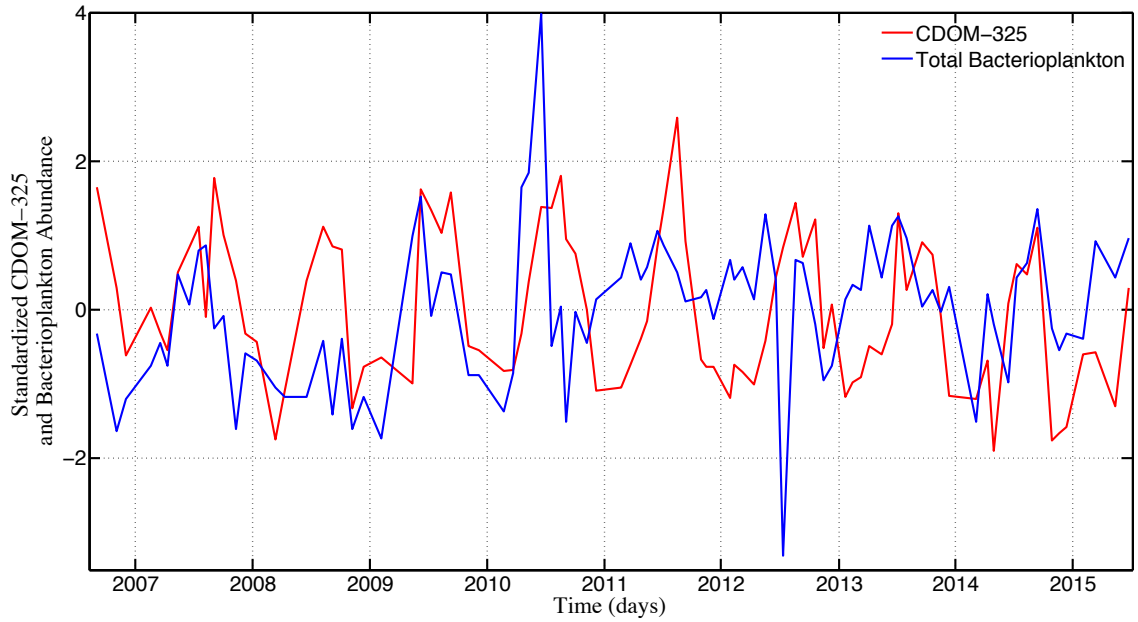

SI Figure 4. Average of 60 – 100 m CDOM-325 and total bacterioplankton (standardized) from BATS (June 2006 - 2015). Pearson's correlation: $R = 0.203$, $p = 0.537$.

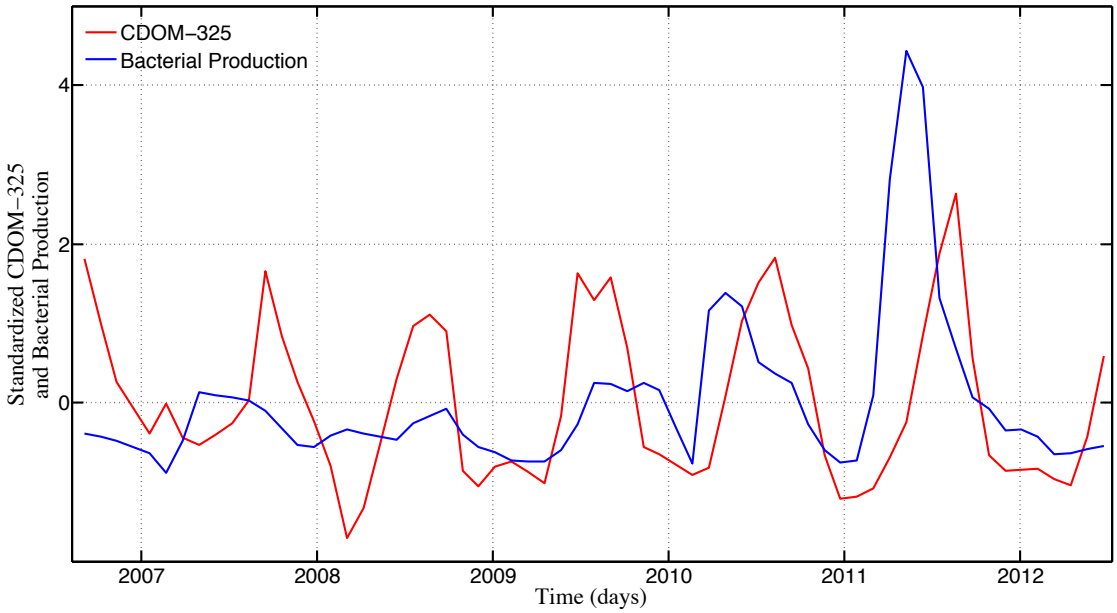

SI Figure 5. Average of 60 – 100 m CDOM-325 and rate bacterial production (standardized) from BATS (June 2006 – July 2012). Note that BP data was not available past July 2012.

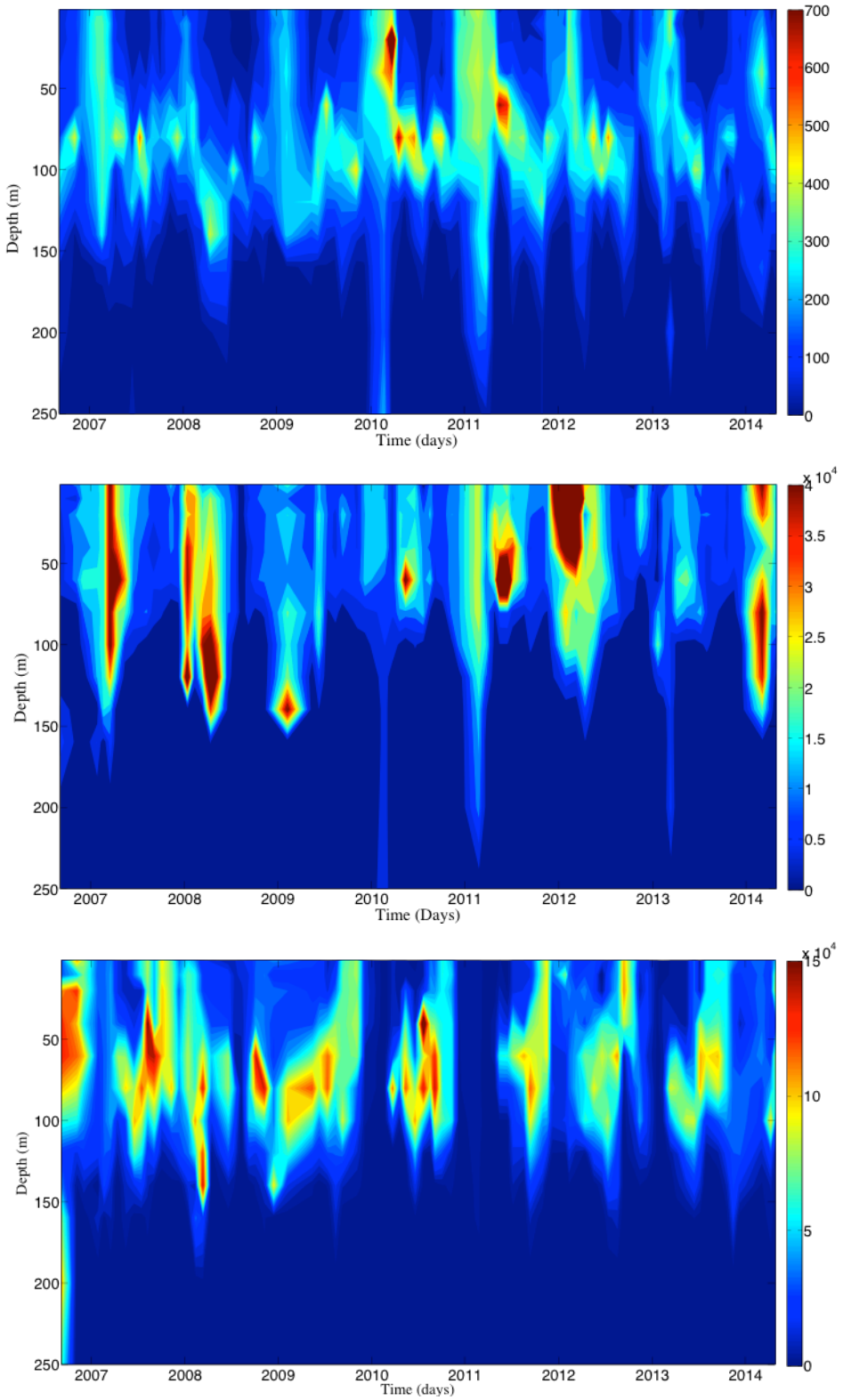

SI Figure 6. Time series of chlorophyll *a* concentration (ng L^{-1}; top panel), *Synechococcus* abundance (cells mL^{-1}; middle panel) and *Prochlorococcus* abundance (cells mL^{-1}; bottom panel) between 1 and 250 m between 2006 – 2014.

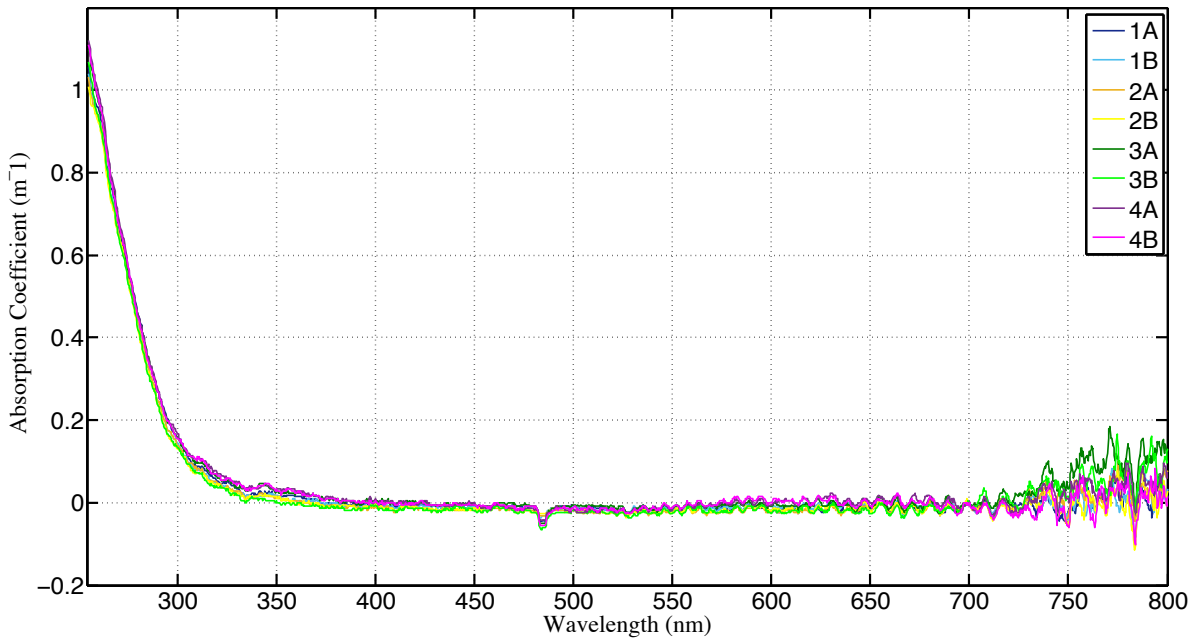

SI Figure 7. CDOM absorption coefficient (m^{-1}) vs. wavelength (nm). 'A' and 'B' denote duplicates of the same treatment. Treatments 1 – 4 are as outlined in SI *Methods*. Paired t-tests revealed no significant difference in absorbance between the samples ($p < 0.01$).

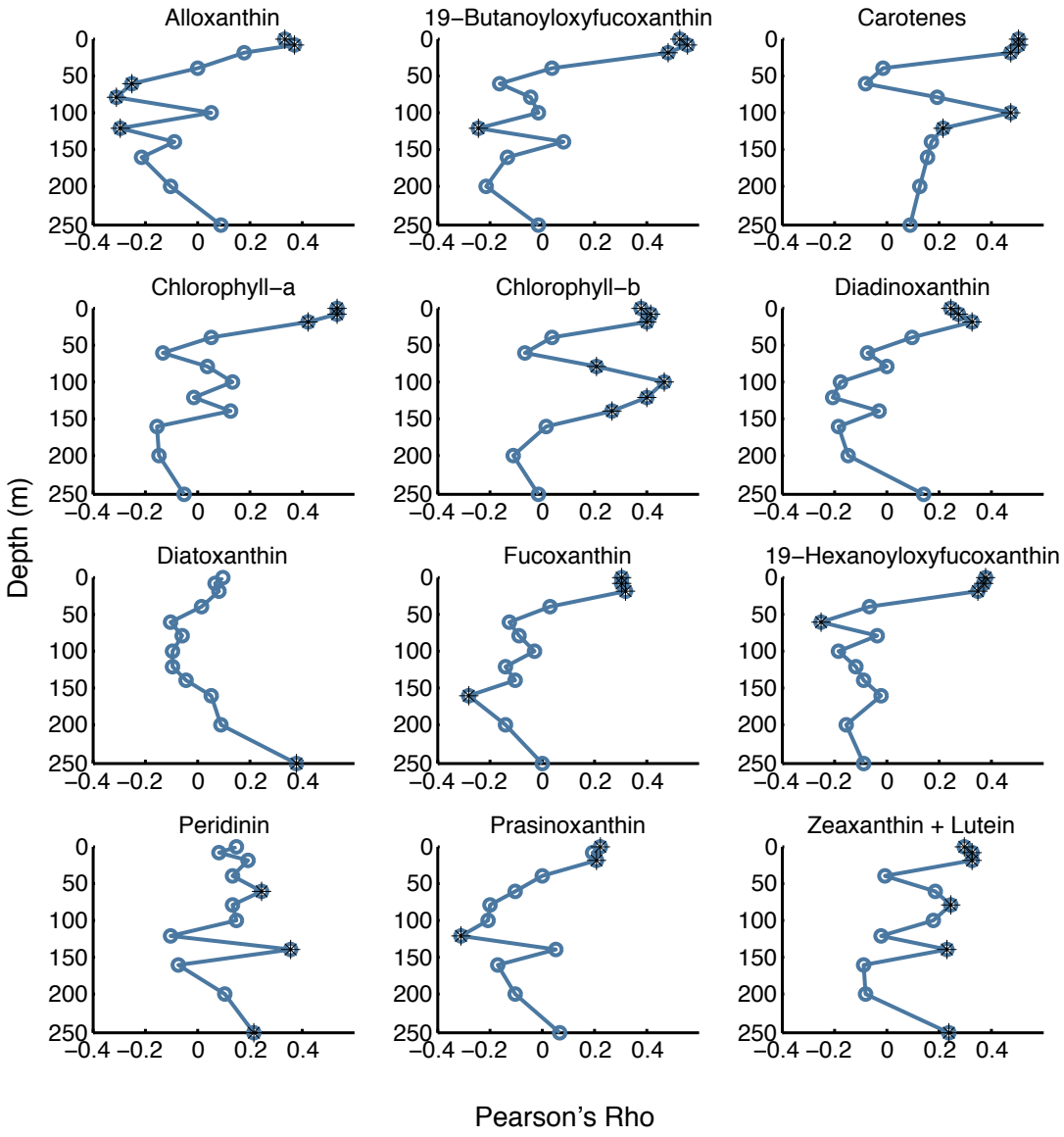

SI Figure 7. Distributions of Pearson's correlation coefficients with depth for CDOM-325 and 12 phytoplankton marker pigments, measured monthly at BATS. *R*-values are shown as solid blue lines. *R*-values, where corresponding *p*-values are < 0.05, are marked with asterisks, and are considered significant (Matlab v. 2014b; Mathworks).

Pigment	**Autotrophic Group**
Alloxanthin	Cryptophytes
19-Butanoyloxyfucoxanthin	Pelagophytes Prymnesiophytes
Carotenes (α + β)	All groups
Chlorophyll a	All groups
Chlorophyll b	Green Algae + *Prochlorococcus*
Diadinoxanthin	Dinoflagelletes

	Prymnesiophytes
Diatoxanthin	Dinoflagelletes Prymnesiophytes
Fucoxanthin	Diatoms Prymnesiophytes Pelagophytes Raphidophytes
19-Hexanoyloxyfucoxanthin	Prymnesiophytes
Peridinin	Autotrophic Dinoflagellates
Prasinoxanthin	Prasinophytes
Zeaxanthin + Lutein	Cyanobacteria (including *Prochlorococcus*) Chlorophytes Rhodophytes

SI Table 1. The twelve phytoplankton marker pigments measured monthly as part of the BATS program (See *Methods* for details) and associated phytoplankton groups.

Intensity		CHO		CHNO		CHOS	
weighted	PRO	O/C_{wt}	H/C_{wt}	O/C_{wt}	H/C_{wt}	O/C_{wt}	H/C_{wt}
averages		0.38 ± 0.10	1.4 ± 0.1	0.38 ± 0.09	1.2 ± 0.1	0.28 ± 0.13	1.7 ± 0.2
common	SYN	O/C_{wt}	H/C_{wt}	O/C_{wt}	H/C_{wt}	O/C_{wt}	$H/C_{wt}C$
formulas		0.40 ± 0.10	1.5 ± 0.2	0.40 ± 0.08	1.2 ± 0.2	0.35 ± 0.14	1.6 ± 0.2
Intensity	PRO	O/C_{wt}	H/C_{wt}	O/C_{wt}	H/C_{wt}	O/C_{wt}	H/C_{wt}
weighted		0.28 ± 0.12	1.6 ± 0.4	0.38 ± 0.15	1.6 + 0.3	0.35 ± 0.12	1.7 ± 0.3
averages							
unique	SYN	O/C_{wt}	H/C_{wt}	O/C_{wt}	H/C_{wt}	O/C_{wt}	H/C_{wt}
formulas		0.60 ± 0.23	1.5 ± 0.3	0.49 ± 0.14	1.2 ± 0.3	0.48 ± 0.08	1.8 ± 0.2
# formulas		CHO	CHNO	CHOS			
	Common	449	315	52			
	PRO	704	255	158			
	SYN	54	177	42			
PRO only	$Mass_{wt}$	O/C_{wt}	H/C_{wt}	DBE_{wt}	# formulas	$\%_{wt}$	
CHO	369 ± 93	0.33 ± 0.12	1.5 ± 0.3	6.2 ± 3.5	1153	67	
CHNO	393 ± 70	0.38 ± 0.13	1.3 ± 0.3	7.3 ± 2.9	570	26	
CHOS	353 ± 54	0.31 ± 0.13	1.7 ± 0.3	3.9 ± 2.3	210	8	
SYN only	$Mass_{wt}$	O/C_{wt}	H/C_{wt}	DBE_{wt}	# formulas	$\%_{wt}$	
CHO	369 ± 78	0.42 ± 0.13	1.5 ± 0.2	6.0 ± 2.2	503	38	
CHNO	355 ± 65	0.42 ± 0.10	1.2 ± 0.2	8.4 ± 2.3	492	49	
CHOS	271 ± 70	0.43 ± 0.13	1.7 ± 0.3	2.8 ± 1.9	94	13	

SI Table 2. Results of FT-ICR-MS analysis of *Synechococcus* and *Prochlorococcus* DOM, including assigned molecular formulae and common vs. unique formulae between the two genera.

Slide ID	Depth	Avg Count	Std	Avg Cell Vol
		VP/mL	VP/mL	μm^3
100% Lysate	0 m	9.5E+06	1.1E+06	11.30
50% Lysate	0 m	5.9E+06	2.7E+05	4.58
25% Lysate	0 m	4.0E+06	4.5E+05	11.27
Permeate	0 m	3.1E+05	5.0E+04	16.23

SI Table 3. Summary of virioplankton (VP) counts for the dilution experiment, as described in SI *Methods*.

References

BIDIGARE, R. R. 1991. *In:* HURD, S. A. (ed.) *The analysis and characterization of marine particles.* Washington, D.C.: American Geophysical Union.

PARSONS, R. J., BREITBART, M., LOMAS, M. W. & CARLSON, C. A. 2011. Ocean time-series reveals recurring seasonal patterns of virioplankton dynamics in the northwestern Sargasso Sea. *The ISME Journal,* 2011**,** 1-12.

SIERACKI, M. E., VERITY, P. G. & STOECKER, D. K. 1993. Plankton Community Response to Sequential Silicate and Nitrate Depletion During the 1989 North Atlantic Spring Bloom. *Deep-Sea Research Part Ii-Topical Studies in Oceanography,* 40**,** 213-225.

WRIGHT, S. W., JEFFREY, S. W., MANTOURA, F. C., LLEWELLYN, C. A., BJORNLAND, T., REPETA, D. AND WELSCHMEYER, N. 1991. Improved HPLC method for the analysis of chlorophylls and carotenoids from marine phytoplankton. *Marine Ecology Progress Series,* 77**,** 183-196.

CHAPTER 5: The Cycling of Deep Ocean Chromophoric Dissolved Organic Matter in the North Atlantic Subtropical Gyre

Abstract

The chromophoric, or light-absorbing, fraction of dissolved organic matter (CDOM) is an important component of the global carbon cycle, but its sources and transport pathways in the ocean are poorly constrained, especially in the bathypelagic zone. The primary source of CDOM to the deep North Atlantic is considered to be terrigenous material, entrained in subducted water masses such as the North Atlantic Deep Water (NADW). However, here, we present a model in which cell abundance of the picocyanobacteria *Prochlorococcus* in the euphotic zone accounts for ca. 30% of the variance in CDOM distribution in the bathypelagic, with a fractional contribution to variance equal to that of deep ocean total organic carbon concentration (ca. 35%). This suggests that *Prochlorococcus* POM may be exported to the deep ocean in the form of aggregated cells or in zooplankton fecal pellets, and is remineralized to form an important component of the deep CDOM pool. The significant correlative relationship between deep CDOM and euphotic zone *Prochlorococcus* abundance indicates the potential for deep CDOM as a tracer of organic carbon export to the bathypelagic zone and highlights a new potential role for *Prochlorococcus* in deep ocean carbon storage.

Introduction

The dissolved organic carbon (DOC) reservoir in the oceans (ca. 660 Pg) is roughly equivalent to the amount of inorganic carbon in the atmosphere (Carlson and Hansell, 2015, Hansell, 2009, Hansell, 2012) and as such, plays an important role in global carbon cycling. A multitude of studies over the past few decades have sought to characterize the ocean organic carbon cycle (Hansell and Carlson, 1998, Nelson et al., 2004, Hansell, 2009, Fasham et al., 2001, Lomas et al., 2010). Many of these studies have focused on dissolved organic matter (DOM) – particularly the light-absorbing, or chromophoric, fraction of dissolved organic matter (CDOM) – due to its role in a range of biogeochemical processes. The impact of CDOM on ocean processes ranges from the regulation of light availability for photosynthesis to serving as an intermediary in chemical reactions, such as the photooxidation of methylated sulfur compounds (Nelson and Siegel, 2002, Nelson et al., 2007, Stedmon and Nelson, 2015, Del Vecchio and Blough, 2002). While many studies have focused on coastal regions, the sources, transport and fate of CDOM in the open ocean, especially in the bathypelagic, are less well understood. In the Pacific and Indian Oceans, there is a strong correlation between CDOM and indicators of organic matter remineralization (apparent oxygen utilization (AOU)), but this correlation is absent in the Atlantic below the euphotic zone (Nelson et al., 2007, Nelson, 2016). Similarly, deep ocean CDOM concentrations in the North Atlantic are elevated (ca. 0.15 m^{-1}) relative to surface waters in the same region, but do not exhibit the high values (> 0.2 m^{-1}) found in the main thermocline of the North Pacific and North Indian Ocean. However, below 2000 m, an average value of ~0.15 m^{-1} is observed globally for CDOM at 325 nm (Nelson and Siegel, 2013). Studies have suggested that deep CDOM in the North Atlantic is allochthonous and is transported to

the subtropical gyres via water mass advection, involving the Antarctic Intermediate Water (AAIW) and North Atlantic Deep Water (NADW). However, vertical distributions of CDOM in the deep North Atlantic are homogenous and show no correlation with *p*CFC-derived water age, which has been attributed to overturning of water masses by isopycnal mixing (Nelson et al., 2007). Terrigenous markers such as lignin are present at depth throughout the NADW and have been cited as evidence for allochthonous deep CDOM; however, the majority of lignin in the North Atlantic exists as POM, likely from atmospheric deposition. Concentrations of lignin phenols in North Atlantic DOM are low (mean for NADW = 39.08 ng L^{-1}), and terrigenous DOC is thought to comprise only 1-2% of DOC in the North Atlantic (Hernes and Benner, 2006). This suggests that while subduction and advection are important mechanisms of DOC export to the deep ocean, the bulk of deep DOM in the North Atlantic Subtropical Gyre does not originate from terrestrial sources.

The primary mechanism for export of organic material to the deep ocean is the sinking of biogenic particles (Carlson et al., 2010, Boyd, 1999), and the leaching of DOM from this particle flux may form a source of deep ocean CDOM. To date, CDOM studies have provided geographical coverage throughout the North Atlantic (Nelson et al., 2007, Carlson et al., 2010, Swan, 2012), but have not allowed for the investigation of short-term (monthly) temporal variations in deep CDOM. In this study, we provide a stationary decadal time-series of CDOM absorbance measurements from the Bermuda Atlantic Time Series Study (BATS) site (31° 40' N; 64° 10' W), showing homogeneity in depth profiles of CDOM from 1 m to depths of 3000 m. Additionally, the entire depth profile exhibits pronounced oscillations in CDOM absorbance with time. The periodicity of these oscillations cannot be explained by the advection of allochthonous material to the deep ocean via the NADW. Using this dataset, we investigate whether autochthonous inputs, including organic particle flux, contribute to the deep CDOM reservoir in the North Atlantic.

Results and Discussion

A decadal time series of CDOM absorbance measurements (m^{-1}; 325 nm; Figure 1) was collected at BATS (2006-2015) and reveals that in the upper mesopelagic, a local CDOM minimum is evident between ~ 250 – 500 m, related to the presence of the advected Subtropical Mode Water (STMW), which is highly photobleached at the surface before subduction (Nelson et al., 1998, Nelson et al., 2007). Below the STMW, a region of elevated CDOM absorbance is evident between 700 m and 3000 m. CDOM absorbance values at 700 m are significantly correlated with values at all lower depths measured at the same time point, indicating a vertical continuity of CDOM through the water column (Figure 2). A Pearson's correlation between CDOM measurements at depths from 700 to 3000 m reveals a mean R value of 0.6068 ($p < 0.001$). A period of 3.91 years (calculated using a Morlet wavelet; Wavelet Toolbox, Matlab2014b; Mathworks) is observed for the decadal time series; however, the average CDOM sampling rate of 34 days and the significant direct correlations between CDOM measurements at all nine discrete depths between 700 and 3000 m suggest that the transfer of chromophoric organic matter from the mesopelagic to the bathypelagic takes place on a monthly timescale. This far exceeds

the timescale on which DOM is transported to the deep ocean, which takes place on annual to multi-decadal timescales. However, DOM can be released from particulate aggregates or fecal pellets as particles sink to the deep ocean (Boyd, 1999, Hansell, 2001) and therefore suggests that the mechanism behind elevated CDOM and consistency from 700-3000 m includes the flux of particulate organic carbon (POC). McDonnell et al. (2010, 2011) found that although sinking rates for particles at BATS were generally lower than in other ocean basins such as the Antarctic (with sinking rates in May at BATS of only 12 – 29 m d^{-1}), rates of up to 316 m d^{-1} were observed in September, especially for the smallest particle size class (~100 μm equivalent spherical diameter).

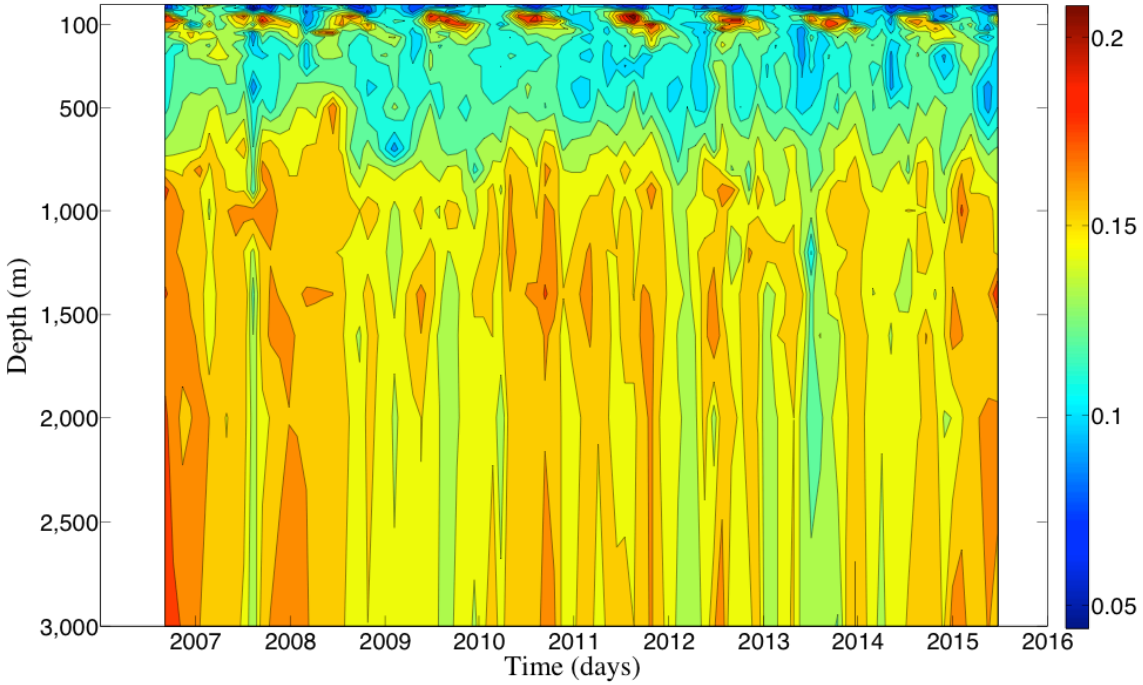

Figure 1. A time series of CDOM at 24 discrete depths throughout the water column at BATS, between 2006 and 2015. The color bar represents absorption coefficient (m^{-1}) at 325 nm.

Sinking rates such as this are more than sufficient to allow particulate matter to reach the bathypelagic in the late summer/fall, when a CDOM maximum is observed in both the epipelagic and bathypelagic.

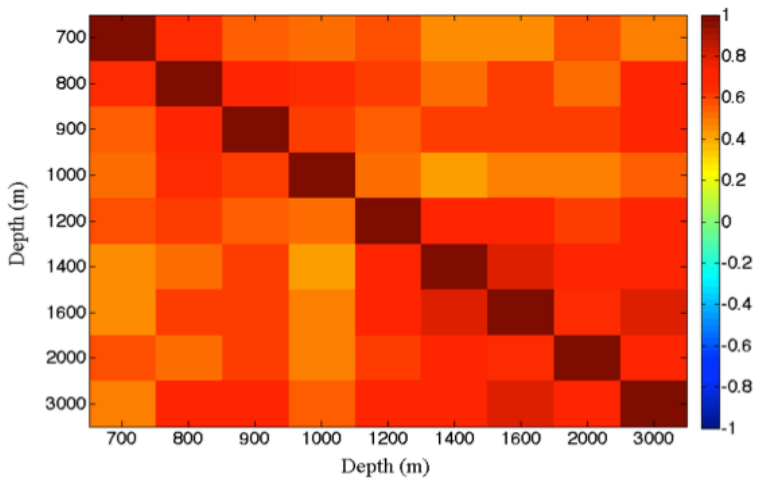

Figure 2. A correlation matrix for CDOM at depths between 700 and 3000 m. The z-axis, as shown by the color bar, represents *R* values between -1 and 1. Values of *p* were < 0.01 for all correlations.

Organic carbon flux rate (C_{org}) measurements from 150 m sediment traps (C_{org150}) deployed at BATS are not statistically different from deep trap data (1500 m and 3200 m at the Ocean Flux Program site; (31° 50' N, 64° 10' W) (Conte, 2001) and can be used as a proxy for deep ocean C_{org} flux. However, the C_{org150} data from 2006 – 2015 reveal that no significant correlation between deep CDOM and C_{org150} is evident, and a cross-correlation analysis reveals that there is no significant indirect correlation between these parameters. However, the maximum C_{org150} values at BATS occur during the spring bloom, and as rates of particle sinking are relatively slow during this period, this flux may not be transported to the deep ocean. Additionally, it is likely that only a portion of POC flux is soluble and leaches into the water as DOM and that only a fraction of that DOM is chromophoric (Stedmon and Nelson, 2015).

Another possible reason for the disconnect between C_{org} and deep CDOM is that *Prochlorococcus* abundance, which is not directly correlated with C_{org}, may contribute to the CDOM signal in the deep ocean. While both *Prochlorococcus* and *Synechococcus* have been shown to produce CDOM *in vitro*, at BATS, only the cell abundance of *Prochlorococcus* correlates strongly with CDOM in the upper water column, and like CDOM, exhibits an annual maximum at ca. 60 – 80 m between August and October. C_{org} flux at 150 m also exhibits an annual periodicity (T = 361.01 days), but is not well correlated with *Prochlorococcus* abundance and instead corresponds to *Synechococcus* and phytoplankton abundance during the annual spring bloom. The lack of significant correlation between CDOM and *Synechococcus* in either the upper water column or below 500 m, suggests that this genus does not contribute to CDOM cycling in the deep ocean (unpublished data). Although the sinking velocity of *Synechococcus* aggregates in laboratory studies were found to be up to 440 m d^{-1} (Deng, 2015), *in situ* studies at BATS showed that during months of maximum *Synechococcus* abundance, sinking velocities were over an order of magnitude lower (McDonnell, 2010). The number of *Prochlorococcus* cells exported during the summer months (> 10^5 cells cm^{-3}) surpasses the number of other autotrophic cells exported during the spring bloom (Brew, 2009); additionally, recent studies have not only shown evidence of *Prochlorococcus* cells in

sediment traps but have estimated that they comprise up to 33% of total POC export at BATS (Lomas and Moran, 2011, Amacher et al., 2013). Furthermore, McDonnell et al. showed that rates of particle sinking do not follow Stokes equation predictions and that the sinking rate appears to increase with decreasing particle size (McDonnell, 2011). Therefore, *Prochlorococcus* cells, with a diameter of only 0.5 – 0.7 μm (Biller et al., 2015), have the potential to sink rapidly throughout the water column to the deep ocean. However, although significant, the correlations between *Prochlorococcus* in the euphotic zone and CDOM at depths below 500 m are weak (mean $R = 0.3427$; $p < 0.05$) and suggest that *Prochlorococcus* export alone cannot account for the deep CDOM signal.

Deep ocean DOC in the North Atlantic has a wide range of reactivities and lifetimes, on the order of months to thousands of years (Hansell, 2012, Dittmar, 2015, Hawkes et al., 2015). Although particle flux plays an important role in the export of organic carbon to the deep ocean, POC comprises less than 14% of TOC (1 – 250 m) during the spring bloom at BATS in the Sargasso Sea, and even less during other seasons (Carlson et al., 1998). Therefore, TOC measurements are largely comprised of DOC at BATS, with deep TOC comprised of both new carbon inputs and accumulated carbon that persists over longer timescales (Druffel, 1996, Hansell et al., 2009). No significant correlation (Pearson's correlation analysis; $p > 0.05$) was evident between TOC and CDOM in the deep ocean. This is likely because CDOM represents only a fraction of TOC and they do not share the same temporal pattern. Older, more stable TOC contains fewer labile aromatic groups and is therefore less likely to be chromophoric (Stedmon and Nelson, 2015).

The presence of the Antarctic Intermediate Water (AAIW) and the North Atlantic Deep Water (NADW) at depth at BATS has led researchers to posit that the deep ocean CDOM signal is the result of the horizontal advection of terrigenous material via these subducted water masses (Carlson et al., 2010, Nelson et al., 2007). However, there is no significant correlation between CDOM and potential density anomaly (σθ) for the depth range of 600 – 4200 m, suggesting that density gradients do not directly influence CDOM behavior in the deep ocean. Neutral density surfaces (γ^n) were calculated for depths between 600 and 4200 m (*Methods*; Table

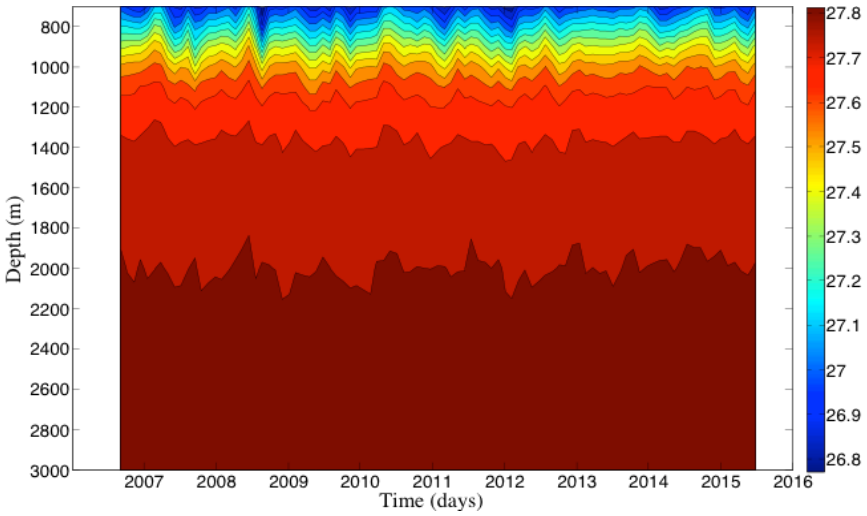

Figure 3. Potential density anomaly (σθ; kg/m^3) at depths of 700 to 3000 m between 2006 and 2015.

1) and Pearson's correlation coefficients were calculated for γ^n and CDOM at matching depths; however, no significant correlations were found.

Layer	Abbreviation	γ^n	Depth range at BATS (m)
Lower Thermocline	LTCL	26.60 – 27.00	600 – 800
Upper Antarctic Intermediate Water	uAAIW	27.00 – 27.50	600 – 1000
Lower Antarctic Intermediate Water	lAAIW	27.50 – 27.80	900 – 1200
Labrador Sea Water	LSW	27.80 – 27.975	1100 – 2000
Iceland-Scotland Overflow Water	ISOW	27.975 – 28.05	2000 – 3000
Denmark Strait Overflow Water	DSOW	28.05 – 28.14	3000 – 4200

Table 1. Values of γ^n and corresponding water mass layers, as outlined in Nelson et al (2007) and the depth ranges in which these layers are present at BATS, during the period from June 2006 to June 2015.

No single variable has been identified that correlates strongly with CDOM in the deep ocean at BATS; however, it is possible that a combination of parameters together contribute to the deep CDOM signal. C_{org}, TOC, potential density and *Prochlorococcus* abundance each possibly contribute to the ocean CDOM pool in some way. As such, a model was created incorporating weighted contributions of these measurements. As none of these parameters account for the period of ca. 3.91 years noted for CDOM at all depths below 500 m, an additional variable was added to the model to represent interdecadal variation, consisting of a cosine wave fitted to the averaged CDOM time series signal for depths of 700 – 3000 m, with an amplitude (A) of 0.015, a period of 1427.15 days and a phase shift (φ) of 2190 as follows in Eq. 1.

$$y = A^* \cos((2\pi/1427.15)x - \varphi) + 0.155, \qquad \text{Eq. (1)}$$

where x represents the dates on which CDOM measurements were collected and 0.155 is the midline. The curve was time-interpolated and standardized (see *Methods*). We first posited a model that entailed the sum of 5 variables over time: C_{org}, TOC, $\sigma\theta$, *Prochlorococcus* abundance and y. Additionally, x_1, x_2, x_3, x_4, and x_5 were chosen to represent the unknown fractional contributions of each parameter, such that

$$CDOM_{mod} = x_1 Pro60 + x_2 C_{org150} + x_3 \sigma\theta_d + x_4 TOC_d + x_5 y \qquad \text{Eq. (2)}$$

and

$$x_1 + x_2 + x_3 + x_4 + x_5 = 1, \qquad \text{Eq. (3)}$$

where $CDOM_{mod}$ represents the modeled CDOM absorption coefficient at discrete depths, *d*; Pro_{60} is *Prochlorococcus* cell abundance at 60 m; C_{org150} is the organic carbon flux (mg m^{-2} d^{-1}) at 150 m, obtained from sediment trap data; $\sigma\theta_d$ (kg m^{-3}) is the potential density anomaly at *d*; TOC_d is the total organic carbon concentration (µmol kg^{-1}) at *d* and *y* is the harmonic oscillator represented by Eq. 1.

Fractional contributions were first weighted equally, yielding the reduced equation:

$$CDOM_{mod} = (Pro_{60} + C_{org150} + \sigma\theta_d + TOC_d + y)*0.2 \quad \text{Eq. (4)}$$

$CDOM_{mod}$ obtained using Eq. 4 was significantly, but only weakly correlated with CDOM for all measured depths between 700 and 3000 m (mean $R = 0.3489$ and $p < 0.01$). The cross correlation of $CDOM_{mod}$ and CDOM at 1400 m is shown in Figure 4.

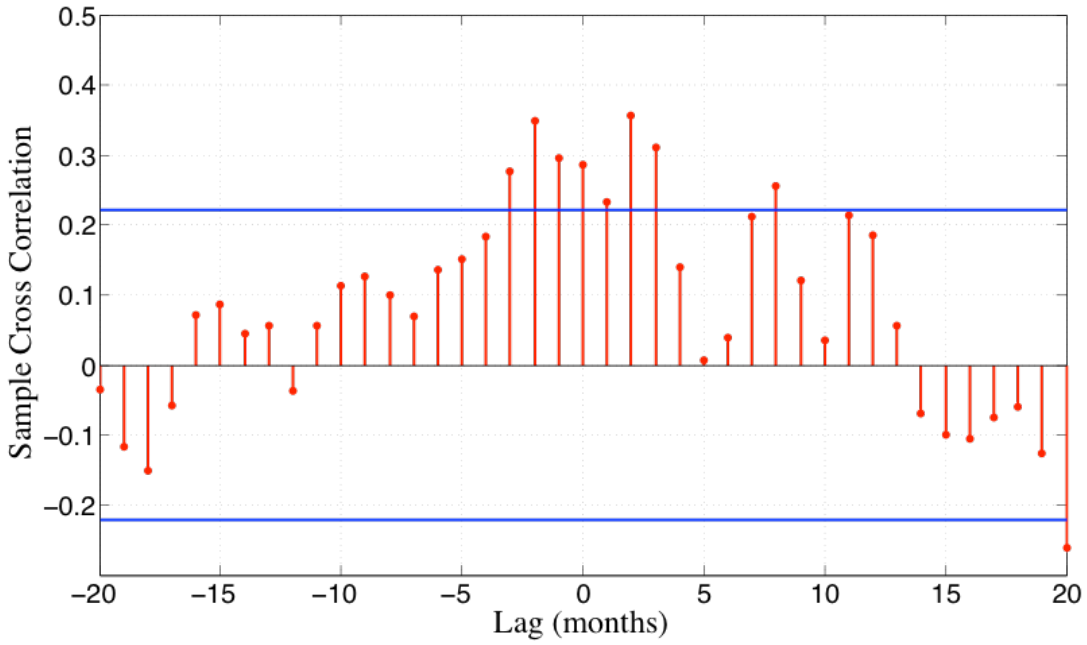

Figure 4. Cross-correlation of CDOM and $CDOM_{mod}$ at 1400 m derived using Eq. 4. Blue lines represent the 95% confidence interval.

Different weighting was then tested to determine the optimal fractional contributions and to attempt to improve the model. To determine if any components of the model were not critical, a principal component analysis of the 5 variables was performed (Figure 5). It was observed that the first principal component accounted for 29.28% of variance and was dominated by Pro_{60}. In the second principal component, $\sigma\theta_d$ and y were the most important factors. C_{org150} was indirectly correlated with Pro_{60} in PC1, which is due to the seasonal lag between the Spring bloom and the *Prochlorococcus* maximum in the early fall. Upon the removal of the C_{org150} component, the variance ascribed to PC1 remained ca. 30% and the model improved by ca. 10% (Figure 6). However, the incompatibility of C_{org150} with the model does not preclude the sinking and leaching of *Prochlorococcus* cells, as it has been shown that *Prochlorococcus* is under-represented in traps (Amacher et al., 2013).

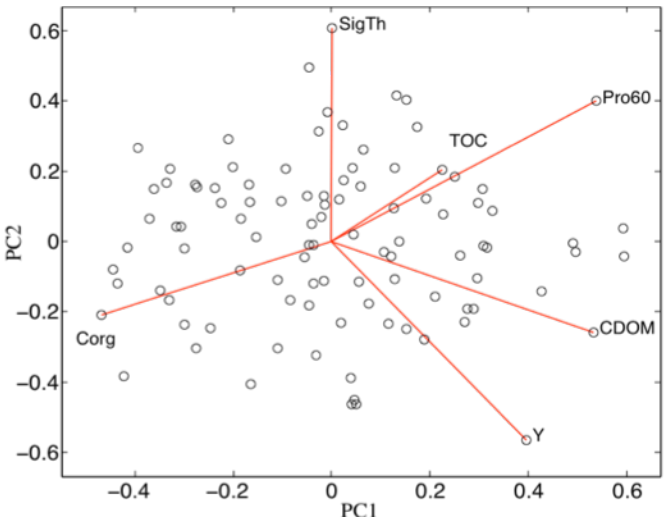

Figure 5. Principal component analysis of the 5 variables used in Eq. 4. Circles represent principle component scores as the representation of the data matrix in principal component space. Red lines represent vectors of the observed variables.

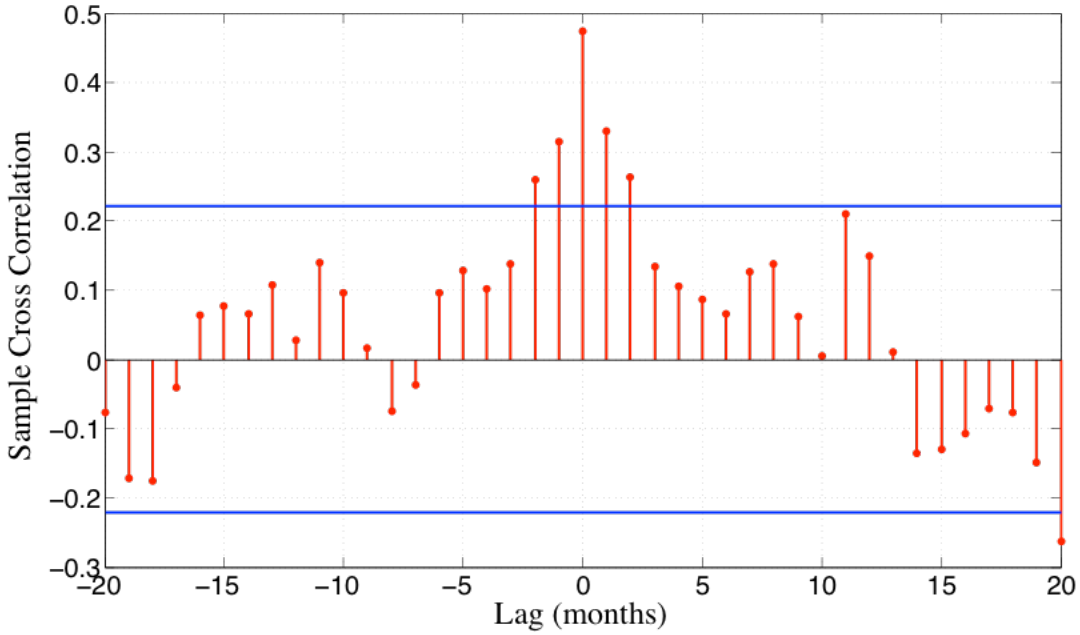

Figure 6. Cross correlation between CDOM and $CDOM_{mod}$ at 1400 m, derived using Eq. 5, which excludes C_{org} from the model. The *R* value has increased from 0.2865 (derived using Eq. 4) to 0.4736 ($p < 0.01$).

The fractional contributions of each remaining component were then optimized to yield the following equation:

$$CDOM_{mod} = 0.35 * Pro_{60} + 0.1 * \sigma\theta_d + 0.35 * TOC_d + 0.2 * y \qquad \text{Eq. (5)}$$

The final model yields a mean *R* of 0.4464 ($p < 0.01$) for measured CDOM depths between 700 and 3000 m. The inclusion of TOC_d and $\sigma\theta_d$ slightly improves the correlation ($R = 0.4736$ and $p < 0.01$ for 1400 m whereas using only Pro_{60} and *y*, $R = 0.4637$ and $p < 0.01$), and the plots of modeled CDOM show that Eq. 5 closely resembles the observed CDOM measurements (Figure 7).

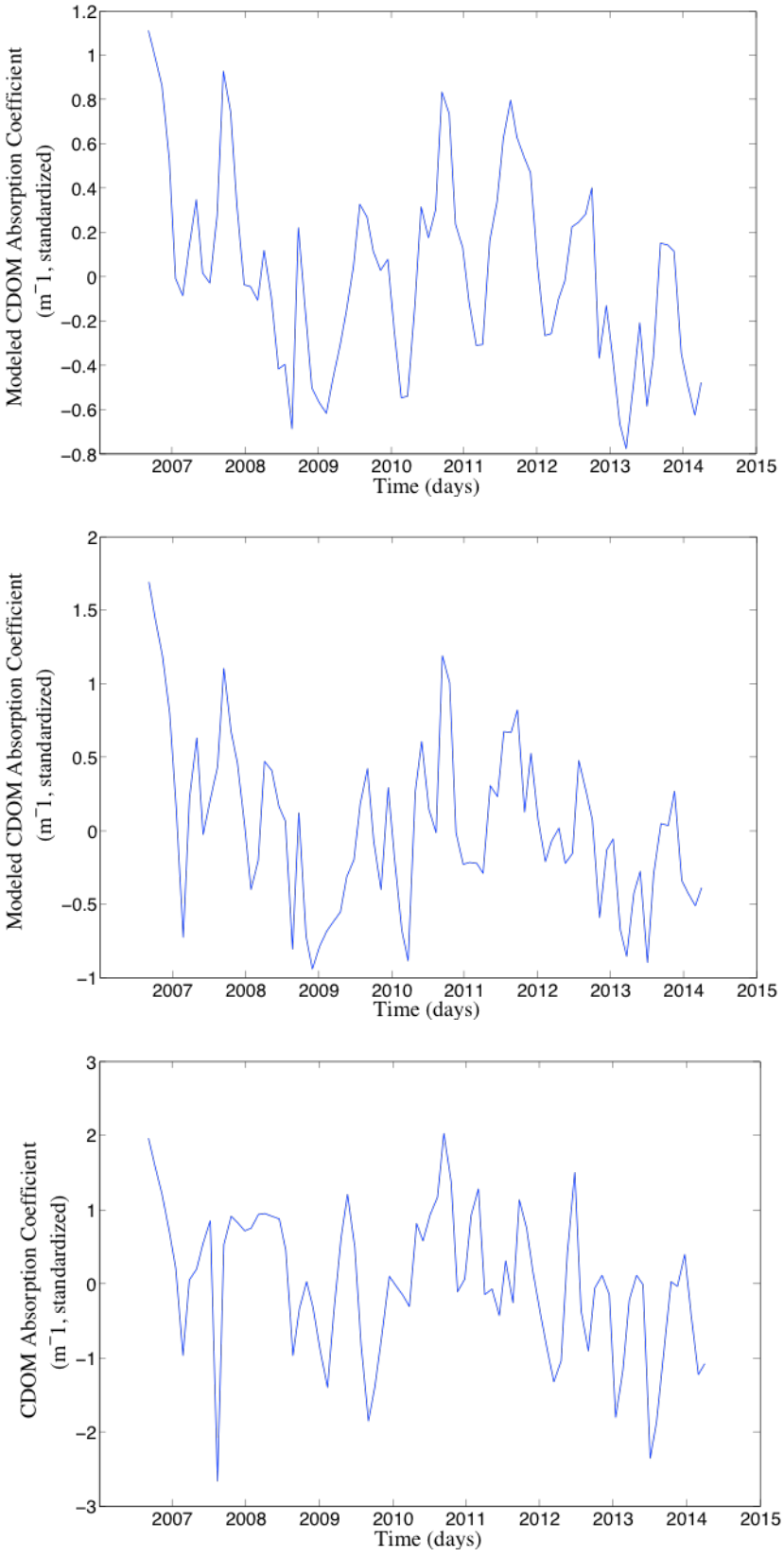

Figure 7. Modeled CDOM at 1400 m derived using only Pro_{60} and y is shown in the top panel. Modeled CDOM at 1400 m derived using Equation 5 is shown in the middle panel and the bottom panel shows CDOM measured from discrete bottle samples at 1400 m.

The model (Eq. 5) indicates that deep ocean CDOM concentrations are significantly correlated with a combination of *Prochlorococcus* abundance at 60 m and a background layer of TOC (largely in the form of DOC). Although the contribution of *Prochlorococcus* to total POC export was originally reported to be negligible due to the small size of the organism (Michaels, 1988), recent studies have shown that *Prochlorococcus*, in the form of aggregates or fecal pellets, can comprise between 1 and 20% of POC flux as measured in sediment traps (Lomas and Moran, 2011, Amacher et al., 2013). The temporal variability exhibited in the deep CDOM signature suggests that *Prochlorococcus*-derived CDOM does not accumulate in the deep ocean and is degraded by some mechanism, leaving a reduced, background layer of organic material, which is likely comprised of a combination of recalcitrant authochthonous CDOM and material advected via the NADW. The contribution of the Pro_{60} component to the model is in agreement with *in vitro* studies that have demonstrated CDOM production by picocyanobacteria; however, while previous studies have demonstrated the chromophoric nature of *Synechococcus*-derived DOM *in vitro* and C_{org} is significantly correlated with *Synechococcus* abundance at BATS, the model is weakened by the addition of the C_{org} parameter. The absence of a significant correlation between CDOM and sediment trap-derived organic carbon flux at BATS indicates that *Synechococcus* does not directly contribute to the deep CDOM pool. A smaller number of *Synechococcus* cells are exported than *Prochlorococus*, but the cells are considerably larger (Lomas and Moran, 2011). The result is that both *Synechococcus* and *Prochlorococcus* contribute equally to POC at BATS (ca. 33% of total POC standing stock each) (Lomas and Moran, 2011, DuRand, 2001). However, it is possible that *Synechococcus*-derived DOM is exported to the mesopelagic but not to the deep ocean. While multiple studies at BATS and in other regions have examined picocyanobacteria export, to our knowledge, no study has successfully detected *Prochlorococcus* or *Synechococcus* cells, marker pigments (such as phycoerythrin and divinyl chlorophyll) or DNA below 500 m. As such, the findings of this study present the possibility that while *Synechococcus* and its degradation products are limited to the euphotic zone and upper mesopelagic, *Prochlorococcus* is a component of POC export to the deep ocean.

Conclusions

This study, although correlative in nature, indicates that *Prochlorococcus* abundance may play a role in the concentration and distribution of CDOM in the deep ocean. This challenges previous studies, which have posited that deep CDOM in the North Atlantic is purely terrigenous and allochthonous. Furthermore, it suggests that *Prochloroccocus* can be exported to the bathypelagic and that this marine autotroph could play a valuable and previously unknown role in the transport of organic material to the deep ocean. The ability to use CDOM as a tracer of *Prochlorococcus* export to the deep ocean would overcome current challenges in the detection of picocyanobacteria in the bathypelagic and could allow for more a comprehensive understanding of the role of *Prochlorococcus* in the deep ocean carbon pool. As studies have indicated that picocyanobacteria will play an increasingly greater role in maintaining a strong biological pump in the North Atlantic as atmospheric CO_2 levels continue to rise (Lomas et al., 2010), the potential for *Prochlorococcus* to enhance carbon sequestration is of great importance to predicted future climate scenarios.

Methods and Materials

Sample Collection
Samples were collected at the Bermuda Atlantic Time-series Site in the Western Sargasso Sea (31° 40' N; 64° 10' W) between June 2006 and June 2015 onboard the *R/V Atlantic Explorer* as part of the Bermuda Bio-Optics Project. Seawater was collected unfiltered or filtered directly from Niskin bottles (General Oceanics) mounted on a steel rosette affixed with a conductivity, temperature and depth (CTD) sensor package (Seabird SBE 9/11 Plus).

CDOM Absorbance Measurements
CDOM samples were filtered through a 0.2 μm capsule filter (Whatman Polycap 75 AS) and collected in amber glass vials (I-Chem; muffled at 500 °C prior to use) with polytetrafluoroethylene-lined caps. Samples were stored in the dark at 4°C until analysis. Samples were analyzed in 10 cm quartz cuvettes using a dual-beam spectrophotometer (Perkin Elmer Lambda 18) equipped with deuterium and tungsten lamps. A slit width of 2 nm was selected and absorbance was measured in 1 nm wavelength increments from 250-750 nm. The instrument was blanked using de-ionized water (Milli-Q, Millipore) and spectra were corrected for baseline offsets according to Green and Blough (1994). Absorbance values are represented as the parameter "absorption coefficient" $_a$cdom (m^{-1}), which is obtained by multiplying the absorbance values by *e* (2.303) and dividing by the cell path length (m). A wavelength of 325 nm was nominally chosen to best represent the CDOM concentrations in the open ocean, as per Nelson and Siegel (2002).

Ancillary Measurements
Ancillary data included measurements collected monthly as part of the BATS time series. Measurements for pressure, temperature, salinity, total organic carbon (TOC) and sediment trap organic carbon flux (C_{org}) were collected according to methods outlined in the Joint Global Ocean Flux Study (JGOFS) protocols and available at www.bats.bios.edu/bats_methods.html. The potential density anomaly ($\sigma\theta$) was defined as $\sigma_{\theta,S,0} = \rho_{\theta,S,0}$ - 1000 kg/m^3, where θ is the potential temperature, S is the *in situ* salinity and ρ_0 is the potential density, referenced to the pressure at the ocean surface.

Neutral density surfaces (γ^n) were calculated using the eos80_gamma_n package (version 3.05.10 for Matlab), which is derived from the UNESCO algorithm for computation of fundamental properties of seawater (1983) and available at www.teos-10.org. γ^n was calculated for 24 depths between 600 and 4200 m. Specific water masses were delineated using the modifications made by Nelson et al (2007) on the definitions outlined by Joyce et al (2001) and are shown in SI Table 1.

Data Analysis
Data were interpolated to remove missing values and then again to create an evenly-spaced time series of CDOM absorbance (325 nm) measurements. Row-wise followed by column-wise linear interpolation of data matrices was used to remove and replace

missing (NA) values and then a linear time interpolation was performed for all variables to create evenly-spaced data. The use of cubic spline instead of linear interpolation resulted in a difference of < 1% in the outcome of modeled data. The interpolated time was defined as t = 732924 : 34.19 : 736138, where the first and last argument are serial date numbers, representing the sampling date range in reference to January 0, 0000, and 34.19 is the average sampling interval (days). Data was then standardized such that all variable vectors had a mean of zero and a standard deviation of one. The time series comprised data from 24 discrete depths ranging from 1 – 3000 m, collected between 2006 and 2015. Significant correlations and confidence intervals were tested by calculating Pearson's correlation coefficients. *P*-values < 0.05 were considered significant, although most values were < 0.01 and noted as such.

Cross correlations were calculated using the fast Fourier transform-based cross correlation theorem, such that $f * g = \mathscr{F}[\overline{F}(\nu)\,\overline{G}(\nu)]$, where $f * g$ is the cross correlation of $f(t)$ and $g(t)$ and $\mathscr{F}$ is the Fourier transform applied to each column of data. The number of degrees of displacement of the first dataset relative to the second, or 'lags', was set to 20 (months), with the center lag set equal to zero. Cross correlation plots included 95% confidence boundaries.

References

AMACHER, J., NEUER, S. & LOMAS, M. 2013. DNA-based molecular fingerprinting of eukaryotic protists and cyanobacteria contributing to sinking particle flux at the Bermuda Atlantic time-series study. *Deep-Sea Research Part Ii-Topical Studies in Oceanography,* 93**,** 71-83.

BILLER, S. J., BERUBE, P. M., LINDELL, D. & CHISHOLM, S. W. 2015. Prochlorococcus: the structure and function of collective diversity. *Nature Reviews Microbiology,* 13**,** 13-27.

BOYD, P., SHERRY, N., BERGES, J., BISHOP, J., CALVERT, S., CHARETTE, M., GIOVANNONI, S., GOLDBLATT, R., HARRISON, P., MORAN, S.B., ROY, S., SOON, M., STROM, S., THIBAULT., VERGIN K., WHITNEY, F., WONG, C. 1999. Transformations of Biogenic Particulates from the Pelagic to the Deep Ocean Realm. *Deep Sea Research Part II,* 46**,** 2761-2792.

BREW, H. S., MORAN, S. B., LOMAS, M. W., BURD, A. B 2009. Plankton Community Composition, Organic Carbon and Thorium-234 Particle Size Distributions, and Particle Export in the Sargasso Sea. *Journal of Marine Research,* 67**,** 845-868.

CARLSON, C. & HANSELL, D. 2015. DOM Sources, Sinks, Reactivity and Budgets. *In:* HANSELL, D. & CARLSON, C. (eds.) *Biogeochemistry of Marine Dissolved Organic Matter 2nd Edition.* San Diego: Academic Press.

CARLSON, C. A., DUCKLOW, H. W., HANSELL, D. A. & SMITH, W. O. 1998. Organic carbon partitioning during spring phytoplankton blooms in the Ross Sea polynya and the Sargasso Sea. *Limnology and Oceanography,* 43**,** 375-386.

CARLSON, C. A., HANSELL, D. A., NELSON, N. B., SIEGEL, D. A., SMETHIE, W. M., KHATIWALA, S., MEYERS, M. M. & HALEWOOD, E. 2010. Dissolved organic carbon export and subsequent remineralization in the mesopelagic and bathypelagic realms of the North Atlantic basin. *Deep-Sea Research Part Ii-Topical Studies in Oceanography,* 57**,** 1433-1445.

CONTE, M., RALPH, N., ROSS, E. 2001. Seasonal and Interannual Variability in the Deep Ocean Particle Fluxes at the Oceanic Flux Program (OFP)/Bermuda Atlantic Time-series (BATS) site in the Western Sargasso Sea near Bermuda. *Deep Sea Research Part II,* 43**,** 891-906.

DEL VECCHIO, R. & BLOUGH, N. V. 2002. Photobleaching of chromophoric dissolved organic matter in natural waters: kinetics and modeling. *Marine Chemistry,* 78**,** 231-253.

DENG, W., MONKS, L., NEUER, S. 2015. Effects of Clay Minerals on the Aggregation and Subsequent Settling of Marine *Synechococcus*. *Limnology and Oceanography,* 60**,** 805-816.

DITTMAR, T. 2015. Reasons Behind the Long-Term Stability of Dissolved Organic Matter. *In:* HANSELL, D. & CARLSON, C. (eds.) *Biogeochemistry of Marine Dissolved Organic Matter.* San Diego: Academic Press.

DRUFFEL, E. R. M., BAUER, J.E., WILLIAMS, P.M., GRIFFIN, S., WOLGAST, D. 1996. Seasonal variability of particulate organic radiocarbon in the northeast Pacific Ocean. *Journal of Geophysical Research,* 101**,** 20543-20552.

DURAND, M., OLSEN, R., CHISHOM, S. 2001. Phtyoplankton Population Dynamics at the Bermuda Atlantic Time-series Study Station in the Sargasso Sea. *Deep Sea Research Part II,* 48**,** 1983-2003.

FASHAM, M. J. R., BALINO, B. M., BOWLES, M. C., ANDERSON, R., ARCHER, D., BATHMANN, U., BOYD, P., BUESSELER, K., BURKILL, P., BYCHKOV, A., CARLSON, C., CHEN, C. T. A., DONEY, S., DUCKLOW, H., EMERSON, S., FEELY, R., FELDMAN, G., GARCON, V., HANSELL, D., HANSON, R., HARRISON, P., HONJO, S., JEANDEL, C., KARL, D., LE BORGNE, R., LIU, K. K., LOCHTE, K., LOUANCHI, F., LOWRY, R., MICHAELS, A., MONFRAY, P., MURRAY, J., OSCHLIES, A., PLATT, T., PRIDDLE, J., QUINONES, R., RUIZ-PINO, D., SAINO, T., SAKSHAUG, E., SHIMMIELD, G., SMITH, S., SMITH, W., TAKAHASHI, T., TREGUER, P., WALLACE, D., WANNINKHOF, R., WATSON, A., WILLEBRAND, J. & WONG, C. S. 2001. A new vision of ocean biogeochemistry after a decade of the Joint Global Ocean Flux Study (JGOFS). *Ambio,* Spec No 10**,** 4-31.

GREEN, S. A. & BLOUGH, N. V. 1994. OPTICAL-ABSORPTION AND FLUORESCENCE PROPERTIES OF CHROMOPHORIC DISSOLVED ORGANIC-MATTER IN NATURAL-WATERS. *Limnology and Oceanography,* 39**,** 1903-1916.

HANSELL, D., CARLSON, C. 2001. Marine Dissolved Orgainc Matter and the Carbon Cycle. *Oceanography,* 14**,** 41-49.

HANSELL, D., CARLSON, C., REPETA, D., AND SCHLITZER, R. 2009. Dissolved Organic Matter in the Ocean: A Controversy Stimulates New Insights. *Oceanography,* 22.

HANSELL, D., CARLSON, C., SCHLITZER, R. 2012. Net Removal of Major Marine Dissolve Organic Carbon Fractions in the Subsurface Ocean. *Global Biogeochemical Cycles,* 26**,** 1-9.

HANSELL, D. A. & CARLSON, C. A. 1998. Deep-ocean gradients in the concentration of dissolved organic carbon. *Nature,* 395**,** 263-266.

HANSELL, D. A., CARLSON, C. A., REPETA, D. J. & SCHLITZER, R. 2009. DISSOLVED ORGANIC MATTER IN THE OCEAN A CONTROVERSY STIMULATES NEW INSIGHTS. *Oceanography,* 22**,** 202-211.

HAWKES, J. A., ROSSEL, P. E., STUBBINS, A., BUTTERFIELD, D., CONNELLY, D. P., ACHTERBERG, E. P., KOSCHINSKY, A., CHAVAGNAC, V., HANSEN, C. T., BACH, W. & DITTMAR, T. 2015. Efficient removal of recalcitrant deep-ocean dissolved organic matter during hydrothermal circulation. *Nature Geoscience,* 8**,** 856-+.

HERNES, P. J. & BENNER, R. 2006. Terrigenous organic matter sources and reactivity in the North Atlantic Ocean and a comparison to the Arctic and Pacific oceans. *Marine Chemistry,* 100**,** 66-79.

JOYCE, T., HERNANDEZ-GUERRA, A., SMETHIE, W. 2001. Zonal Circulation in the NW Atlantic and Caribbean from a Meridional World Ocean Circulation Experiment Hydrographic Section at 66W. *Journal of Geophysical Research,* 106**,** 22095-22113.

LOMAS, M. W. & MORAN, S. B. 2011. Evidence for aggregation and export of cyanobacteria and nano-eukaryotes from the Sargasso Sea euphotic zone. *Biogeosciences,* 8**,** 203-216.
LOMAS, M. W., STEINBERG, D. K., DICKEY, T., CARLSON, C. A., NELSON, N. B., CONDON, R. H. & BATES, N. R. 2010. Increased ocean carbon export in the Sargasso Sea linked to climate variability is countered by its enhanced mesopelagic attenuation. *Biogeosciences,* 7**,** 57-70.
MCDONNELL, A. M. P. 2011. *Marine particle dynamics: sinking velocities, size distributions, fluxes and microbial degradation rates.* PhD, Massachusetts Institute of Technology.
MCDONNELL, A. M. P., BUESSELER, K.O. 2010. Variability in the average sinking velocity of marine particles. *Limnology and Oceanography,* 55**,** 2085-2096.
MICHAELS, A., SILVER, M.W. 1988. Primary Production, Sinking Fluxes, and the Microbial Food Web. *Deep Sea Research Part I,* 35**,** 473-490.
NELSON, N. B., CARLSON, C. A. & STEINBERG, D. K. 2004. Production of chromophoric dissolved organic matter by Sargasso Sea microbes. *Marine Chemistry,* 89**,** 273-287.
NELSON, N. B. & SIEGEL, D. A. 2002. Chromophoric DOM in the Open Ocean. *In:* HANSELL, D. & CARLSON, C. (eds.) *Biogeochemistry of Marine Dissolved Organic Matter.* Academic Press.
NELSON, N. B. & SIEGEL, D. A. 2013. The Global Distribution and Dynamics of Chromophoric Dissolved Organic Matter. *Annual Review of Marine Science***,** 447-76.
NELSON, N. B., SIEGEL, D. A., CARLSON, C. A., SWAN, C., SMETHIE, W. M. & KHATIWALA, S. 2007. Hydrography of chromophoric dissolved organic matter in the North Atlantic. *Deep-Sea Research Part I-Oceanographic Research Papers,* 54**,** 710-731.
NELSON, N. B., SIEGEL, D. A. & MICHAELS, A. F. 1998. Seasonal dynamics of colored dissolved material in the Sargasso Sea. *Deep-Sea Research Part I-Oceanographic Research Papers,* 45**,** 931-957.
NELSON, N. B. A. G., J.M. 2016. Optical Signatures of Dissolved Organic Matter Transformation in the Global Ocean. *Frontiers in Marine Science,* 2.
STEDMON, C. A. & NELSON, N. B. 2015. The Optical Properties of DOM in the Ocean. *In:* HANSELL, D. A. C., C. (ed.) *Bioegeochemistry of Marine Dissolved Organic Matter* San Diego: Academic Press.
SWAN, C., NELSON, N.B., SIEGEL, D.A., KOSTADINOV, T.S. 2012. The Effect of Surface Irradiance on the Absorption Spectrum of Chromophoric Dissolved Organic Matter in the Global Ocean. *Deep Sea Research Part I,* 63**,** 52-64.

CHAPTER 6: Final Discussion and Future Work

Impetus for the study

This study was largely driven by the paucity of knowledge about CDOM cycling in the open ocean. As CDOM accounts for up to 50% of blue light absorption in the ocean and has been shown to influence ocean color algorithms that predict primary production (Nelson et al., 1998, Siegel et al., 2002, Siegel et al., 2005, Maritorena and Siegel, 2005, Nelson and Siegel, 2013), a better understanding of the sources and fate of CDOM in the open ocean is crucial. Studies such as the CLIVAR Repeat Hydrography Program have elucidated spatial variation in oceanic CDOM distributions, but measurements along the cruise tracks allowed for only 'snapshots' of CDOM cycling over time (Nelson et al., 2007, Carlson et al., 2010). The decade-long time-series of monthly CDOM measurements collected at the Bermuda Atlantic Time-series Study site (31.666° N, 64.166° W), as part of the NASA-funded Bermuda Bio-Optics Project has provided the temporal resolution necessary to deconstruct CDOM signals, to determine patterns in CDOM cycling at depths ranging from the surface ocean to the bathypelagic zone and to link these patterns to previously unknown sources of CDOM in the North Atlantic.

Autochthonous sources of CDOM

The existence and distribution of CDOM in the open ocean was once thought to be solely the result of advection of terrigenous material from coastal regions and the subpolar gyres (Bricaud et al., 1981, Blough and Del Vecchio, 2002). The gradient of increasing salinity that is observed when transitioning from coastal zones to the open ocean corresponds to a decrease in CDOM concentration (Blough and Del Vecchio, 2002). This led a number of researchers to conclude that ocean CDOM is simply diluted material originating from coastal waters. As a result, studies focused on terrigenous markers such as humic and fulvic acids and lignin phenols (Del Vecchio and Blough, 2004, Boyle et al., 2009, McCarthy et al., 1996, Hernes and Benner, 2002, Hernes and Benner, 2003). However, in the past two decades, production of CDOM by marine microbes has been demonstrated. Incubations of natural assemblages of heterotrophic bacteria in seawater from the Sargasso Sea exhibited an increase in CDOM corresponding to an increase in bacterial cell abundance (Nelson et al., 2004, Steinberg et al., 2004). These incubations were performed in the dark to preclude the growth of marine autotrophs. Although many marine heterotrophs can be difficult to culture in the laboratory, a number of axenic cultures have been successful and have demonstrated the production of CDOM *in vitro*.

The role of marine heterotrophs in CDOM production and degradation

The lack of correlation between CDOM and chlorophyll *a* in the North Atlantic subtropical gyre, as well as the fact that CDOM exhibits a seasonal peak in the summer instead of during the Spring bloom, has led researchers to hypothesize a non-phytoplankton source of biogenic CDOM in the open ocean (Nelson et al., 1998, Siegel et al., 2002, Nelson and Siegel, 2002, Siegel et al., 2005, Nelson et al., 2007, Carlson et al., 2010, Nelson, 2016). It has been shown that summer depth profiles of bacterial abundance are qualitatively similar to CDOM profiles in the upper water column during these months (Nelson et al., 1998, Nelson and Siegel, 2013). Additionally, CDOM production has been demonstrated in controlled incubations of natural seawater

assemblages of marine heterotrophs. In these studies, filtered surface water from the BATS site was inoculated with unfiltered water from the bacterial maximum, amended with various nutrient treatments and incubated in the dark. Even in control samples without added nutrients, an increase in CDOM absorbance was observed to coincide with an increase in bacterial cell abundance (Nelson et al., 2004). These studies also revealed that the chemical composition of nutrient amendments affected not only microbial community composition, but also decay rates of subsequently produced CDOM. In incubations amended with labile neutral sugars such as glucose, CDOM was produced rapidly in conjunction with a dramatic increase in bacterial abundance, but was removed within days. Conversely, in those incubations amended with a more complex substrate such as zooplankton exudate, CDOM persisted in the samples for weeks to months. Although these studies demonstrated the production of CDOM by heterotrophic microbes, they did not examine which species were present. In other similar amended incubations in which CDOM was not measured, species were found to vary depending on the composition of nutrient amendments (Carlson et al., 2002, Carlson et al., 2009, Nelson and Carlson, 2012, Nelson et al., 2013). In incubations amended with dissolved neutral sugars such as glucose, copiotrophic groups of bacteria, such as Alteromonas, quickly outcompeted other species. In unamended controls with limited nutrients, oligotrophs such as SAR11 were dominant. In our study, heterotrophic community response was examined in relation to CDOM production and removal. In addition to heterotrophic bacteria, the role of Archaea was examined. At discrete time points throughout the incubations, measurements were collected for dissolved organic carbon (DOC), bacterial cell abundance, CDOM, Fluorescence In-Situ Hybridization (FISH) and Catalyzed Reporter Deposition (CARD)-FISH. Incubations were amended with either a labile 'cocktail' containing glucose, ammonia and phosphate, or left unamended as controls. Alternatively, some incubations were amended with lignin, a terrigenous and purportedly 'semi-refractory' substrate. It has been previously shown that lignin can be used by microbes over extended (> 1 year) timescales, or after prior degradation by photolysis or hydroxyl radicals. However, our results showed a 21-25% decrease in CDOM at wavelengths corresponding to lignin (~ 340 nm) that coincided with an increase in bacterial cell abundance after less than 8 days of incubation. This effectively demonstrated that some marine microbes are able to alter portions of the lignin macromolecule on timescales of days. Furthermore, an analysis of the microbial community composition throughout the lignin-amended samples revealed that in addition to several species of copiotrophic bacteria, two types of Archaea – Thaumarcheota and Euryarcheota – grew in correlation with the decrease in lignin absorbance (at 340 nm). These findings are novel in that they demonstrate for the first time the ability for microbes in the open ocean to alter un-degraded lignin on short timescales. The results highlight the important and under-investigated role of Archaea in the degradation of terrigenous DOM and subsequent production of marine organic matter and suggest a greater interconnection between cycles of terrigenous and biogenic organic matter in the open ocean, whereby portions of terrigenous DOM can be altered by marine heterotrophs that subsequently leads to the production of autochthonous CDOM – either through the production of new DOM or the alteration of existing molecules to produce new chromophores.

Marine autotrophic production of CDOM in the upper ocean

Studies suggesting a predominantly heterotrophic source of CDOM in the North Atlantic subtropical gyre have pointed to the fact that the CDOM seasonal maximum at BATS does not occur during the Spring bloom and does not correlate with concentrations of Chlorophyll *a* (Nelson et al., 1998, Siegel et al., 2005, Nelson and Siegel, 2013). This is in contrast to *in vitro* studies that have measured production of CDOM in axenic cultures of marine eukaryotic phytoplankton, including diatoms, dinoflagellates and green algae (Rochelle-Newall and Fisher, 2002). The fact that a link between CDOM seems to exist in cultures but not *in situ* suggests the possibility of a removal mechanism of CDOM in the upper water column that prevents its accumulation. This mechanism could be grazing by heterotrophic organisms or the rapid export of autotrophs out of the euphotic zone. While primary productivity is at a minimum during the occurrence of the summer CDOM maximum, this does not preclude a phytoplankton origin. The picocyanobacteria *Prochlorococcus* exhibits peak cell abundance between August and November, at the same time and depths as the CDOM maximum. While *Prochlorococcus* are extremely small in size, they are the most abundant photosynthetic organism on earth (Becker et al., 2014, Biller et al., 2015), and their contribution to CDOM distributions in the North Atlantic warrants investigation. In our study, possible correlations between CDOM and 7 indicators of biological processes, as well as phytogenic marker pigments, were investigated to identify possible links between CDOM and marine autotrophs. While significant correlations were found between CDOM and Chlorophyll *a* in surface waters, we concluded that the factors governing the temporal distribution of surface CDOM were different than those driving Chlorophyll *a* concentrations at the surface and that the correlation was coincidental. However, as reported in other studies, no significant correlation was found between the CDOM and chlorophyll *a* time series at either the local CDOM maximum (ca. 60 – 100 m) or the deep chlorophyll maximum. Similarly, CDOM was significantly correlated with other phytopigments at the surface but not at the local CDOM maximum. A significant correlation was found between CDOM and α + β-carotenes as well as chlorophyll *b* at ca. 100 – 120 m, suggesting that CDOM at these depths is produced by green algae. This is in agreement with studies that have demonstrated production of CDOM *in vitro* by axenic cultures of green algae. However, the lack of a significant correlation between CDOM and prasinoxanthin at these depths suggests that these algae are not prasinophytes. The fact that correlations with chlorophyll *b* are not significant at other depths may be due to the fact that green algae at BATS proliferate in deeper parts of the euphotic zone, below diatoms, cyanobacteria and prymnesiophytes (Steinberg et al., 2001, Bidigare, 1990). Additionally, studies have shown that the chemical composition of phytoplankton-derived DOM varies widely amongst different species (Becker et al., 2014), suggesting that CDOM from certain groups will be utilized more readily by marine heterotrophs, thus creating a decoupling between phytoplankton abundance and CDOM concentration. However, it should be noted that the BATS method of HPLC analysis does not separate divinyl chlorophyll (*a* or *b*) and so these correlations could in fact be indicative of a link between CDOM and *Prochlorococcus,* which contains both divinyl chlorophylls *a* and *b*. Our study found a significant correlation ($R = 0.58$, $p < 0.01$) between *Prochlorococcus* abundance and CDOM absorbance at the depths of the CDOM seasonal maximum and the *Prochlorococcus* maximum. A significant direct correlation was not found between

another picocyanobacteria, *Synechococcus*, despite evidence that this species can produce CDOM *in vitro.* The lack of accumulation of CDOM during the Spring bloom may be due to convective overturn that takes place in the winter and spring months, when the sea surface temperature at BATS is at an annual low. Additionally, CDOM exhibits varying degrees of lability, determined by its chemical composition as well as the community structure present in the water column. CDOM produced during the Spring bloom could be rapidly utilized by marine heterotrophs or could be mixed with deeper waters, creating a homogenous and amorphous depth profile. In contrast, waters in the summer and early fall are highly stratified. Furthermore, the number of depth-integrated *Prochlorococcus* cells present during these months is greater than the depth-integrated abundances of *Synechococcus* and pico-eukaryotic cells (6,000 and 200 cells cm^{-2}, respectively) during the Spring bloom (Brew, 2009). In our study, we also demonstrated that the chemical composition of *Prochlorococcus*-derived DOM is different than that *Synechococcus*, and it is possible that the community of grazers and/or viruses in the summer months are more efficient at utilizing *Prochlorococcus*. We also found that total virioplankton abundance was strongly correlated with CDOM absorbance ($R = 0.65$, $p < 0.01$) and *Prochlorococcus* abundance ($R = 0.73$, $p < 0.01$) at 80 m, presenting a possible scenario whereby CDOM is produced by the viral lysis of these picocyanobacteria. The combination of physical and biological features during the summer/fall likely facilitates the accumulation of CDOM and is responsible for the seasonal maximum that occurs in the euphotic zone at BATS. The demonstrated correlation between CDOM, *Prochlorococcus* and virioplankton highlights the fact that neither marine autotrophs nor viruses should be discounted as important factors governing the distribution of CDOM in the open ocean.

Picocyanobacteria contribution to deep ocean CDOM

CDOM in the euphotic zone at BATS exhibits a distinct seasonality and correlates with apparent oxygen utilization (AOU). In the mesopelagic, a local CDOM minimum is attributed to the presence of the Subtropical Modewater (STMW), comprised of highly irradiated organic material. Below the STMW, CDOM values increase and remain elevated throughout the water column, into the bathypelagic (Nelson et al., 1998, Nelson and Siegel, 2013). While studies have pointed to an autochthonous microbial source of CDOM in the upper water column of the open ocean (Nelson and Siegel, 2002, Nelson et al., 2004, Steinberg et al., 2004), a number of researchers maintain that CDOM in the deep ocean is solely allochthonous, and the result of water masses that have been subducted and horizontally advected to the subtropical gyres (Nelson et al., 2007, Carlson et al., 2010, Nelson, 2016). The presence of terrigenous markers in the deep ocean such as lignin phenols have supported this theory, though concentrations of these markers are low and terrigenous material is thought to account for only 1-2% of DOC in the North Atlantic (Hernes and Benner, 2006). Furthermore, recent analyses of fluorescent DOM (FDOM) at BATS have revealed that deep ocean DOM has a similar chemical composition to DOM produced by piocyanobacteria in culture and is comprised largely of CHNO groups and H-N bonds indicative of pyrollic rings, which suggest a biogenic source (Zhao et al., 2017). In spatial studies carried out throughout the North Atlantic, there was no correlation between *p*-CFC water mass age and deep CDOM, and depth profiles were revealed to be largely homogenous below the permanent thermocline.

Although a strong correlation between CDOM and AOU exists in the Pacific and Indian Oceans, no such correlation exists in the bathypelagic zone of the North Atlantic (Carlson et al., 2010). This has been attributed to more rapid ventilation in the North Atlantic compared to the Pacific and Indian oceans, where it has been ~ 900 years since deep waters were in contact with the surface (Nelson and Siegel, 2013). However, evidence of mixing and water mass advection is observed in the North Atlantic AOU signature (Carlson et al., 2010) and so a lack of correlation implies a source of deep CDOM other than the NADW. Additionally, the decade-long time series of CDOM at BATS shows significant correlations between CDOM measurements (325 nm; m^{-1}) at each of 9 discrete depths below 500 m for a given time point, suggesting that vertical export of organic material may contribute to deep CDOM reservoirs. Temporal variations in the time-series suggest that the export of DOC could not explain the short timescales over which CDOM was transported to depth. We therefore hypothesize that export of particulate organic matter (POM), which can release DOM upon sinking, plays a major role in deep ocean CDOM. However, there was no significant correlation between deep CDOM and organic carbon flux (C_{org}) as measured in sediment traps. C_{org} is strongly associated with the spring bloom, though cells exported in the summer and early fall by *Prochlorococcus* outnumber those exported by other autotrophs during the bloom season (Brew, 2009). Furthermore, recent studies have demonstrated the ability of *Prochlorococcus* to form aggregates and to sink into sediment traps (Amacher et al., 2013). A mathematical model consisting of multiple input variables was devised to predict deep CDOM. In the final optimized model, *Prochlorococcus* cell abundance at 60 m and total organic carbon (TOC) at the given depth each comprised ca. 1/3 of the model variance, with potential density anomaly and a fitted harmonic oscillator, *y* also included. There was a significant correlation between the CDOM values predicted by the model and measured CDOM data from BATS. The model suggests that deep CDOM may be partly autochthonous and is possibly the result of particulate flux of *Prochlorococcus* to the bathypelagic, and therefore indicates that advection of terrigenous DOM alone cannot account for deep CDOM cycling in the North Atlantic. This 'newly produced' CDOM is coupled with a background of accumulated TOC, consisting of refractory autochthonous material and organic matter advected via the NADW.

Implications for our understanding of the role of Prochlorococcus in open ocean carbon cycling

This study reveals a potentially important role of *Prochlorococcus* in the cycling of open ocean CDOM. Although laboratory incubations highlight the role of heterotrophic bacteria and Archaea in both the production and utilization of marine CDOM, *Prochlorococcus* abundance, along with virioplankton, appear to be the primary factors in determining the composition and distribution of CDOM throughout the water column at BATS. Here, we have shown that although a number of marine autotrophs produce CDOM *in vitro*, most of the CDOM assumed to be produced during the Spring phytoplankton bloom does not accumulate in the upper water column, nor does it appear to be transported to the bathypelagic, as evidenced by the lack of correlation between C_{org} flux and deep CDOM. The exact set of factors that enable the accumulation of *Prochlorococcus*-derived CDOM in the summer and early autumn are not entirely clear. However, the highly-stratified nature of the water column during this time likely plays an

important role. Additionally, the work of Zhao et al. (2019) suggests that the viral lysate of *Prochlorococcus* can be made relatively refractory upon microbial processing, positing an additional explanation for the accumulation of this CDOM. Furthermore, the inherent biological and chemical properties of *Prochlorococcus* cells may play a role in allowing not only the accumulation of CDOM in the euphotic zone during these months, but its export to the deep ocean. *Prochlorococcus* has a notably small cell size of 0.5-0.7 μm (Lomas and Moran, 2011, De Martini, 2017), and it has been hypothesized that the large surface area to volume ratio of these cells results in the species being more susceptible to grazing than larger autotrophs (Lomas and Moran, 2011). The small cell size was previously thought to preclude *Prochlorococcus* from sinking; however, recent studies have shown that it can form aggregates that have been found in sediment traps. While studies of *Prochlorococcus* at BATS have not been carried out below the mesopelagic zone, our work suggests that it may be transported to at least 3000 m. Our work suggests that the seasonal flux of these cells to the deep ocean may be responsible for the autochthonous component of deep CDOM and may explain the temporal variation in deep CDOM that occurs on more rapid timescales than the transport of DOC to the deep ocean without the aid of particulate flux. Additionally, the findings of this study have important implications for our understanding of *Prochlorococcus* cycling in the open ocean. As *Prochlorococcus* is the most abundant photosynthetic organism on earth, the notion that it may play an important role in particulate flux of organic carbon to the deep ocean is critical. Over the past decade, our understanding of the contribution of *Prochlorococcus* to POC flux has changed considerably. It was once thought to contribute negligibly to total POC (Michaels, 1988); however in recent years, estimates suggest that it contributes up to a third of total POC in the open ocean (Lomas and Moran, 2011, DuRand, 2001). In our study, *Synechococcus* does not appear to be linked to deep CDOM and does not appear to be exported below the mesopelagic. The processes suggested by the results of our model could therefore indicate that *Prochlorococcus* is the only known species of marine picoplankton that is transported to the deep ocean, which has vast implications for export of organic matter and sequestration of carbon in the deep ocean.

Knowledge gaps and future work

A number of knowledge gaps and the need for future research are highlighted by the findings of this study. It is clear that the cycling of CDOM in the open ocean is complex and that CDOM has multiple sources, many of which appear to be interconnected. Much of open ocean CDOM in both the upper water column and the deep ocean is authochthonous. However, *in situ* data does not fully correlate with *in vitro* findings. The *in vitro* demonstration that a number of marine autotrophs and heterotrophs can produce CDOM is generally not observed throughout the water column. The exact reasons for this are not fully known, but are hypothesized to be a combination of the chemical composition of DOM produced by these organisms, the community composition of marine species at particular depths in the ocean, and physical processes such as turbulent mixing, convective overturn and stratification. Measurements from amended incubations suggest that DOM may be produced by some organisms and subsequently consumed by others. In this manner, terrigenous CDOM may play a valuable role in ocean DOM cycling, even when it does not accumulate throughout the water column. Future work

into the role of heterotrophic microbes in CDOM cycling should include further in-depth studies characterizing the community composition of bacterial and archaeal lineages. There are a number of analytical techniques, which while beyond the scope of the present study, could foreseeably benefit future investigations. For instance, analysis of gross changes in DOC concentrations could be achieved utilizing $\delta^{13}C$ measurements. The slight mass difference between ^{12}C and ^{13}C results in the former being preferentially uptaken during photosynthesis and leaves ^{13}C depleted in marine DOC relative to the DIC from which it originated. This signal can be used to identify organic carbon that is produced autochthonously, and in some instances can be used to identify the controls on these measurements (such as temperature and CO_2 partial pressure) (Beaupre and Druffel, 2012, St-Jean, 2003, Osburn and St-Jean, 2007, Beaupre, 2015). Recent work has shown that $\delta^{13}C$ measurements coupled with ultra-high resolution mass spectrometry such as Fourier-transform ion-cyclotron resonance mass spectrometry (FT-ICR-MS) and lignin phenol measurements can delineate terrigenous DOM in ocean samples, providing a more robust method of differentiating carbon source (Medeiros et al., 2016). Stable isotope probing (SIP) and 16S amplicon sequencing of species present in these incubations could be useful tools of analysis (Nelson and Carlson, 2012, Vergin et al., 2013, Koch et al., 2005) to better determine taxon-specific differences in the ability to uptake (and/or produce) organic carbon and to determine if genetic differences within the same species govern carbon utilization. Although SIP could not be used in conjunction with natural abundance measurements of $\delta^{13}C$, it has been shown to be useful in determining which species incorporate certain organic macromolecules. These ^{13}C-labeled compounds exhibit an altered buoyant density, which allows them to be separated on a density gradient for analysis. When coupled with 16S amplicon sequencing, it can determine which species can or cannot utilize a substrate of interest. This would be of particular use for determining definitively if Archaea actually utilize lignin. 16S amplicon sequencing, although considerably more expensive than FISH or TRFLP, allows for previously sequenced and catalogued species present to be identified and is therefore a much more robust and comprehensive technique. FT-ICR-MS could additionally be useful in further characterizing the organic compounds produced autochthonously and subsequently consumed in incubations of natural microbial assemblages. Studies have shown that this technique can be used to identify molecular markers in seawater, unique to heterotrophic bacterial metabolism (Kujawinski et al., 2009, Kujawinski et al., 2004). Using FT-ICR-MS to track changes in molecular composition at discreet time points in an incubation could reveal compositional differences between terrigenous and autochthonous DOM, and also demonstrate whether differences in molecular structure determine whether organic compounds will be utilized by specific microbial communities.

In addition to characterizing the chemical composition of DOM produced by heterotrophs in incubations, future work should comprise FT-ICR-MS and proton-nuclear magnetic resonance (p-NMR) analyses of DOM *in situ* at BATS (Zhao et al., 2017). The exact reasons that *Synechococcus* does not appear to contribute to the accumulation of CDOM in the euphotic zone are not currently known, nor is it clear why it is not correlated with CDOM in the deep ocean. The physiology of *Synechococcus* appears to differ from that of *Prochlorococcus*, and the DOM produced by each species is chemically different. However, the microbial community present during the Spring bloom is fundamentally different from that present during the summer/autumn months. The chemical composition

of the DOM becomes irrelevant if the microbes present are unable to utilize it. The winter mixing that upwells nutrients from deeper waters during the Spring bloom may also transport lower dwelling copiotrophs to the upper euphotic zone. Unlike SAR11, which usually dominates the community composition in shallower waters, these organisms can readily utilize a diverse range of organic compounds and can quickly outcompete oligotrophs in the presence of labile nutrients (Goldberg et al., 2009, Carlson et al., 2009, Goldberg et al., 2011, Nelson and Carlson, 2012, Nelson et al., 2013). This may explain the lack of accumulation of CDOM during these months and should be further investigated.

This study raises a number of questions about the nature of export of picocyanobacteria to the deep ocean. The lack of correlation between *Synechococcus* and deep CDOM suggests that this species is not exported below the mesopelagic zone. It is currently unknown how *Prochlorococcus* could be transported to depths of at least 3000 m, but not *Synechochoccus*. Aggregate formation of *Synechococcus* has been demonstrated, as has the existence of fecal pellets containing lysed *Synechococcus* cells. Additionally, its export out of the euphotic zone has been evidenced (Lomas and Moran, 2011, Amacher et al., 2013). Future work should examine whether grazing or other removal mechanisms exist in the mesopelagic, precluding its transport to the bathypelagic, or if the chemical composition of *Synechococcus* is such that its chromophoric activity is rapidly extinguished in the water column.

This is by no means an exhaustive summary of the techniques and experiments that could be employed in future studies; however, these measurements would provide further information about the exact mechanisms by which marine heterotrophs and autotrophs contribute to CDOM cycling in the open ocean. They could elucidate how terrigenous, semi-refractory DOM is transformed and utilized by marine microbes and the resulting autochthonous DOM produced. They would also allow for the full identification of all microbial species present in the incubation that contribute to the utilization and production of DOM. Furthermore, a better understanding of why *Prochlorococcus* appears to drive the accumulation and transport of CDOM in the North Atlantic Subtropical Gyre could be achieved. With this knowledge, an empirical model could be created to predict spatial and temporal concentrations of DOC using in-situ or remote absorbance and fluorescence measurements. This would greatly advance our understanding of oceanic carbon and its role in the global carbon cycle.

References

AMACHER, J., NEUER, S. & LOMAS, M. 2013. DNA-based molecular fingerprinting of eukaryotic protists and cyanobacteria contributing to sinking particle flux at the Bermuda Atlantic time-series study. *Deep-Sea Research Part Ii-Topical Studies in Oceanography,* 93**,** 71-83.

BEAUPRE, S. R. 2015. The Carbon Isotopic Composition of Marine DOC. *In:* HANSELL, D. & CARLSON, C. (eds.) *Biogeochemistry of Marine Dissolved Organic Matter.* San Diego: Academic Press.

BEAUPRE, S. R. & DRUFFEL, E. R. M. 2012. Photochemical reactivity of ancient marine dissolved organic carbon. *Geophysical Research Letters,* 39.

BECKER, J. W., BERUBE, P. M., FOLLETT, C. L., WATERBURY, J. B., CHISHOLM, S. W., DELONG, E. F. & REPETA, D. J. 2014. Closely related phytoplankton species produce similar suites of dissolved organic matter. *Frontiers in Microbiology,* 5.

BIDIGARE, R. R., MARRA, J., DICKEY, T.D., ITURRIAGA, R., BAKER, K.S., SMITH, R.C., PAK, H. 1990. Evidence for phytoplankton succession and chromatic adaptation in the Sargasso Sea during spring 1985. . *Marine Ecology Progress Series 60,* 113-122.

BILLER, S. J., BERUBE, P. M., LINDELL, D. & CHISHOLM, S. W. 2015. Prochlorococcus: the structure and function of collective diversity. *Nature Reviews Microbiology,* 13**,** 13-27.

BLOUGH, N. V. & DEL VECCHIO, R. 2002. Chromophoric DOM in the Coastal Environment. *In:* HANSELL, D. A. C., C. (ed.) *Biogeochemistry of Marine Dissolved Organic Matter.* Academic Press.

BOYLE, E. S., GUERRIERO, N., THIALLET, A., DEL VECCHIO, R. & BLOUGH, N. V. 2009. Optical Properties of Humic Substances and CDOM: Relation to Structure. *Environmental Science & Technology,* 43**,** 2262-2268.

BREW, H. S., MORAN, S. B., LOMAS, M. W., BURD, A. B 2009. Plankton Community Composition, Organic Carbon and Thorium-234 Particle Size Distributions, and Particle Export in the Sargasso Sea. *Journal of Marine Research,* 67**,** 845-868.

BRICAUD, A., MOREL, A. & PRIEUR, L. 1981. ABSORPTION BY DISSOLVED ORGANIC-MATTER OF THE SEA (YELLOW SUBSTANCE) IN THE UV AND VISIBLE DOMAINS. *Limnology and Oceanography,* 26**,** 43-53.

CARLSON, C. A., GIOVANNONI, S. J., HANSELL, D. A., GOLDBERG, S. J., PARSONS, R., OTERO, M. P., VERGIN, K. & WHEELER, B. R. 2002. Effect of nutrient amendments on bacterioplankton production, community structure, and DOC utilization in the northwestern Sargasso Sea. *Aquatic Microbial Ecology,* 30**,** 19-36.

CARLSON, C. A., HANSELL, D. A., NELSON, N. B., SIEGEL, D. A., SMETHIE, W. M., KHATIWALA, S., MEYERS, M. M. & HALEWOOD, E. 2010. Dissolved organic carbon export and subsequent remineralization in the mesopelagic and bathypelagic realms of the North Atlantic basin. *Deep-Sea Research Part Ii-Topical Studies in Oceanography,* 57**,** 1433-1445.

CARLSON, C. A., MORRIS, R., PARSONS, R., TREUSCH, A. H., GIOVANNONI, S. J. & VERGIN, K. 2009. Seasonal dynamics of SAR11 populations in the euphotic and mesopelagic zones of the northwestern Sargasso Sea. *Isme Journal,* 3**,** 283-295.

DE MARTINI, F., NEUER, S., HAMILL, D., ROBIDART, J., LOMAS, M. 2017. Clade and Strain Specific Contributions of *Synechococcus* and *Prochlorococcus* to Carbon Export in the Sargasso Sea. *Limnology and Oceanography*.

DEL VECCHIO, R. & BLOUGH, N. V. 2004. On the origin of the optical properties of humic substances. *Environmental Science & Technology,* 38**,** 3885-3891.

DURAND, M., OLSEN, R., CHISHOM, S. 2001. Phtyoplankton Population Dynamics at the Bermuda Atlantic Time-series Study Station in the Sargasso Sea. *Deep Sea Research Part II,* 48**,** 1983-2003.

GOLDBERG, S. J., CARLSON, C. A., BRZEZINSKI, M., NELSON, N. B. & SIEGEL, D. A. 2011. Systematic removal of neutral sugars within dissolved organic matter across ocean basins. *Geophysical Research Letters,* 38.

GOLDBERG, S. J., CARLSON, C. A., HANSELL, D. A., NELSON, N. B. & SIEGEL, D. A. 2009. Temporal dynamics of dissolved combined neutral sugars and the quality of dissolved organic matter in the Northwestern Sargasso Sea. *Deep-Sea Research Part I-Oceanographic Research Papers,* 56**,** 672-685.

HERNES, P. J. & BENNER, R. 2002. Transport and diagenesis of dissolved and particulate terrigenous organic matter in the North Pacific Ocean. *Deep-Sea Research Part I-Oceanographic Research Papers,* 49**,** 2119-2132.

HERNES, P. J. & BENNER, R. 2003. Photochemical and microbial degradation of dissolved lignin phenols: Implications for the fate of terrigenous dissolved organic matter in marine environments. *Journal of Geophysical Research-Oceans,* 108.

HERNES, P. J. & BENNER, R. 2006. Terrigenous organic matter sources and reactivity in the North Atlantic Ocean and a comparison to the Arctic and Pacific oceans. *Marine Chemistry,* 100**,** 66-79.

KOCH, B. P., WITT, M. R., ENGBRODT, R., DITTMAR, T. & KATTNER, G. 2005. Molecular formulae of marine and terrigenous dissolved organic matter detected by electrospray ionization Fourier transform ion cyclotron resonance mass spectrometry. *Geochimica Et Cosmochimica Acta,* 69**,** 3299-3308.

KUJAWINSKI, E. B., DEL VECCHIO, R., BLOUGH, N. V., KLEIN, G. C. & MARSHALL, A. G. 2004. Probing molecular-level transformations of dissolved organic matter: insights on photochemical degradation and protozoan modification of DOM from electrospray ionization Fourier transform ion cyclotron resonance mass spectrometry. *Marine Chemistry,* 92**,** 23-37.

KUJAWINSKI, E. B., LONGNECKER, K., BLOUGH, N. V., DEL VECCHIO, R., FINLAY, L., KITNER, J. B. & GIOVANNONI, S. J. 2009. Identification of possible source markers in marine dissolved organic matter using ultrahigh resolution mass spectrometry. *Geochimica Et Cosmochimica Acta,* 73**,** 4384-4399.

LOMAS, M. W. & MORAN, S. B. 2011. Evidence for aggregation and export of cyanobacteria and nano-eukaryotes from the Sargasso Sea euphotic zone. *Biogeosciences,* 8**,** 203-216.

MARITORENA, S. & SIEGEL, D. A. 2005. Consistent merging of satellite ocean color data sets using a bio-optical model. *Remote Sensing of Environment,* 94**,** 429-440.
MCCARTHY, M., HEDGES, J. & BENNER, R. 1996. Major biochemical composition of dissolved high molecular weight organic matter in seawater. *Marine Chemistry,* 55**,** 281-297.
MEDEIROS, P. M., SEIDEL, M., NIGGEMANN, J., SPENCER, R. G. M., HERNES, P. J., YAGER, P. L., MILLER, W. L., DITTMAR, T. & HANSELL, D. A. 2016. A novel molecular approach for tracing terrigenous dissolved organic matter into the deep ocean. *Global Biogeochemical Cycles,* 30**,** 689-699.
MICHAELS, A., SILVER, M.W. 1988. Primary Production, Sinking Fluxes, and the Microbial Food Web. *Deep Sea Research Part I,* 35**,** 473-490.
NELSON, C. E. & CARLSON, C. A. 2012. Tracking differential incorporation of dissolved organic carbon types among diverse lineages of Sargasso Sea bacterioplankton. *Environmental Microbiology,* 14**,** 1500-1516.
NELSON, C. E., GOLDBERG, S. J., KELLY, L. W., HAAS, A. F., SMITH, J. E., ROHWER, F. & CARLSON, C. A. 2013. Coral and macroalgal exudates vary in neutral sugar composition and differentially enrich reef bacterioplankton lineages. *Isme Journal,* 7**,** 962-979.
NELSON, N. B., CARLSON, C. A. & STEINBERG, D. K. 2004. Production of chromophoric dissolved organic matter by Sargasso Sea microbes. *Marine Chemistry,* 89**,** 273-287.
NELSON, N. B. & SIEGEL, D. A. 2002. Chromophoric DOM in the Open Ocean. *In:* HANSELL, D. & CARLSON, C. (eds.) *Biogeochemistry of Marine Dissolved Organic Matter.* Academic Press.
NELSON, N. B. & SIEGEL, D. A. 2013. The Global Distribution and Dynamics of Chromophoric Dissolved Organic Matter. *Annual Review of Marine Science***,** 447-76.
NELSON, N. B., SIEGEL, D. A., CARLSON, C. A., SWAN, C., SMETHIE, W. M. & KHATIWALA, S. 2007. Hydrography of chromophoric dissolved organic matter in the North Atlantic. *Deep-Sea Research Part I-Oceanographic Research Papers,* 54**,** 710-731.
NELSON, N. B., SIEGEL, D. A. & MICHAELS, A. F. 1998. Seasonal dynamics of colored dissolved material in the Sargasso Sea. *Deep-Sea Research Part I-Oceanographic Research Papers,* 45**,** 931-957.
NELSON, N. B. A. G., J.M. 2016. Optical Signatures of Dissolved Organic Matter Transformation in the Global Ocean. *Frontiers in Marine Science,* 2.
OSBURN, C. L. & ST-JEAN, G. 2007. The use of wet chemical oxidation with high-amplification isotope ratio mass spectrometry (WCO-IRMS) to measure stable isotope values of dissolved organic carbon in seawater. *Limnology and Oceanography-Methods,* 5**,** 296-308.
ROCHELLE-NEWALL, E. J. & FISHER, T. R. 2002. Production of chromophoric dissolved organic matter fluorescence in marine and estuarine environments: an investigation into the role of phytoplankton. *Marine Chemistry,* 77**,** 7-21.
SIEGEL, D. A., MARITORENA, S., NELSON, N. B., BEHRENFELD, M. J. & MCCLAIN, C. R. 2005. Colored dissolved organic matter and its influence on the

satellite-based characterization of the ocean biosphere. *Geophysical Research Letters,* 32.

SIEGEL, D. A., MARITORENA, S., NELSON, N. B., HANSELL, D. A. & LORENZI-KAYSER, M. 2002. Global distribution and dynamics of colored dissolved and detrital organic materials. *Journal of Geophysical Research-Oceans,* 107.

ST-JEAN, G. 2003. Automated quantitative and isotopic (C-13) analysis of dissolved inorganic carbon and dissolved organic carbon in continuous-flow using a total organic carbon analyser. *Rapid Communications in Mass Spectrometry,* 17**,** 419-428.

STEINBERG, D. K., CARLSON, C. A., BATES, N., JOHNSON R. J., F., M. A. & KNAP, A. H. 2001. Overview of the US JGOFS Bermuda Atlantic Time-series Study (BATS): a decade-scale look at ocean biology and biogeochemistry. *deep-Sea Research II,* 48**,** 1405-1447.

STEINBERG, D. K., NELSON, N. B., CARLSON, C. A. & PRUSAK, A. C. 2004. Production of chromophoric dissolved organic matter (CDOM) in the open ocean by zooplankton and the colonial cyanobacterium Trichodesmium spp. *Marine Ecology Progress Series,* 267**,** 45-56.

VERGIN, K. L., BESZTERI, B., MONIER, A., THRASH, J. C., TEMPERTON, B., TREUSCH, A. H., KILPERT, F., WORDEN, A. Z. & GIOVANNONI, S. J. 2013. High-resolution SAR11 ecotype dynamics at the Bermuda Atlantic Time-series Study site by phylogenetic placement of pyrosequences. *Isme Journal,* 7**,** 1322-1332.

ZHAO, Z., GONSIOR, M., LUEK, J., TIMKO, S., IANIRI, H., HERTKORN, N., SCHMITT-KOPPLIN, P., FANG, X. T., ZENG, Q. L., JIAO, N. Z. & CHEN, F. 2017. Picocyanobacteria and deep-ocean fluorescent dissolved organic matter share similar optical properties. *Nature Communications,* 8.

ZHAO, Z., GONSIOR, M., SCHMITT-KOPPLIN, P., ZHAN, Y., ZHANG, R., JIAO, N. & CHEN, F. 2019. Microbial transformation of virus-induced dissolved organic matter from picocyanobcteria: coupling of bacterial diversity and DOM chemodiversity. *The ISME Journal*.